TORSIONAL COUPLING IN SEISMIC RESPONSE OF REACTOR SYSTEMS

by

MAGDI F. ISHAC, B.Sc. (Eng.), M.Eng.

A Thesis

Submitted to the School of Graduate Studies

in Partial Fulfilment of the Requirements

for the Degree

Doctor of Philosophy

McMaster University

June, 1979

TORSIONAL COUPLING IN SEISMIC RESPONSE OF REACTOR SYSTEMS

DOCTOR OF PHILOSOPHY (1979)
(Civil Engineering and
Engineering Mechanics)

McMASTER UNIVERSITY
Hamilton, Ontario

TITLE: Torsional Coupling in Seismic
Response of Reactor Systems

AUTHOR: Magdi F. Ishac, B.Sc. (Eng.) (Cairo University) Egypt
M.Eng. (McMaster University) Canada

SUPERVISOR: Dr. A.C. Heidebrecht

NUMBER OF PAGES: xii, 160

ABSTRACT

The design of a nuclear power station to resist the effects of a strong motion earthquake represents one of the most significant considerations confronting the electric power generating industry today. The prevailing view in the nuclear industry is that structures are designed to remain essentially elastic and functionally-important equipment to remain fully functional during and/or after an earthquake.

In seismic analysis of reactor buildings it is usual to consider planar models along each of the two principal axes, and to independently analyse the response of each model to the in-plane horizontal component of ground motion. Analysis on this basis is strictly valid only for structures with coincident centers of mass and rigidity. The lateral and torsional motions of the structure are coupled if the centers of mass and rigidity do not coincide.

It is the purpose of this thesis to consider the torsional effect in the seismic analysis of Nuclear Power Plant Reactor Systems and to illustrate the effect of the lateral-torsional coupling on the equipment response. The equipment response is represented by floor response spectra. It is usually impractical to include such equipment in the dynamic model representing the building structure because of the large difference between the mass of the equipment and that of the building. Therefore, the equipment and the building are treated separately and the building response are used as inputs for the equipment analysis.

A torsionally coupled reactor model is developed considering the effect of eccentricities between the center of mass and the center of

rigidity for each floor level of the corresponding uncoupled model, and a detailed coupled analysis is investigated. To consider the effect of torsion, lateral floor spectra are developed for more than one location on each floor level. Uncoupled and coupled lateral floor spectra are presented for excitation due to several different earthquakes with the objective of evaluating the effect of torsional coupling and its influence on the equipment response.

The second object of this study is to develop a simple procedure to compute floor response spectra of the torsionally coupled reactor building without a time-history analysis. And finally, the effect of torsional ground motion is investigated, in which, a rotational time-history ground motion is generated in addition to the recorded lateral component and these two time-history excitations are used as input motions applied at the base of the torsionally reactor building. The floor response spectra are determined and analysed with the objective of evaluating the influence of the estimated torsional ground motion on the response parameters.

ACKNOWLEDGEMENTS

I would like to express my sincere appreciation to my research supervisor, Dr. A.C. Heidebrecht, for his guidance, interest and encouragement during every stage of this research project. It has been a privilege and a pleasure to work under his supervision.

I am greatly indebted to the other members of my supervisory committee, Dr. W.K. Tso, Dr. G.A. Oravas, Dr. M. Dokainish, from McMaster University, and Mr. C.G. Duff from Atomic Energy of Canada Limited, for their valuable comments and suggestions.

I wish to thank the National Research Council of Canada for providing the financial support for this investigation, Atomic Energy of Canada Limited for making available the data used in the numerical examples and the Computer Center of McMaster University for making possible the computations involved in this work.

I would also like to thank Mrs. Linda Espeut for making this thesis presentable.

And finally, and personally more important, for their understanding and encouragement, this thesis is dedicated to my parents.

TABLE OF CONTENTS

LIST OF TABLES

LIST OF FIGURES

CHAPTER I

INTRODUCTION

1.1 Seismic Design of Nuclear Power Plant Structures and Systems

The design of a nuclear power station to resist the effects of a strong motion earthquake represents one of the most significant considerations confronting the electric power generating industry today. Earthquake motions induce inertial forces in all parts of a structural system, including the soil or rock underlying the structure, secondary components including mechanical and electrical systems, equipment and piping, and any human beings present. Early approaches to the seismic design of nuclear facilities included static loading coefficients of the seismic effect. By the late 1950s dynamic analyses were being performed on certain critical subsystems, including reactor core assemblies, piping, and some heavy equipment.

In the early 1960s, the first designs of a power plant incorporating seismic analysis were being prepared. By the late 1960s, dynamic analyses of nuclear power plant structures and equipment had become commonplace.

At the present time the seismic design of nuclear power plants has become a sophisticated technique, and from a structural engineering point of view a nuclear power plant is one of the most sophisticated structures engineered by man.

From the standpoint of dynamic analysis of nuclear power plants subjected to seismic disturbance, the plant structure can be divided into two categories: namely, primary structures and secondary systems.

This is necessary because it is not feasible to formulate one mathematical model which could, in addition to the primary structures, include all of the equipment, piping systems and other light weight structures. Consequently, it is necessary to consider decoupling of the secondary system from the primary system whenever feasible.

Some rules have been developed to determine the conditions when decoupling is possible (14). Usually, the basis of such decoupling is the mass ratio (equipment to structure). Although a comparison of frequencies is more appropriate, the problem is simplified by assuming resonance conditions and then determining the corresponding mass ratio that would justify decoupling. Recently, a family of new decoupling criteria has been presented by Aziz and Duff (1,2). These new criteria are consistent for any mass ratio and any frequency ratio.

In the analysis of the seismic response of an entire power plant structure, it is essential to obtain:

1. the interaction effect of subsystems on each other, and
2. the detailed response of individual subsystems.

For example, if the reactor vessel and the turbine-generator building rest on a common foundation, the dynamic response of each is affected by the presence of the other. Therefore, an analysis including the interaction is required to determine the response. The design of the reactor vessel itself requires a knowledge of the maximum seismic stresses at various points. Such information is obtained from the detailed response of the vessel.

Calculations yielding the desired information are accordingly divided into two categories:

1. General analysis
2. Detailed analysis.

The general analysis is concerned with the evaluation of the interaction effects among the various subsystems (including the soil-structure interaction) as well as with the detailed response of the major subsystems. The various subsystems included in this analysis are usually connected by structural elements or resting on the same foundation. In developing a dynamic model, the masses of the building structure and major subsystems together with the masses of other heavy equipment must be included. A lumped mass model can be used for most conditions but if more detail is needed a finite element model can be used. The results of this analysis permit the engineer to investigate the amplification of ground motion transmitted to each individual power plant structure and to check the clearance tolerances provided for the major subsystems.

The detailed analysis is used to compute stress and strain information for any individual structural or mechanical component. Finite element models, even non-linear analysis, may be used in this case. The accelerations and displacements calculated in the general analysis are now imposed on the components to determine their capacity under such loads. Detailed stress calculations are carried out, usually by computer methods.

Once the primary structural model is formulated, the seismic and operating forces must be applied to the model and the desired response parameters (displacement, acceleration, and stress) must be calculated. Currently the nuclear industry assumes that seismic loading consists of ground vibratory motion, although considerable thought is given to ensure

that Tsunamis, soil liquefaction, landslides, and compaction will not endanger the plant. Engineers generally consider that proper geological investigations and site selection will eliminate the possibility of ground faulting immediately under the plant.

The seismic design input for the site of the nuclear power plant are usually presented by sets of ground response spectrum curves. A response spectrum is a plot of the maximum response (acceleration, velocity, or displacement) of a family of single mass oscillators with a given critical damping ratio which have been subjected to a specific input motion. These curves can be plotted on arithmetic or logarithmic scale of acceleration versus period or frequency and on tripartite log paper with acceleration, displacement, and velocity plotted versus period or frequency. Typical design seismic response spectra are shown in Figure 1.1.

The concept of the response spectrum is used to reflect the frequency content of the ground motion. Studies of strong motion records indicate that frequency content is affected, among other factors, by site subsurface materials and distance to the earthquake postulated for the site. It is simpler to develop a response spectrum that reflects these factors than it is to modify an acceleration time-history record (46).

After the response spectrum curves have been determined for the site, including the peak ground acceleration, an acceleration time-history is developed to match the response spectrum curves. Several methods (50, 14) are available to create artificial earthquake time-histories, but it is usually difficult to obtain a reasonably close match for all required damping values (0.5%, 1.0%, 2.0%, 5.0%, 7.0%, and 10.0%).

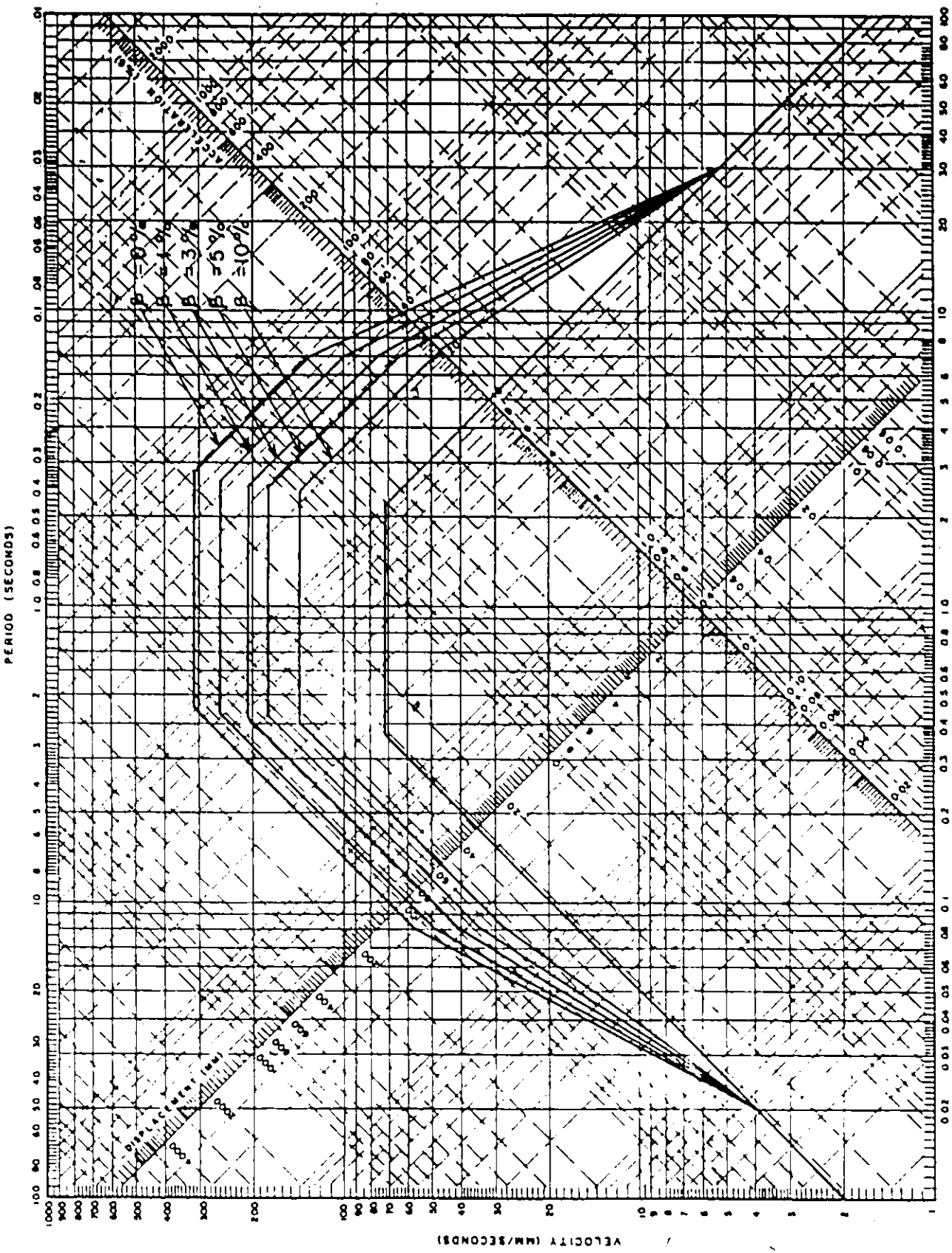

FIG 1:1 STANDARD GROUND RESPONSE SPECTRA
(Ground Acceleration 10% g)

The selection of damping values, to be used, often appear very low, because the main structures are designed to remain elastic even during very large seismic excitations. The damping values expressed as a percentage of critical damping vary between 2% and 5% for the primary structure and between 0.5% and 2% for secondary systems (8).

In the nuclear industry, the response spectrum modal superposition method is generally used for the seismic analysis of structures (8,55). This method provides an estimate of the maximum response of a structure and does not require the computation of the complete time history of the response. Since the maximum values of individual modes do not necessarily occur at the same time, the exact manner in which various modes combine cannot be precisely determined. The common method of modal combination is to compute the square root of the sum of the squares of each individual modal response. Usually in building analysis only those modes having frequencies less than about 33 Hz have to be considered (8,55). This frequency has been used since evaluation of ground response spectra generally shows little or no amplification of seismic motion for frequencies higher than 33 Hz.

As mentioned previously, the smaller items such as light equipment and piping located at the various elevations in the building structure are not included in the general seismic analysis of such primary structure.

The seismic analysis of these secondary components (equipment and piping) requires a dynamic input to determine their response. If a time history analysis is used the resulting acceleration response of the primary structure is considered as input motion to the secondary

system. This procedure is costly; several schemes have been reported (5) to avoid the time domain solution for the analysis of such secondary systems:

1. Use of maximum ground acceleration
2. Use of ground response spectra
3. Use of maximum floor accelerations
4. Use of floor response spectra
5. Use of maximum floor spectral acceleration

The use of the maximum ground acceleration assumes that both the building and equipment are rigid (natural frequency greater than 33 Hz). This is of course an erroneous conclusion and can lead to a very unconservative design.

The use of the specified site ground response spectra neglects the amplifying effect of the building on the equipment response which in most cases is a significant consideration.

The use of maximum floor accelerations obtained from the building dynamic analysis recognizes the amplifying effects of the building but assumes the equipment to be rigid.

The generation of floor response spectra for a particular building to be used as base input to equipment or equipment supports mounted directly on the floor, represents the best solution for specifying dynamic loadings for equipment.

The use of the maximum floor spectral acceleration assumes that the need to determine the frequency of the equipment has been eliminated in as much as the maximum possible spectral value is used. It, however, assumes that all equipment can be represented by a single degree of freedom

system, in resonance condition, which is not always the case and which can result in very high design forces. A graphical comparison of these different criteria is shown in Figure 1.2.

It is important to note that the response of equipment supported on ground is mainly a function of the frequency content of the earthquake ground motion; whereas, the response of equipment mounted on structures is mainly a function of the natural frequencies of the supporting structure.

As was noted previously, the floor response spectra represent the most appropriate representation of the phenomenon of the building amplification of the ground motion. This, then, should be the loading condition utilized for the dynamic analysis of the secondary systems. The analytical and modelling techniques necessary for this type of analysis have been widely described in the literature.

1.2 Development of Floor Response Spectra

The various qualification procedures usually involve computer-aided analysis for large systems and structures and tend towards shaking table tests for small equipment and components. The significance of a general building analysis is to provide dynamic inputs to the internal equipment and the term used to define this environment in a generalized form is the "Floor Response Spectrum". The floor response spectrum is a concept for defining the floor motion in such a manner as to depict the general frequency content, energy content, and maximum amplitude contained within it. The floor spectrum can then be used by the qualifying agency to develop a test motion or analytical motion that contains the same characteristics: the same frequency content, energy content,

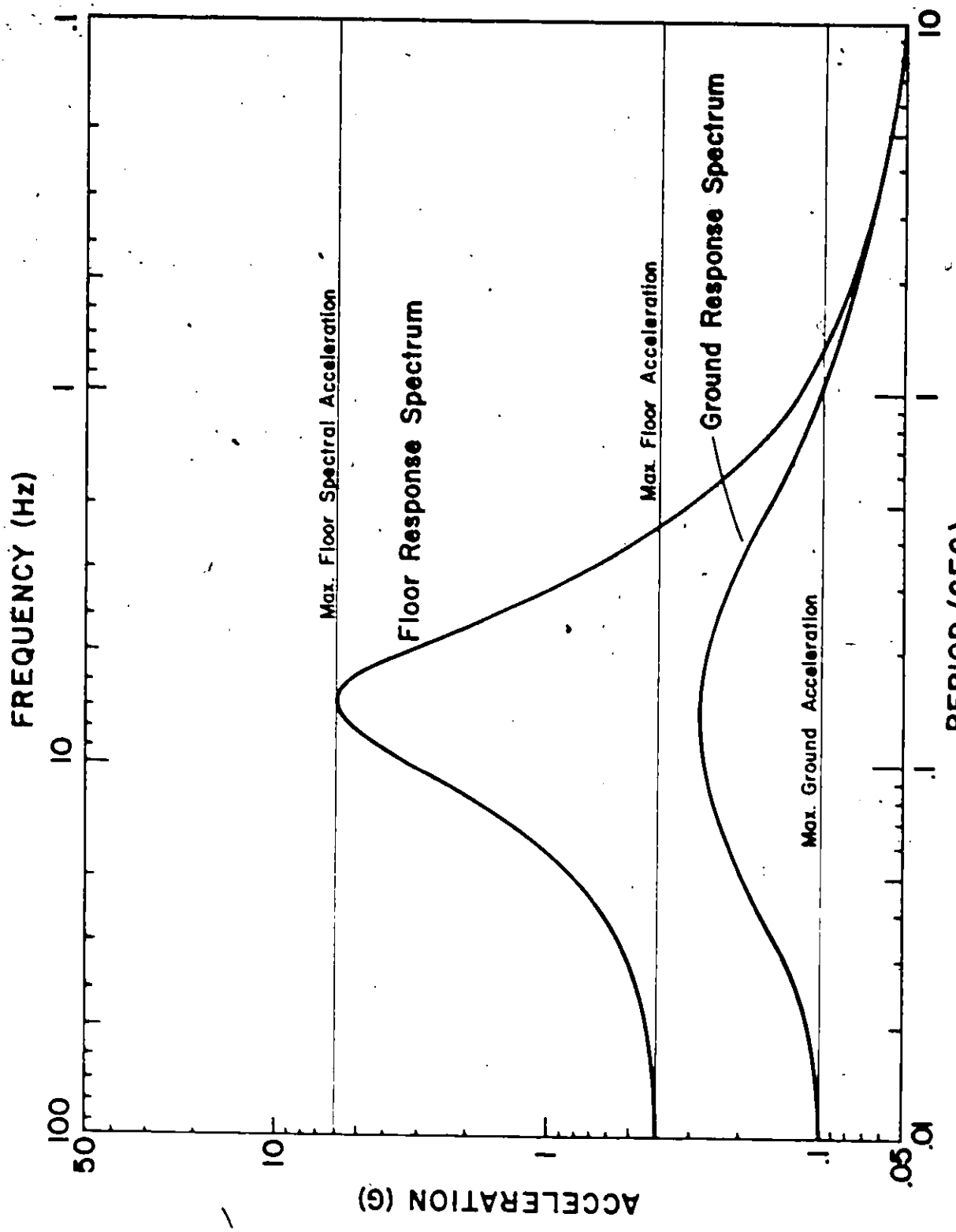

FIG. 1.2 Comparison of Design Criteria

and peak amplitudes.

Usually, floor response spectra are developed for each floor level, or other principal points of support within the building and the spectra are then used as dynamic input to pieces of equipment installed in the plants. There are several methods available to determine floor response spectra.

The most popular method to generate floor response spectra is the time history method; it is the most straightforward one as far as the theory is concerned. The basic assumption used in the time history approach is that the mass of the equipment is so small in relation to that of the structure such that there is no feedback from the equipment to the structure.

This procedure is costly, especially as several independent earthquake records must be used to avoid large statistical fluctuations. Several methods have been proposed to avoid the time domain step in generation of floor spectra directly from ground spectra.

The simplified procedures for the construction of floor response spectra are based on the concept of amplification of the ground design spectrum. The one developed by Biggs (6,7) is empirically derived and simple to apply. It is based on the results of a response spectrum analysis of the supporting structure; the effects of the structure's modes are computed separately and then combined by an empirical procedure. This method has not been adopted by some theoretically oriented groups because of the empirical nature. Later, Kapur and Shao (30) have modified Biggs' method into a mathematically more consistent form. Both of the above methods yield conservative results in comparison to time-history

solutions.

One of the widely-used methods to generate floor response spectra in Canada is the Duff method (12,13). This method is based on the dynamic response of the supporting structure subjected to a ground motion in the form of a decaying sinusoid. The resulting harmonic motion of the structure is similarly imparted to the equipment to determine its peak response. A well-proven equipment-to-structure amplification envelope is also included.

Peters, Schmitz and Wagner (41) developed a method, to determine floor response spectra, based on the modal analysis of a support structure with interaction-free one-degree-of-freedom system attached. Jeanpierre and Livolant (26) used the Fourier transform of the ground movement to determine directly the floor response spectra.

Recently, Selcuk Atalik (43) has proposed an alternative definition of Instructure Response Spectra. He showed that for a given simple oscillator (with specific damping and natural frequency) the corresponding spectral acceleration of the structural response of the ith-degree-of-freedom, when the structural system is subjected to a prescribed ground motion, is equal to the maximum absolute acceleration of that degree-of-freedom when the system is excited by a support motion which is obtained by filtering the prescribed ground motion through the single oscillator. Utilizing this alternative definition, a procedure is formulated to construct the floor response spectra, using as input a derivative of ground design spectrum (43).

None of the above methods considers the torsional response of the primary structure and its effect on the floor response spectra generated. Since earthquake motions occur randomly and not necessarily

along the orthogonal axes of structures, some torsional response may be induced in symmetrical or nearly symmetrical buildings as well as non-symmetrical structures. This fact is recognized in the National Building Code of Canada (36), where 5% accidental torsion must be considered for symmetrical structures. Of course, when a structure is not symmetrical, a torsional analysis must be made. Because torsional response of the structure may modify floor response spectra values significantly, especially at the extreme edges, it may be appropriate to investigate the effect of torsion on such floor spectra values.

1.3 Torsional Effect in Seismic Analysis

It is usual to consider planar models of the structure in each of the two orthogonal directions and to independently analyze the response of each model to the in-plane horizontal component of earthquake ground motion. The mode shapes for such a model are said to be uncoupled.

In asymmetric structures, the mode shapes would be composed of both translational and rotational components (16,4,32,25,22) and hence, the lateral and torsional motions of the structure are coupled.

In most studies of torsional coupling in seismic response of buildings (23,28,32), planar mathematical models have been extended to include the torsional degree of freedom. It is obvious that torsional coupling in seismic response is due to the asymmetric arrangement of structural elements, i.e., the center of mass at the floor does not coincide with the center of rigidity of the same floor; furthermore, these mass centers and rigidity centers of different floors are not on the same vertical axis. If the eccentricity between the center of mass and rigidity is large, lateral and torsional motions will be strongly coupled.

This strong coupling is also observed in structures with close lateral and torsional frequencies even for those structures with nearly coincident center of mass and rigidity (23,28,32).

In the nuclear industry at least two studies (9,45) have considered the torsional effect in seismic analysis of a coupled stubby asymmetric building of a nuclear power plant. In the first study, Chen (9) has assigned three dynamic degrees of freedom to each floor diaphragm: two translational in its own plane and one rotational about the vertical axis. Due to the rotational effect two floor design spectra corresponding to the two translational degrees of freedom of the diaphragm have been obtained for each directional input ground motion. In the second study, Scavuzzo and Lam (45) have used a three-mass structural model with eccentrically located dynamic masses and the results of their investigation indicate that it is possible to increase the seismic loads significantly from torsional excitation. No general conclusion has been drawn with respect to torsional coupling effect in both studies.

Asymmetric multi-storey structures have been analyzed by various different techniques and the possibility of inducing torsional response in structures has been studied by several investigators (16,4,32,35,22, 28). However, a recent torsional problem has been investigated; this problem is the torsional ground motion. Relations between lateral and torsional ground motions are obtained by several investigators (27, 11, 21, 35, 47, 57). If these relations are really true and comprehensive ones, then torsional ground motion will have large effects in the results of the response analysis and torsional effect will be of major significance.

1.4 Object and Scope of Present Investigation

The main object of this investigation is to consider the torsional effect in the seismic analysis of nuclear power plant systems and to illustrate the effect of the lateral-torsional coupling on both the input motions and the response of the internal equipment. The equipment response is represented by floor response spectra.

It is usually impractical to include such equipment in the dynamic model representing the building structure because of the large difference between the mass of the equipment and that of the building. Therefore, the equipment and the building are treated separately and the building responses are used as inputs for the equipment analysis.

A torsionally coupled reactor model is developed considering the effect of eccentricities between the center of mass and the center of rigidity for each floor level of the corresponding uncoupled model, and a detailed coupled analysis is investigated. Due to torsional coupling, the reactor building induces two different input motions to the equipment contained: lateral motion and rotational motion. Hence, the response analysis of the equipment requires both lateral and rotational floor response spectra. The concept of the rotational floor response spectrum is developed and examined in this investigation.

To consider the effect of torsion, lateral floor spectra are developed for more than one location on each floor level. Uncoupled and coupled lateral floor spectra are presented for excitation due to several different earthquakes with the objective of evaluating the effect of torsional coupling and its influence on the seismic response.

The second object of this study is to develop a simple procedure

to compute the lateral and rotational floor response spectra of the torsionally coupled reactor building without a time-history analysis. It is shown that the spectral values obtained by filtering the prescribed ground motion first through the structure and the resulting lateral-rotational motions through simple oscillators are equal to the maximum lateral-rotational responses of the structure developed when the order of filtration is reversed. Based on the preceding concept a deterministic method is presented to construct the lateral-rotational floor response spectra utilizing the response spectrum technique.

And finally, the effect of torsional ground motion is investigated. A rotational time-history ground motion is generated in addition to the recorded lateral component and these two time-history excitations are used as input motions applied at the base of the torsionally reactor building. The lateral-rotational floor response spectra are determined and analyzed with the objective of evaluating the influence of the estimated torsional ground motion on the response parameters.

CHAPTER II

DYNAMIC ANALYSIS OF A TORSIONALLY COUPLED REACTOR BUILDING

2.1 Introduction

The prevailing view in the nuclear industry is that structures are designed to remain essentially elastic under seismic loading. Although foundation soils exhibit nonlinear stress-strain relationships, analysis of containments including soil-structure interaction effect assumes equivalent linear properties of the soil. Generally, the structural components of nuclear reactor containments are walls, shells and slabs which have irregular openings and complex spatial arrangements. To obtain a general analysis, the nuclear industry currently creates a much simplified discrete lumped mass model. In this case, all the mass of the physical structure is assumed to be concentrated at a finite number of locations on the structure, usually the floors, and structural elements between these lumped mass points, which provide the system stiffness, are considered weightless. Most calculations indicate that shear is the dominant response in nuclear containments.

In dynamic analysis of the response of reactor buildings to earthquake ground motion, it is usual to consider planar models along each of the two principal axis, and to analyse independently the response of each model to the in-plane horizontal component of ground motion. Analysis on this basis is strictly valid only for structures with coincident centers of mass and rigidity. The lateral and torsional motions

of the structure are coupled if the centers of mass and rigidity do not coincide.

In this chapter, an asymmetric one storey building structure consisting of a rigid deck supported on massless, axially inextensible stiffness elements is studied to give an understanding of the lateral-torsional coupling and its effect on the structural dynamic properties. The influence of the basic coupling parameters on the response is investigated.

Extending the coupled analysis to consider a multi-degree-of-freedom system, a mathematical model for a torsionally coupled reactor building is developed.

The coupled model consists of 13 mass points representing the internal structure, containment wall and concrete vault, and takes into consideration the effect of eccentricities between the center of mass and of rigidity for each floor level. A special case of the coupled lateral-torsional model may be analysed by ignoring the eccentricity effect to give an uncoupled lateral torsional model. Due to coupling, lateral and rotational modal participation factors are determined. The concept of the rotational modal participation factor is developed and examined in this chapter. To express the degree of torsional coupling, a modal coupling parameter is proposed. Finally, a comparison of natural frequencies and modal participation factors computed by both mathematical models is made with the objective of evaluating the effect of torsional coupling on the dynamic properties of the reactor building.

2.2 Asymmetric One Storey Building Structure

The linear system studied is an idealized one storey structure consisting of a rigid deck supported on massless, axially inextensible stiffness elements. The three degrees of freedom of the system are: horizontal displacements u_z and u_y of the center of mass of the deck, relative to the ground, along the principal axes of rigidity of the structure, Z and Y, and the rotation u_θ of the deck about the vertical X-axis. For the objective of this study it is most appropriate to assume one axis of symmetry. Figure 2.1 shows the coordinate system for a typical one storey building structure with the Z-axis as the axis of symmetry and M and R are the center of mass and the center of rigidity of the system, respectively.

The center of rigidity is the point in the plan of the rigid deck through which a horizontal force must be applied in order that it may cause horizontal displacement without torsion. The location of the center of rigidity can be determined from elementary principles of mechanics.

2.2.1 Equations of Motion

The equations of motion of an asymmetric one storey building with one axis of symmetry, subjected to base ground excitation $\ddot{u}_{gy}(t)$ may be expressed as

$$\begin{bmatrix} m & 0 \\ 0 & m \end{bmatrix} \begin{Bmatrix} \ddot{u}_y \\ \ddot{u}_\theta \end{Bmatrix} + \begin{bmatrix} K_y & -\frac{e}{r} K_y \\ -\frac{e}{r} K_y & \tilde{K}_\theta \end{bmatrix} \begin{Bmatrix} u_y \\ \tilde{u}_\theta \end{Bmatrix} = -\begin{Bmatrix} m\, \ddot{u}_{gy}(t) \\ 0 \end{Bmatrix} \qquad (2.1)$$

in which m is the mass of the deck, r is the radius of gyration of the deck about a vertical axis through the center of mass, K_y is the

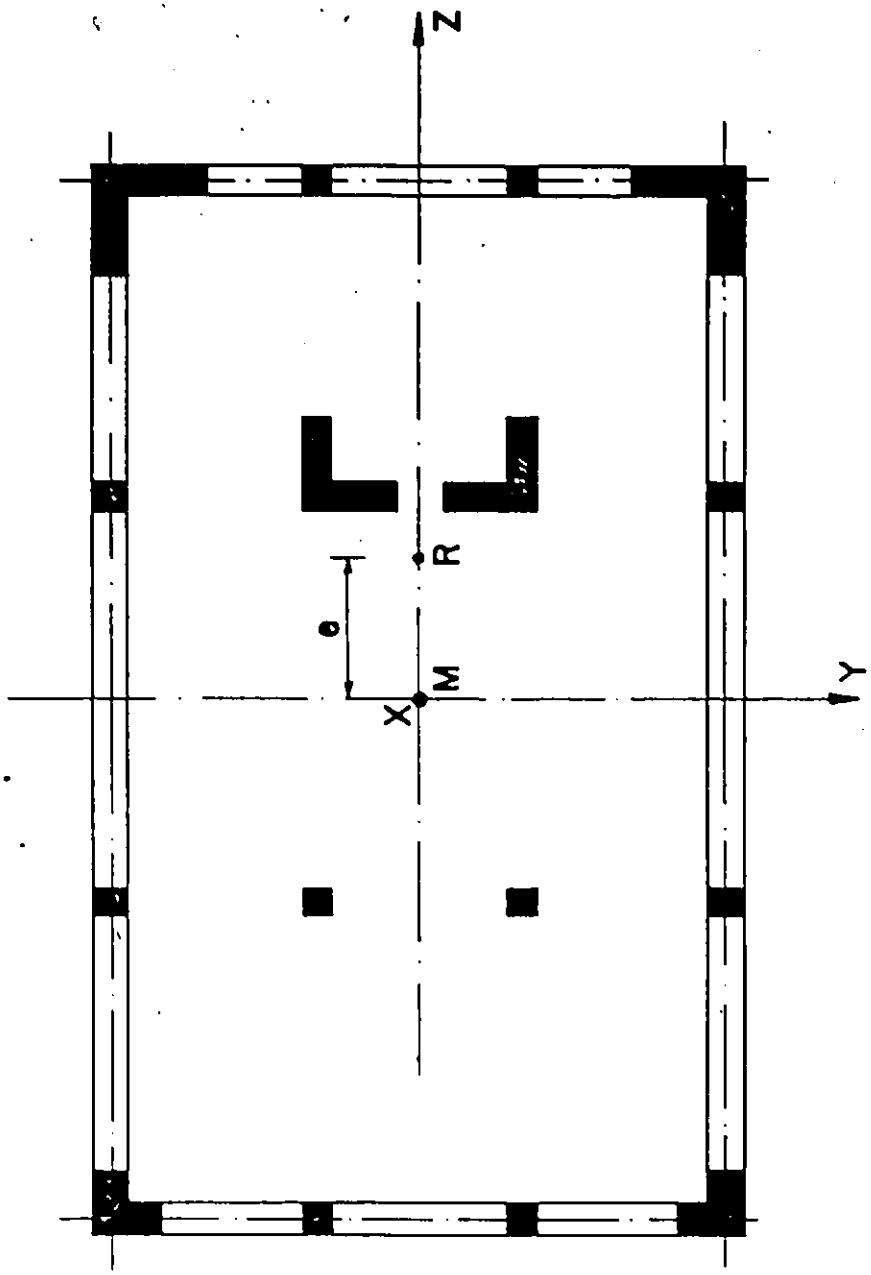

FIG. 2.1 Typical One Storey Building Structure with One Axis of Symmetry

translational stiffness of the structure in y direction, $\tilde{K}_\theta$ is the normalized torsional stiffness of the structure defined at the center of mass (Appendix 2.1), u_y and $\tilde{u}_\theta$ are the lateral and the normalized rotational ($\tilde{u}_\theta = r u_\theta$) displacements of the center of mass, and "e" is the static eccentricity between the center of rigidity (R) and the center of mass (M). The superscript "~" means that the rotational component is normalized to the same dimension of the translational component.

Damping is defined directly in each of the two natrual modes of vibration of the system. The viscous damping ratio "ζ" expressed as a fraction of critical damping is assumed to be the same in each mode of vibration. The corresponding eigenvalue problem takes the form

$$\begin{bmatrix} \left(1 - \frac{\omega^2}{\omega_y^2}\right) & -\frac{e}{r} \\ -\frac{e}{r} & \left(\lambda^2 + \frac{e^2}{r^2} - \frac{\omega^2}{\omega_y^2}\right) \end{bmatrix} \begin{Bmatrix} \alpha_y \\ \tilde{\alpha}_\theta \end{Bmatrix} = \begin{Bmatrix} 0 \\ 0 \end{Bmatrix} \qquad (2.2)$$

in which

$$\omega_y^2 = \frac{K_y}{m}, \quad \omega_\theta^2 = \frac{K_\theta}{mr^2}, \quad \lambda^2 = \frac{\omega_\theta^2}{\omega_y^2}$$

and leads to the vibration frequencies (ω_1, ω_2) and the coupled lateral-rotational mode shapes $\begin{bmatrix} \alpha_{y1} & \alpha_{y2} \\ \tilde{\alpha}_{\theta 1} & \tilde{\alpha}_{\theta 2} \end{bmatrix}$.

The coupled natural frequencies may be computed by

$$\left(\frac{\omega}{\omega_y}\right)^2_{1,2} = \frac{a + \lambda^2}{2} \mp \sqrt{\left(\frac{a + \lambda^2}{2}\right)^2 - \lambda^2} \qquad (2.3)$$

in which

$$a = 1 + \left(\frac{e}{r}\right)^2$$

and the coupled lateral-rotational mode shapes take the form

$$\alpha_{yi} = \frac{\frac{e}{r}}{\sqrt{\left(\frac{e}{r}\right)^2 + \left[1 - \left(\frac{\omega_i}{\omega_y}\right)^2\right]^2}} \qquad i = 1,2 \qquad (2.4.a)$$

$$\tilde{\alpha}_{\theta i} = \frac{\left[1 - \left(\frac{\omega_i}{\omega_y}\right)^2\right]}{\sqrt{\left(\frac{e}{r}\right)^2 + \left[1 - \left(\frac{\omega_i}{\omega_y}\right)^2\right]^2}} \qquad i = 1,2 \qquad (2.4.b)$$

It is clear from the above equations that the coupled dynamic properties depend only on the two dimensionless parameters $\left(\frac{\omega_\theta}{\omega_y}, \frac{e}{r}\right)$. Figure 2.2 shows the relationship between the coupled and the uncoupled natural frequencies for different values of $\frac{e}{r}$.

2.2.2 Response Parameters

In determining the response time history, it can be assumed that

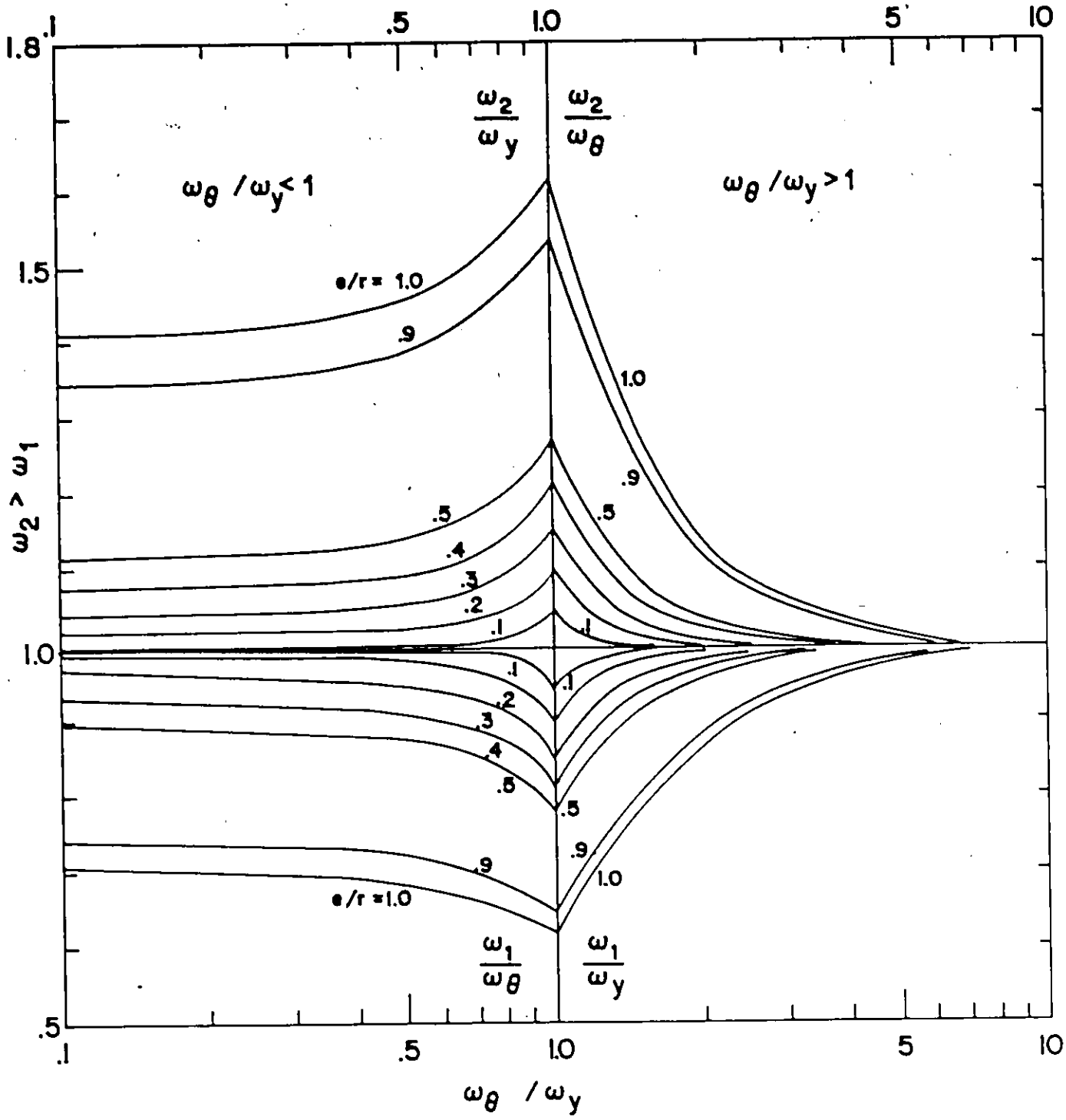

FIG. 2.2 Relationship Between Coupled and Uncoupled Natural Frequencies

$$\begin{Bmatrix} u_y(t) \\ \tilde{u}_\theta(t) \end{Bmatrix} = \begin{bmatrix} \alpha_{y1} & \alpha_{y2} \\ \tilde{\alpha}_{\theta 1} & \tilde{\alpha}_{\theta 2} \end{bmatrix} \begin{Bmatrix} A_1(t) \\ A_2(t) \end{Bmatrix} \tag{2.5}$$

in which $A_i(t)$ represents the variation with time (t) of the i^{th} mode of vibration (i=1,2).

Substituting equation (2.2) and (2.5) into equation (2.1), premultiplying the resulting equation by $[\alpha_{yi}, \tilde{\alpha}_{\theta i}]$ and writing that equation in a convenient form yields

$$\ddot{A}_i(t) + \omega_i^2 A_i(t) = - \Gamma_i \ddot{u}_{gy}(t) \tag{2.6}$$

where Γ_i, the modal participation factor is given by

$$\Gamma_i = \frac{\alpha_{yi}}{\alpha_{yi}^2 + \tilde{\alpha}_{\theta i}^2} \tag{2.7}$$

In general, the coupled mode shapes are normalized in a way that

$$\alpha_{yi}^2 + \tilde{\alpha}_{\theta i}^2 = 1 \tag{2.8}$$

Accordingly,

$$\Gamma_i = \alpha_{yi} \tag{2.9}$$

For the objectives of this study it is most appropriate to characterize ground motion by its response spectrum.

Using the response spectrum approach, the amplitude $\ddot{A}_i(t)$ attains its maximum value at

$$\max[\ddot{A}_i(t)] = \Gamma_i \, S_a(\omega_i,\zeta) \tag{2.10}$$

where $S_a(\omega_i,\zeta)$ is the spectral acceleration for the y-direction ground motion $\ddot{u}_{gy}(t)$.

The maximum coupled responses may be computed by

$$(\ddot{u}_{yi})_{max} = \alpha_{yi}^2 \, S_a(\omega_i,\zeta) \qquad i = 1,2, \tag{2.11.a}$$

$$(\ddot{\tilde{u}}_{\theta i})_{max} = \alpha_{yi} \, \tilde{\alpha}_{\theta i} \, S_a(\omega_i,\zeta) \qquad i = 1,2 \tag{2.11.b}$$

The maximum uncoupled response is determined by

$$(\ddot{u}_{y0})_{max} = S_a(\omega_y,\zeta) \tag{2.12}$$

Expressing the coupled response quantities in normalized form

$$(\bar{\ddot{u}}_{yi})_{max} = \frac{(\ddot{u}_{yi})_{max}}{(\ddot{u}_{y0})_{max}} = \alpha_{yi}^2 \, \frac{S_a(\omega_i,\zeta)}{S_a(\omega_y,\zeta)} \tag{2.13.a}$$

$$(\bar{\ddot{\tilde{u}}}_{\theta i})_{max} = \frac{(\ddot{\tilde{u}}_{\theta i})_{max}}{(\ddot{u}_{y0})_{max}} = \alpha_{yi}\tilde{\alpha}_{\theta i} \, \frac{S_a(\omega_i,\zeta)}{S_a(\omega_y,\zeta)} \tag{2.13.b}$$

Assuming two alternative idealized response spectra: (1) flat acceleration spectrum and (2) hyperbolic acceleration spectrum (or flat velocity spectrum), the normalized coupled lateral-torsional response takes the form

(1) For flat spectrum

$$(\ddot{\bar{u}}_{yi})_{max} = \alpha_{yi}^2 \tag{2.14.a}$$

$$(\ddot{\tilde{u}}_{\theta i})_{max} = \alpha_{yi}\tilde{\alpha}_{\theta i} \tag{2.14.b}$$

(2) For hyperbolic spectrum

$$(\ddot{\bar{u}}_{yi})_{max} = \alpha_{yi}^2 \frac{\omega_i}{\omega_y} \tag{2.15.a}$$

$$(\ddot{\tilde{u}}_{\theta i})_{max} = \alpha_{yi}\tilde{\alpha}_{\theta i} \frac{\omega_i}{\omega_y} \tag{2.15.b}$$

For these two idealized spectra the normalized responses do not depend on ω_i and ω_y separately but on the ratios ω_i/ω_y. The frequency ratios ω_i/ω_y and the mode shapes $(\alpha_{yi},\tilde{\alpha}_{\theta i})$ depend on the two dimensionless parameters $(\omega_\theta/\omega_y, e/r)$. The variation of the normalized modal responses, in the case of flat spectra, with these two dimensionless parameters are shown in Figures 2.3.a and 2.4.a. Those of the case of hyperbolic spectra are presented in Figures 2.3.b and 2.4.b.

In the case of flat spectrum, the two parameters α_{yi}^2 and $\alpha_{yi}\tilde{\alpha}_{\theta i}$ are the measures of the degree of coupling. The first term (α_{yi}^2) expresses the relationship between the coupled lateral response and the corresponding uncoupled response. The second term $(\alpha_{yi}\tilde{\alpha}_{\theta i})$ expresses the relationship between the induced rotational response, due to coupling, and the uncoupled lateral response. It can be seen that the effect of torsional coupling depends strongly on ω_θ/ω_y, the ratio of natural frequencies for uncoupled torsional and lateral motions of the corresponding

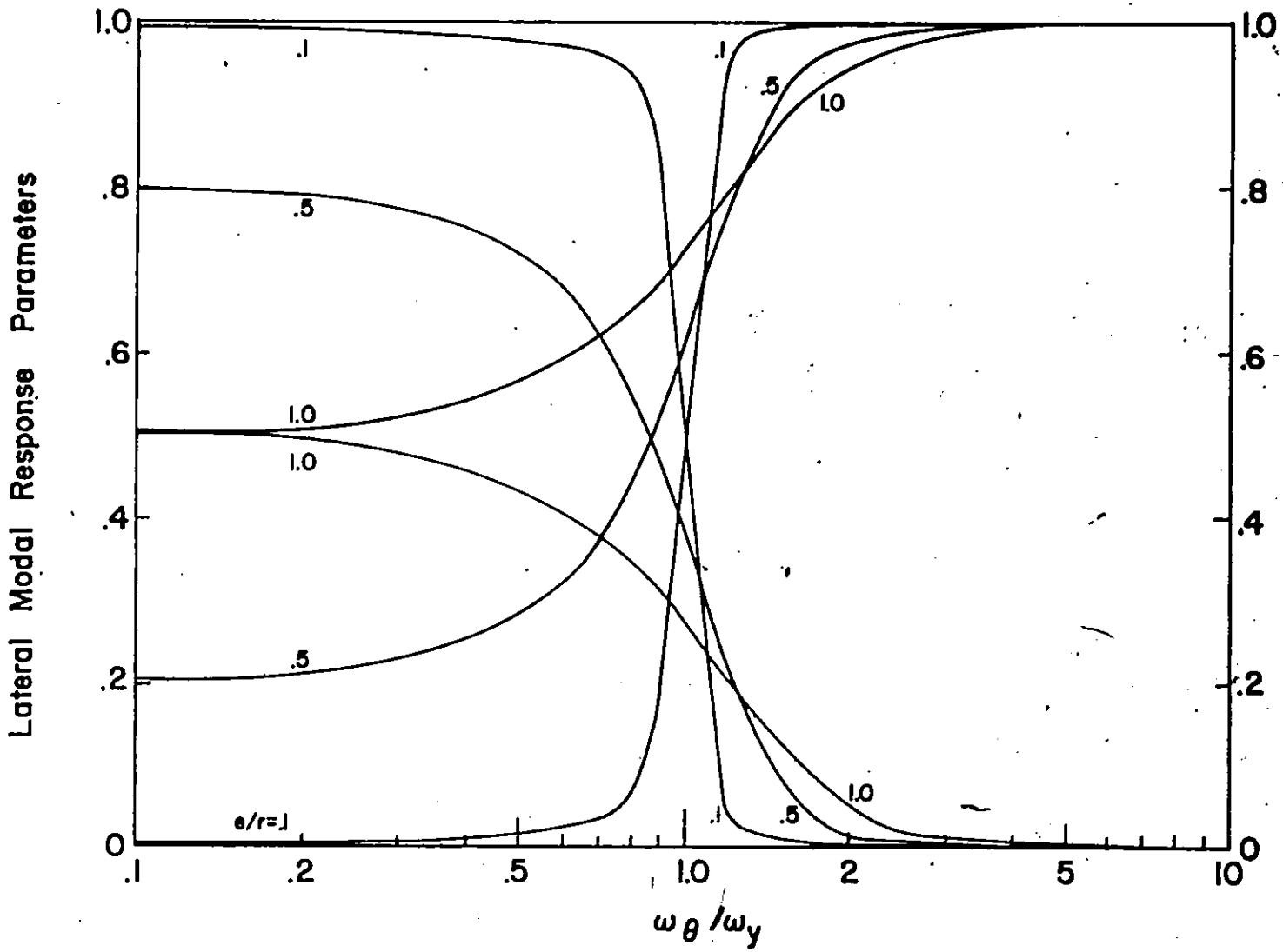

FIG. 2.3.a Lateral Modal Response Parameter-Flat Spectrum

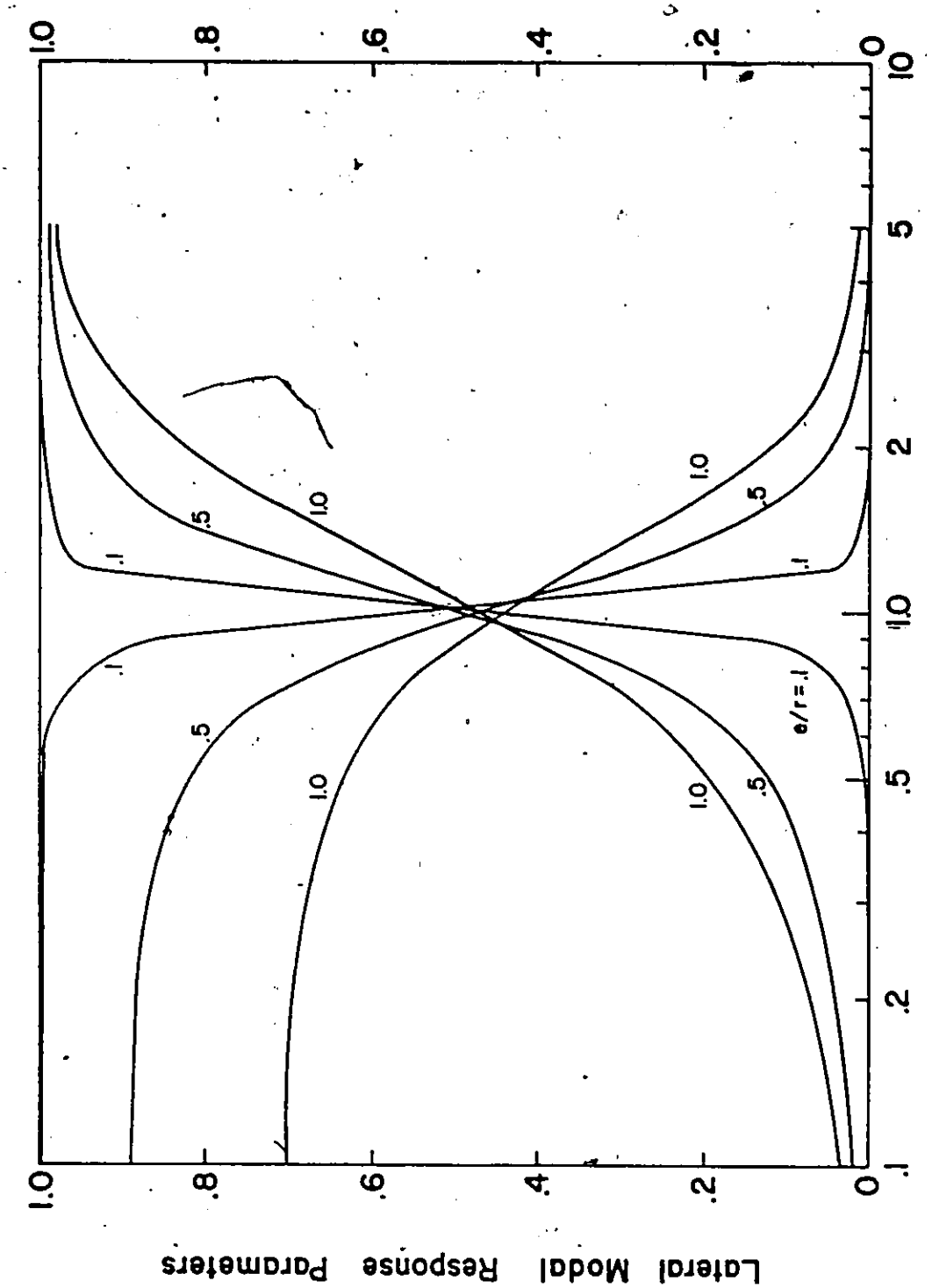

FIG. 2.3.b Lateral Modal Response Parameter-Hyperbolic Spectrum

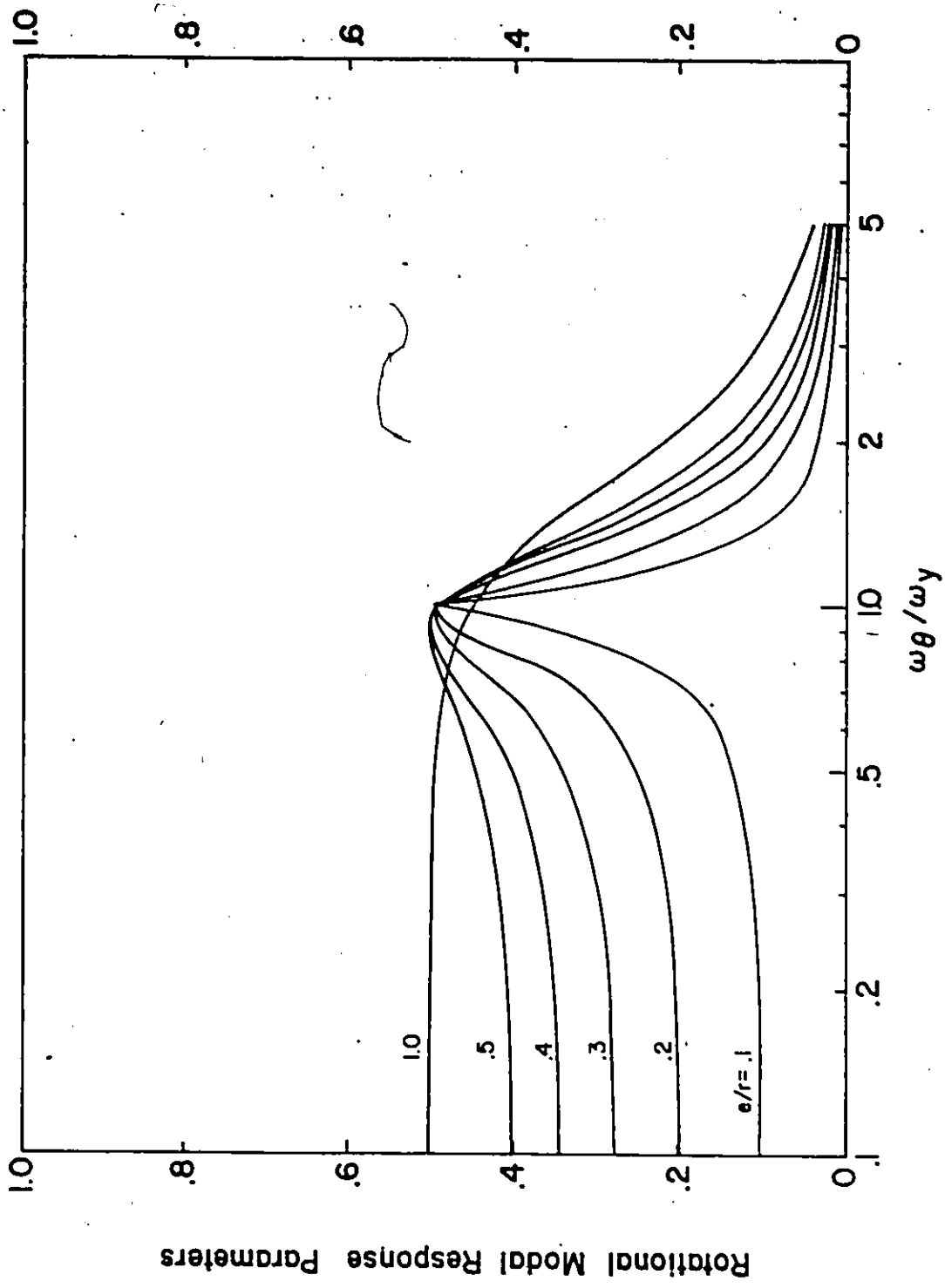

FIG. 2.4.a Rotational Modal Response Parameter-Flat Spectrum

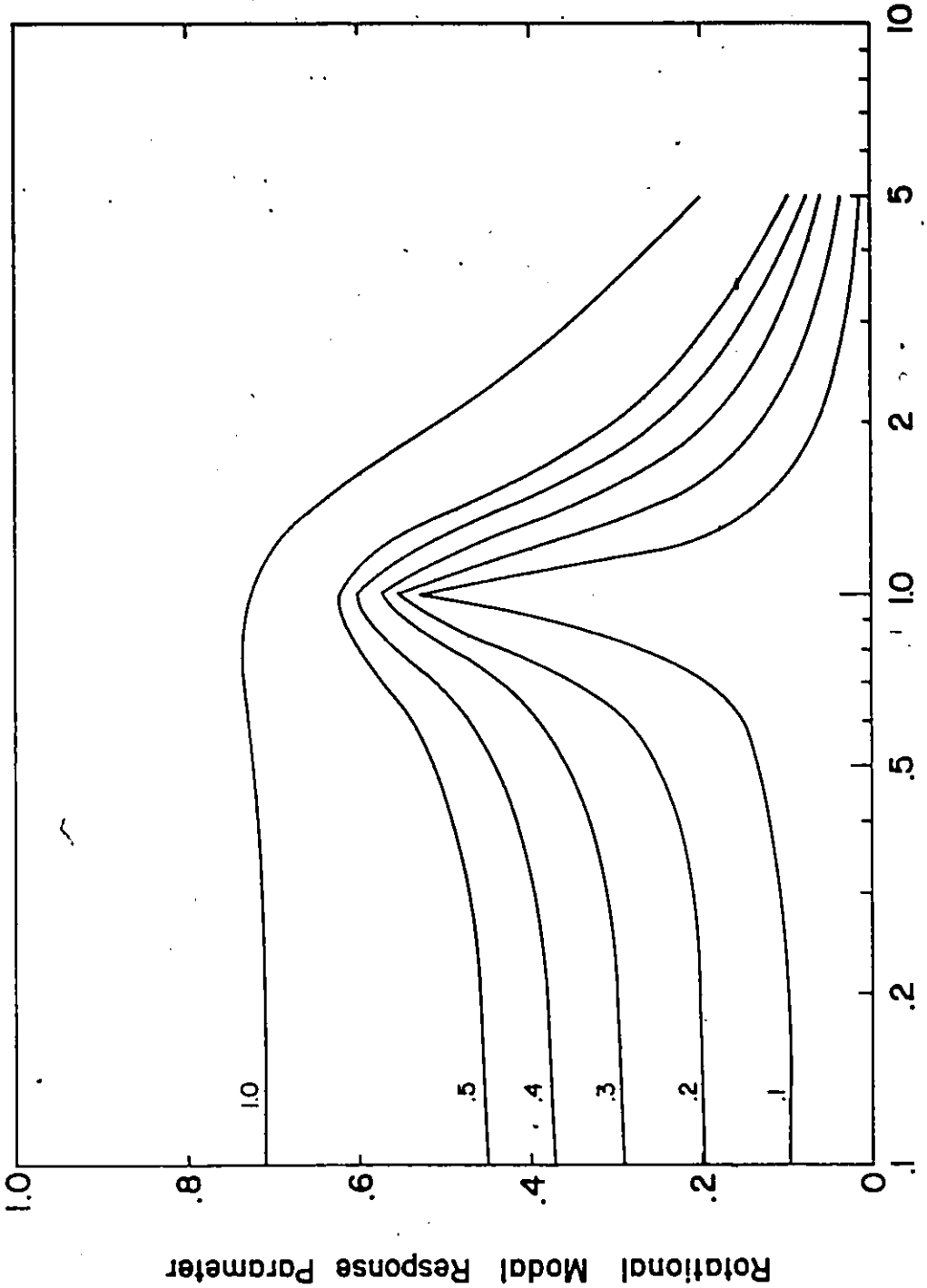

FIG. 2.4.b Rotational Modal Response Parameter-Hyperbolic Spectrum

uncoupled system. If the ratio ω_θ/ω_y is very small the coupling depends only on e/r and if ω_θ/ω_y is very large the coupling vanishes.

In the case of hyperbolic spectrum, the above parameters are scaled by the frequency ratio $\frac{\omega_i}{\omega_y}$ and the same conclusions can be drawn.

An estimate of the maximum response is determined by combining the modal maximum according to the relation given in Reference (28).

$$S^2 = \sum_{i=1}^{2} S_i^2 + \sum_{i=1}^{2} \sum_{\ell=1}^{2} a_{i\ell} S_i S_\ell \qquad (2.16)$$

in which

$$a_{i\ell} = \frac{1}{1 + \epsilon_{i\ell}^2} \quad \text{and} \quad \epsilon_{i\ell} = \sqrt{\frac{1 - \zeta^2}{\zeta^2}} \frac{\omega_i - \omega_\ell}{\omega_i + \omega_\ell}$$

The first term in equation (2.16) represents the more commonly used combination rule: square-root-of-the-sum-of-the-squares of the modal maxima. The second term is important under certain conditions, in particular when the two natural frequencies of the structure are close.

For a specific damping ratio (ζ=0.05), the maximum normalized responses in both cases of flat and hyperbolic spectra are determined and the variation of the response parameters with (ω_θ/ω_y, e/r) are shown in Figures 2.5.a and 2.5.b, respectively.

It can be shown numerically (Figures 2.5.a and 2.5.b) and also analytically (Appendix 2.1) that the normalized responses in a one storey structure, due to earthquake motion characterized by either a flat or hyperbolic acceleration spectrum, satisfy the interaction equation

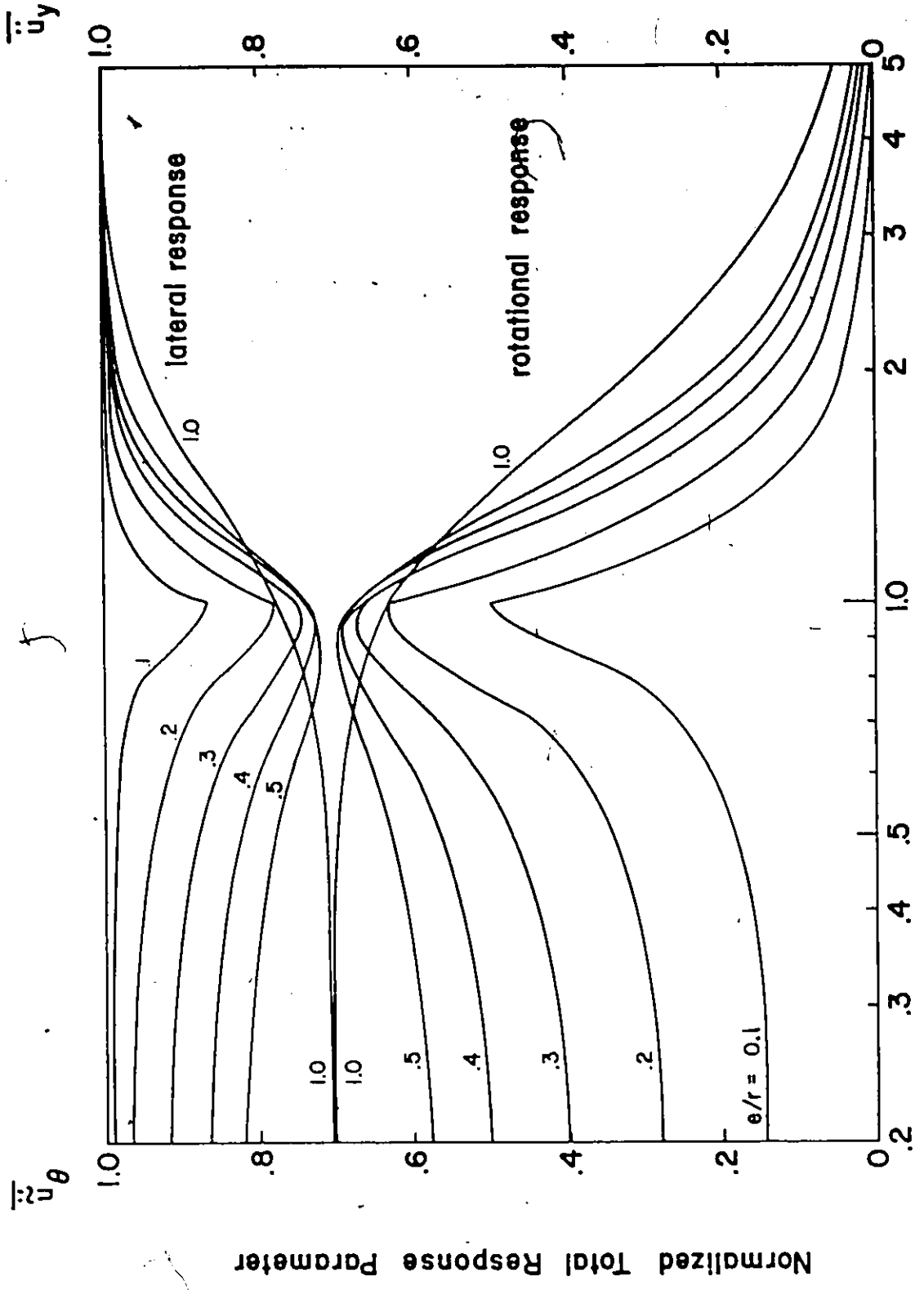

FIG. 2.5.a Variation of Normalized Total Response Parameters-Flat Spectrum

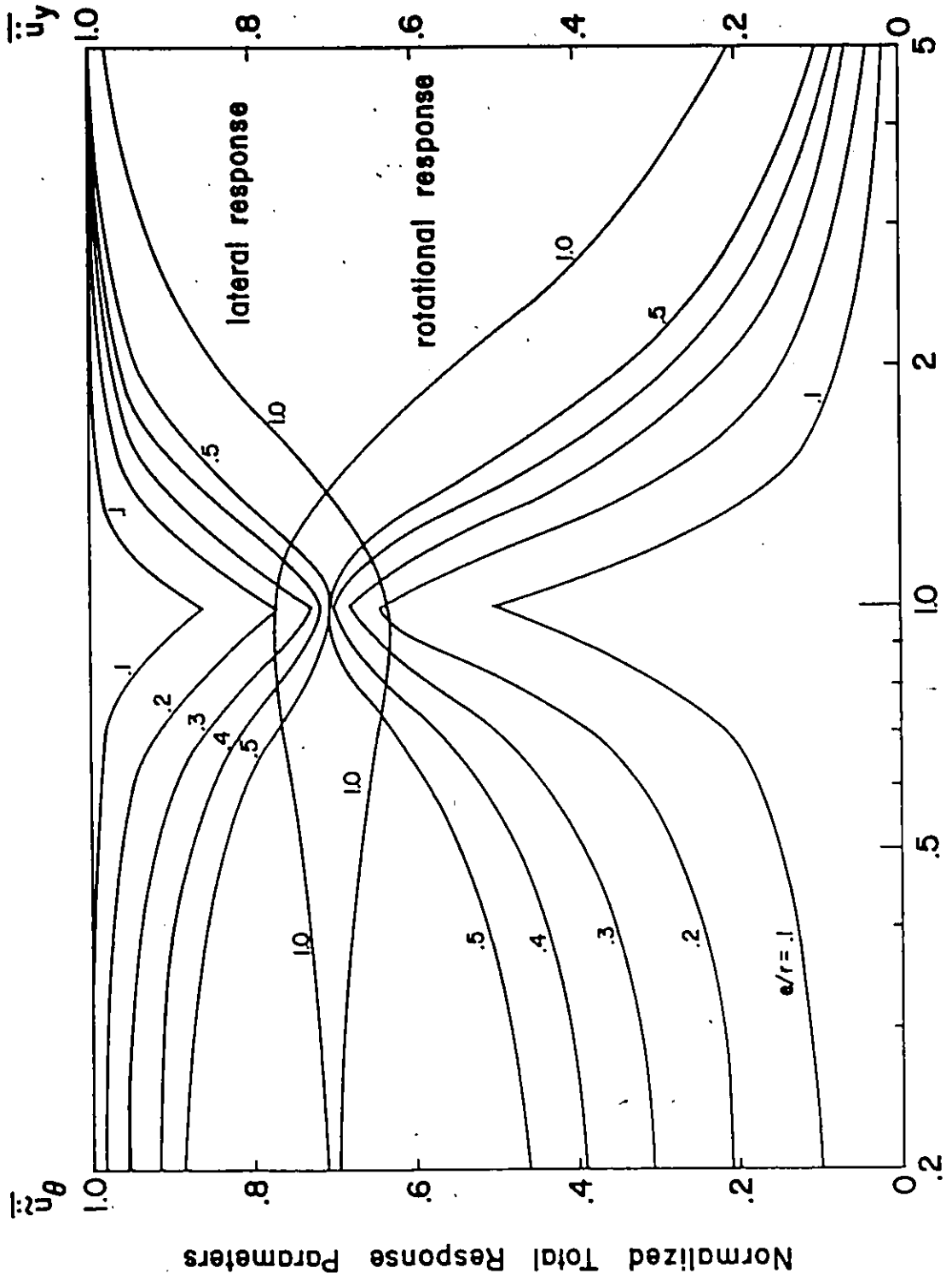

FIG. 2.5.b Variation of Normalized Total Response Parameters-Hyperbolic Spectrum

$$\ddot{\bar{u}}_y^2 + \ddot{\bar{u}}_\theta^2 = 1 \qquad (2.17)$$

It is obvious from this interaction equation that the coupled lateral acceleration response is less than the lateral acceleration computed by ignoring torsional coupling. Hence one may conclude that torsional coupling reduces the maximum lateral floor motion at the center of a torsionally coupled system.

2.3 Asymmetric Reactor Building Structure

One of the major steps in the seismic analysis is the construction of an appropriate analytical model to represent the physical structure. Basically, all dynamic models consist of masses and stiffness elements or springs. The degree of complexity of such a model will depend upon the extent of information to be obtained from the analysis. In any case, the model should closely simulate the expected dynamic behaviour of the real structure, yet be simple enough to allow any interpretation of results and economic computation. This requires careful evaluation of the assumption on which the model is based.

A commonly used analytical model is the discrete lumped mass system. In this case, all the mass of the physical structure is assumed to be concentrated at a finite number of locations on the structure, and structural elements between the lumped mass points, which provide the system stiffness, are considered weightless. The use of this lumped mass model permits development of a general matrix analysis (digital computer solution) which can be applied to structures of various types and configuration.

Most nuclear power plant structures are complex systems. They are asymmetric in plan, with heavy concrete slabs at the various floor elevators interconnected with numerous concrete shear walls or heavy cross-braced members. Here, asymmetry means the center of mass at the floor does not coincide with the center of rigidity of the same floor; furthermore, these mass centers and rigidity centers of different floors are not on the same vertical axis. These buildings, also, generally, have similar dimensions in height as in plan, that is, have an aspect ratio near to unity. Most of the literature on the subject of the dynamic analysis of power plant structures indicates it is common practice to model these structures as shear beam lateral load resisting elements.

2.3.1 Equations of Motion

The equations of motion for a lumped mass torsionally coupled system, with one axis of symmetry, subjected to base ground excitation $\ddot{u}_{gy}(t)$ may be expressed as

$$\underset{2n\times 2n}{\begin{bmatrix}[M] & [0]\\ [0] & [M]\end{bmatrix}}\underset{2n\times 1}{\begin{Bmatrix}\ddot{\underline{u}}_y\\ \ddot{\underline{u}}_\theta\end{Bmatrix}} + \underset{2n\times 2n}{\begin{bmatrix}[K_{yy}] & [K_{y\theta}]\\ [K_{y\theta}]^T & [K_{\theta\theta}]\end{bmatrix}}\underset{2n\times 1}{\begin{Bmatrix}\underline{u}_y\\ \underline{u}_\theta\end{Bmatrix}} = -\underset{2n\times 1}{\begin{Bmatrix}[M]\{1\}\ddot{u}_{gy}(t)\\ [M]\{r\}0\end{Bmatrix}} \quad (2.18)$$

in which

$$\underline{u}_y = \begin{Bmatrix}u_{y1}\\ u_{y2}\\ \vdots\\ u_{yn}\end{Bmatrix} \quad (2.19.a) \qquad \underline{u}_\theta = \begin{Bmatrix}r_1 u_{\theta 1}\\ r_2 u_{\theta 2}\\ \vdots\\ r_n u_{\theta n}\end{Bmatrix} \quad (2.19.b)$$

where r_j is the radius of gyration of the jth floor deck about a vertical axis through the center of mass; the mass sub-matrix is

$$[M] = \begin{bmatrix} m_1 & & & \\ & m_2 & & \\ & & \ddots & \\ & & & m_n \end{bmatrix} \tag{2.20}$$

where m_j is the lumped mass of floor "j"; the general form of the stiffness sub-matrix may be written as

$$[K_{yy}] = \begin{bmatrix} (K_{y1}+K_{y2}) & -K_{y2} & & & \\ -K_{y2} & (K_{y2}+K_{y3}) & -K_{y3} & & \\ & -K_{y3} & \ddots & & \\ & & & \ddots & -K_{yn} \\ & & & -K_{yn} & K_{yn} \end{bmatrix} \tag{2.21.a}$$

$$[K_{\theta\theta}] = \begin{bmatrix} \left(\frac{1}{r_1}\right)^2 (K_{\theta1}+K_{\theta2}) & -\frac{1}{r_1 r_2} K_{\theta2} & & & \\ -\frac{1}{r_1 r_2} K_{\theta2} & \left(\frac{1}{r_2}\right)^2 (K_{\theta2}+K_{\theta3}) & -\frac{1}{r_2 r_3} K_{\theta3} & & \\ & -\frac{1}{r_2 r_3} K_{\theta3} & \ddots & & \\ & & & \ddots & -\frac{1}{r_{n-1} r_n} K_{\theta n} \\ & & & -\frac{1}{r_{n-1} r_n} K_{\theta n} & \left(\frac{1}{r_n}\right)^2 (K_{\theta n}) \end{bmatrix} \tag{2.21.b}$$

$$[K_{y\theta}] = \begin{bmatrix} \frac{1}{r_1}(e_1K_{y1}+e_2K_{y2}) & -\frac{1}{r_2}e_2K_{y2} & & & \\ -\frac{1}{r_1}e_2K_{y2} & \frac{1}{r_2}(e_2K_{y2}+e_3K_{y3}) & -\frac{1}{r_3}e_3K_{y3} & & \\ & -\frac{1}{r_2}e_3K_{y3} & \cdot & & \\ & & \cdot & \cdot & -\frac{1}{r_n}e_nK_{yn} \\ & & & -\frac{1}{r_{n-1}}e_nK_{yn} & \frac{1}{r_n}e_nK_{yn} \end{bmatrix} \qquad (2.21.c)$$

where e_j is the static eccentricity for storey "j", K_{yi} and $K_{\theta j}$ are the stiffness of storey "j" in y translation and in torsion, respectively, and n is the number of masses.

Damping is introduced as viscous damping ratio ζ in each natural mode of vibration.

Equation (2.18) is the generalization of equation (2.1) for a multi-degree-of-freedom system consisting of n lumped masses representing the floors in which their centers of mass do not coincide with their centers of rigidity.

In dynamic analysis of structural response to earthquake ground motion it is usual to consider planar models along each of the two principal axis, and to analyse independently the response of each model to the in-plan horizontal component of ground motion. It is obvious that analysis on this basis is strictly valid only if the center of mass of floor "j" is coincident with the center of rigidity of storey "j" and this is true for every floor (j=1,2,...,n).

The coupled analysis of asymmetric structure requires solution of an eigenvalue problem of order 2n. The two coupled displacement vectors may be assumed to take the form

$$\begin{Bmatrix} \underline{u}_y \\ \underline{\tilde{u}}_\theta \end{Bmatrix} = \sum_{i=1}^{2n} \begin{Bmatrix} \underline{\phi}_{yi} \\ \underline{\tilde{\phi}}_{\theta i} \end{Bmatrix} T_i(t) \tag{2.22}$$

in which $T_i(t)$ represents the variation with time (t) for the ith mode of vibration and $[\underline{\phi}_{yi}, \underline{\phi}_{\theta i}]^T$ represent the coupled mode shapes for this mode of vibration.

The eigenvalue problem takes the form

$$\begin{bmatrix} [K_{yy}] - \omega^2[M] & [K_{y\theta}] \\ [K_{y\theta}]^T & [K_{\theta\theta}] - w^2[M] \end{bmatrix} \begin{Bmatrix} \underline{\phi}_y \\ \underline{\tilde{\phi}}_\theta \end{Bmatrix} = \begin{Bmatrix} \underline{\phi} \\ \underline{0} \end{Bmatrix} \tag{2.23}$$

and leads to the vibration frequencies ω_i and the coupled lateral-rotational mode shapes $\underline{\phi}_{yi}$ and $\underline{\tilde{\phi}}_{\theta i}$ subvectors of the mode shape $\underline{\phi}_i$, $(i=1,2,\ldots,2n)$.

In order to be able to evaluate the effect of coupling between lateral and torsional response, it is necessary to determine the uncoupled response as well. In the uncoupled case, the effect of eccentricities in equation (2.1) is ignored and the decoupled equations of motion take the form

$$[M]\ddot{\underline{u}}_y + [K_{yy}]\underline{u}_y = [M]\{1\}\ddot{u}_{gy}(t) \tag{2.24.a}$$

$$[M]\ddot{\underline{u}}_\theta + [K_{\theta\theta}]\underline{u}_\theta = 0 \tag{2.24.b}$$

The eigenvalue problems become

$$[[K_{yy}] - \omega_y^2[M]]\{\psi_y\} = 0 \tag{2.25.a}$$

$$[[K_{\theta\theta}] - \omega_\theta^2[M]]\{\tilde{\psi}_\theta\} = 0 \tag{2.25.b}$$

and lead to the uncoupled vibration frequencies ω_{yi}, $\omega_{\theta i}$ and the uncoupled lateral and rotational mode shapes ψ_{yi} and $\tilde{\psi}_{\theta i}$, (i=1,2,...,n).

2.3.2 Modal Participation Factors

The modal participation factor is a number developed from a mathematical expression which involves the mass, mode shapes and direction of the excitation of a system for the evaluation of the modal response of a particular mode of vibration (8). For the coupled analysis, both lateral modal participation factor and rotational modal participation factor, for each mode, may be determined.

Inserting equations (2.22) and (2.23) into equation (2.18) yields for the ith mode of vibration

$$\begin{bmatrix} [M] & [0] \\ [0] & [M] \end{bmatrix} \begin{Bmatrix} \underline{\phi}_{yi} \\ \underline{\tilde{\phi}}_{\theta i} \end{Bmatrix} \ddot{T}_i(t) + \omega_i^2 \begin{bmatrix} [M] & [0] \\ [0] & [M] \end{bmatrix} \begin{Bmatrix} \underline{\phi}_{yi} \\ \underline{\tilde{\phi}}_{\theta i} \end{Bmatrix} T_i(t) = \begin{Bmatrix} [M]\{1\}\ddot{u}_{gy}(t) \\ [M]\{r\}0 \end{Bmatrix} \tag{2.26}$$

in which

$$\{r\} = \begin{Bmatrix} r_1 \\ r_2 \\ \vdots \\ r_n \end{Bmatrix} \tag{2.27}$$

Premultiplying equation (2.26) by $\{\phi_{yi}\}^T\{\tilde{\phi}_{\theta i}\}^T$ and using the orthogonality-normality relationship given by

$$\{\phi_{yi}\}^T[M]\{\phi_{yi}\} + \{\tilde{\phi}_{\theta i}\}^T[M]\{\tilde{\phi}_{\theta i}\} = 1 \tag{2.28}$$

equation (2.26) takes the form

$$\ddot{T}_i(t) + \omega_i^2 T_i(t) = -\{\phi_{yi}\}^T[M]\{1\}\ddot{u}_{gy}(t) - \{\tilde{\phi}_{\theta i}\}^T[M]\{r\}0 \tag{2.29}$$

$\{\phi_{yi}\}^T[M]\{1\}$ is the lateral modal participation factor for mode i (Γ_{yi})
$\{\tilde{\phi}_{\theta i}\}^T[M]\{r\}$ is the rotational modal participation factor for mode i ($\Gamma_{\theta i}$)

The second term of the right hand side of equation (2.29) is usually ignored in the coupled analysis by introducing the input ground motion only in the lateral direction and assuming that no rotational input ground motion is occurring. Even though this term is zero in the analysis investigated in this chapter, it is of some interest to study the variation of the rotational modal participation factor through a numerical example (Section 2.4). It is believed that the concept of the rotational modal participation factor is a straight forward analogy to the well known concept of the lateral modal participation factor. This rotational modal participation factor may be used in the case of rotational input motion.

For the uncoupled analysis, the modal participation factor is determined using the same procedure described above. In this case, the orthogonality-normality relationship is expressed by

$$\{\psi_{yi}\}^T[M]\{\psi_{yi}\} = 1 \tag{2.30}$$

and the uncoupled modal participation factor Γ^u_{yi} can be calculated by

$$\Gamma^{u}_{yi} = \frac{\sum_j m_j \psi_{yij}}{\sum_j m_j \psi^2_{yij}} \tag{2.31}$$

2.3.3 Modal Response Factors and Modal Coupling Parameters

For the objectives of this study it is most appropriate to develop modal response factors to express the contribution of each mode in the total response of a specific mass m_j.

In the coupled analysis, the coupled modal response factors associated with the response parameters $(\ddot{u}_{yj}, \ddot{u}_{\theta j})$ of mass m_j are $\Gamma_{yi}\,\phi_{yij}$ and $\Gamma_{yi}\,\tilde{\phi}_{\theta ij}$, respectively.

The term $(\Gamma_{yi}\,\phi_{yij})$ is a direct measure of the coupled lateral response due to lateral input motion and the corresponding term $(\Gamma_{yi}\tilde{\phi}_{\theta ij})$ is the induced rotational modal response factor due to torsional coupling. Strong torsional coupling is associated with the modes contributing large values of rotational modal response factors.

In the uncoupled analysis, the modal response factors are $(\Gamma^{u}_{yi}\psi_{yij})$. The effect of torsional coupling on the modal lateral response can be studied by comparing the values of the uncoupled modal response factors $(\Gamma^{u}_{yi}\psi_{yij})$ to the corresponding coupled values $(\Gamma_{yi}\phi_{yij})$. These values of modal response factors have to be determined for each mass point. The large deviation between the uncoupled and the coupled modal response factors will be associated with the masses contributing major torsional coupling (large eccentricity between center of mass and rigidity). From the previous discussion one may conclude that these modal response factors, which can be measures of torsional coupling, are mode and mass dependent.

To express an overall modal coupling parameter to be a direct measure of torsional coupling in each mode of vibration, such modal coupling parameter has to be mode dependent only. The overall modal coupling parameters are the generalization of the response parameters associated with the single mass model studied in Section 2.2.

The overall modal coupling parameters expressing the relation between the coupled lateral response and the corresponding uncoupled response may be written in the form

$$(OMCP)_{yi} = \frac{\sum_{j=1}^{n} m_j \phi_{yij}^2}{\sum_{j=1}^{n} m_j \phi_{yij}^2 + \sum_{j=1}^{n} m_j r_j^2 \phi_{\theta ij}^2} \tag{2.32}$$

The $(OMCP)_{yi}$ are analogies to the lateral modal response parameters $\frac{\alpha_{yi}^2}{\alpha_{yi}^2 + \tilde{\alpha}_{\theta i}^2}$ of the single mass model (Figures 2.3.a and 2.3.b).

The overall modal coupling parameters expressing the relation between the induced rotational response, due to coupling, and the uncoupled lateral response takes the form

$$(OMCP)_{\theta i} = \frac{\sum_{j=1}^{n} m_j \phi_{yij} r_j \phi_{\theta ij}}{\sum_{j=1}^{n} m_j \phi_{yij}^2 + \sum_{j=1}^{n} m_j r_j^2 \phi_{\theta ij}^2} \tag{2.33}$$

The $(OMCP)_{\theta i}$ are analogies to the rotational modal response parameters $\frac{\alpha_{yi} \tilde{\alpha}_{\theta i}}{\alpha_{yi}^2 + \tilde{\alpha}_{\theta i}^2}$ of the single mass model (Figures 2.4.a and 2.4.b).

2.4 Numerical Example - CANDU 600 Reactor Building

The planar mathematical model of the CANDU reactor building, provided by AECL*, consists of 13 mass points representing the internal structure, containment wall and concrete vault (Figure 2.6). The internal structure consists of walls and floors. In addition to the wall supporting elements, shielding walls are also present. A typical structural plan for the CANDU reactor building is shown in Figure 2.7. It is clear from the orientation of the structural elements that the building plan can be considered to have one axis of symmetry (BD-axis). The stick model considers the internal structure as a multi-mass system connected by springs representing the inter-storey lateral stiffness.

In this study, the torsional degree of freedom for each mass point is included in the analysis and an uncoupled lateral-torsional model (ULTM) is developed. The inter-storey torsional stiffnesses are computed and represented by torsional springs connecting the multi-mass system.

Taking into consideration the effect of eccentricities between the center of mass and rigidity for each floor level of the uncoupled model, a more sophisticated coupled lateral-torsional model (CLTM) is presented. The purpose of analysing the two models (ULTM and CLTM) is to evaluate the effect of torsional coupling on the dynamic properties of the CANDU reactor building.

---

*Atomic Energy of Canada Limited.

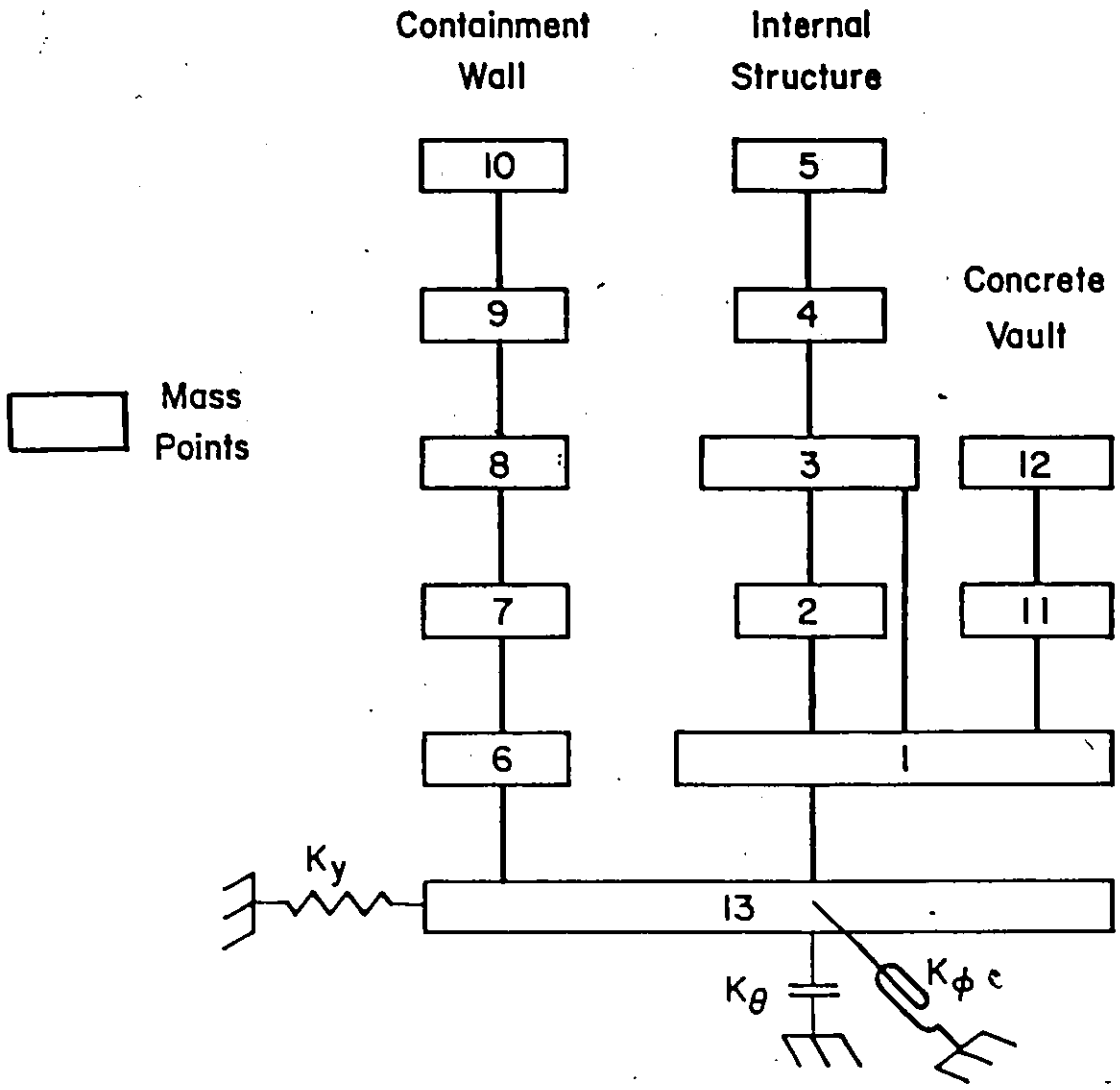

FIG. 2.6 Stick Lumped Mass Model for Example Reactor Building

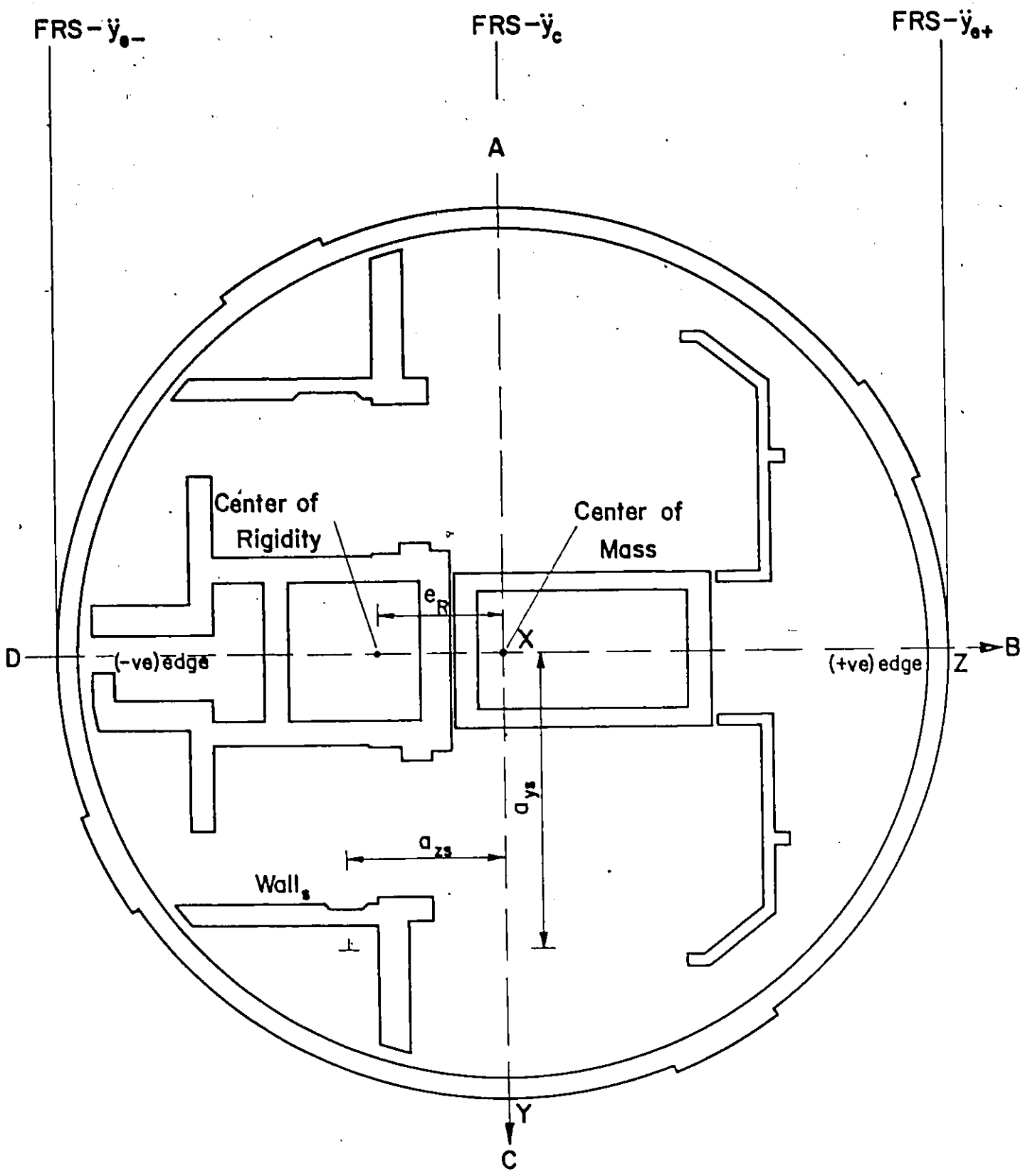

FIG. 2.7 Structural Plan for a Typical CANDU Reactor Building

2.4.1 Uncoupled Lateral-Torsional Model (ULTM)

In modelling, it is necessary to include as much as possible the essential characteristics of the stiffness and mass distribution while at the same time developing a model which is simple enough for easy interpretation of the results. A compromise is usually necessary in order to optimize both these objectives.

To reveal the torsional effect about the vertical axis of the reactor building, the floor is assumed to behave like a diaphragm rigid in its own plane and with two degrees of freedom, one translational and one torsional. A parametric study of the reactor building's behaviour shows that the flexibility of the walls is controlled by the shear deformation; therefore the warping torsional effect can be neglected and the St. Venant torsional stiffness may be estimated by

$$\overline{GJ} = \sum_{s} (GJ_s + a_{zs}^2\, GA_{ys} + a_{ys}^2\, GA_{zs}) \qquad (2.34)$$

in which GA_{ys} and GA_{zs} are the shear stiffnesses in the y and z directions respectively. GJ_s is the St. Venant torsional stiffness and (a_{ys}, a_{zs}) are the coordinate position of the wall "s". The torsional mass moment of inertia (IM_T) is computed assuming that each floor is acting as circular disc.

The mathematical model is shown in Figure 2.8.a and the physical and geometric properties of the elements are given in Table 2.1 and 2.2, respectively. The soil spring constants are assumed to be ∞ as the structure is considered to be totally fixed to its foundation.

The ULTM is analysed using SAP IV computer programme (3) and the dynamic properties are determined for the first 12 modes of vibration.

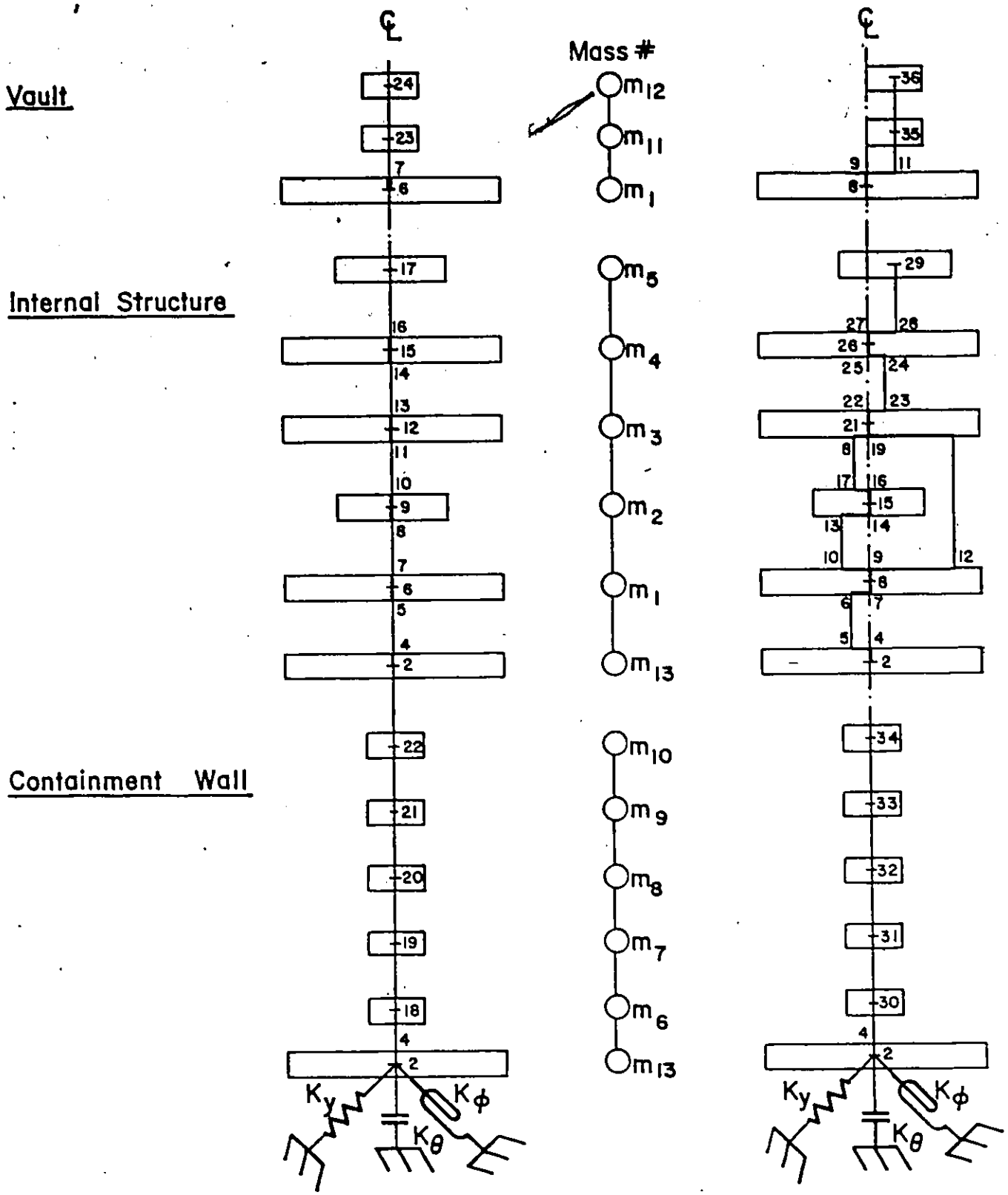

(a) Uncoupled Lateral Torsional Model

(b) Coupled Lateral Torsional Model

FIG. 2.8 Mathematical Models for Reactor Building

Table 2.1: Physical Properties of the 13-Mass Model

	Mass No.	Node No. ULTM	Node No. CLTM	$M_{A/C}$ K. sec^2/ft	IM_T K. sec^2/ft	e_M (ft)
Vault	m_{12}	24	36	67.42	--	+13.50
	m_{11}	23	35	128.14	--	+13.50
Internal Structure	m_5	17	29	147.97	385,840	+13.50
	m_4	15	26	246.86	469,600	--
	m_3	12	21	138.41	500,780	--
	m_2	9	15	244.57	438,070	--
	m_1	6	8	682.24	1,779,900	--
Containment Wall	m_{10}	22	34	716.77	1,677,000	--
	m_9	21	33	208.93	--	--
	m_8	20	32	208.93	--	--
	m_7	19	31	208.93	--	--
	m_6	18	30	174.11	--	--
	m_{13}	2	2	926.15	4,100,000	--

ULTM : Uncoupled Lateral Torsional Model

CLTM : Coupled Lateral-Torsional Model

$M_{A/C}$: Mass in Direction A/C

IM_T : Torsional Mass Moment of Inertia (I_X)

e_M : Eccentricity of Center of Mass

Table 2.2: Geometrical Properties of Structural Elements

	Location			Area (ft^2)	$A_{A/C}$ (ft^2)	Length (ft^2)	$I_{B/D}$ (ft^4)	J (ft^4)	e_R (ft)
		ULTM	CLTM						
Vault	m_{12}-m_{11}	24-23	36-35	211.3	211.3	29.16	37,986	129,103	+13.50
	m_{11}-m_{11}	23- 7	35-11	211.3	211.3	19.75	31,514	129,103	+13.50
Internal Structure	m_5 -m_4	17-16	29-28	564.0	144.9	23.75	34,253	224,300	+13.50
	m_4 -m_3	14-13	24-23	1293.0	1293.0	13.25	1,220,757	2,721,910	+ 8.00
	m_3 -m_2	11-10	18-17	952.0	952.0	14.00	1,749,524	2,022,018	- 7.95
	m_2 -m_1	8 - 7	13-10	1446.7	1446.7	20.50	193,298	4,150,000	-22.30
	m_3 -m_1	11- 7	30-12	221.0	221.0	40.00	3,069	40,277	+38.75
	m_1 -m_{13}	5 - 4	6 - 5	2485.4	2485.4	14.50	482,047	4,150,000	-11.00
Containment Wall	m_{10}-m_9	22-21	34-33	1534.0	813.0	30.00	3,733,600	7,467,200	--
	m_9 -m_8	21-20	33-32	1534.0	813.0	30.00	3,733,600	7,467,200	--
	m_8 -m_7	20-19	32-31	1534.0	813.0	30.00	3,733,600	7,467,200	--
	m_7 -m_6	19-18	31-30	1534.0	813.0	30.00	3,733,600	7,467,200	--
	m_6 -m_{13}	18- 4	30- 4	1534.0	813.0	20.00	3,733,600	7,467,200	--

$A_{A/C}$ = Shear Area in Direction A/C

$I_{B/D}$ = Moment of Inertia about BD-Axis (I_z)

J = Torsional Moment of Inertia (I_o)

e_R = Eccentricity of Center of Rigidity

NOTE: Structural elements not included in the table are considered as rigid members.

2.4.2 Coupled Lateral-Torsional Model (CLTM)

From the typical structural plan of the CANDU reactor building shown in Figure 2.7, it is clear that the internal structure is made up of an asymmetrically arranged grouping of walls located in a particular fashion and forming an asymmetric structural system with one axis of symmetry (BD axis). Hence, the translational motion along the AC axis and the torsional motion are coupled.

Assuming the coordinate X-axis, positive upwards, is located at the center of the building, which coincides with the center of mass of the typical floor; the location of the center of rigidity of each floor may be estimated by

$$e_R = \frac{\sum_s a_{zs} GA_{ys}}{\sum_s GA_{ys}} \qquad (2.35)$$

Taking into consideration the effect of eccentricities between the center of mass and of rigidity for each floor level, the CLTM is developed for the same physical and geometrical properties of the ULTM and a detailed coupled dynamic analysis is investigated. The CLTM is shown in Figure 2.8.b and the eccentricities are given in Tables 2.1 and 2.2. The coupled dynamic properties are computed for the first 12 modes of vibration.

2.4.3 Effect of Torsional Coupling on Dynamic Properties

The natural frequencies (f_i) and the modal participation factors Γ_{yi} and $\Gamma_{\theta i}$ of the reactor building structure are given in Table 2.3.

Table 2.3: Natural Frequencies and Modal Participation Factors

	ULTM			CLTM		
Mode	Frequency (Hz)	Γ_{yi}	$\Gamma_{\theta i}$	Frequency (Hz)	Γ_{yi}	$\Gamma_{\theta i}$
1	4.94	35.44	---	4.94	35.44	---
2	5.82	27.96	---	5.78	28.03	83
3	10.00	11.04	---	9.97	11.12	86
4*	10.65	---	1043	10.68	0.41	1040
5*	14.20	---	1297	14.20	---	1297
6	16.29	10.98	---	16.25	10.93	16
7	18.24	15.78	---	18.24	15.78	---
8*	19.66	---	1337	19.18	8.42	1278
9	23.88	28.15	---	24.40	23.13	649
10	27.89	12.92	---	27.74	12.44	436
11	28.69	6.57	---	28.69	6.57	179
12	29.46	1.31	---	29.40	1.90	67

*Torsional mode of vibration

The modal response factors for the internal structure, containment wall and concrete vault are given in Tables 2.4.2, 2.4.b and 2.4.c respectively.

The overall modal coupling parameters are shown in Table 2.5. The corresponding values of the uncoupled model are also given with the objective of evaluating such modal coupling parameters.

Mass j / Mode i	m_1			m_2			m_3			m_4			m_5		
	ULTM	CLTM		ULTM	CLTM		ULTM	CLTM		ULTM	CLTM		ULTM	CLTM	
	$r^{u}_{yi\phi yij}$	$r_{yi\phi yij}$	$r_{yi\phi\theta ij}$	$r^{u}_{yi\phi yij}$	$r_{yi\phi yij}$	$r_{yi\phi\theta ij}$	$r^{u}_{yi\phi yij}$	$r_{yi\phi yij}$	$r_{yi\phi\theta ij}$	$r^{u}_{yi\phi yij}$	$r_{yi\phi yij}$	$r_{yi\phi\theta ij}$	$r^{u}_{yi\phi yij}$	$r_{yi\phi yij}$	$r_{yi\phi\theta ij}$
1	--	--	--	0.0002	0.0002	--	0.0003	0.0003	--	0.0004	0.0004	--	0.0007	0.0007	--
2	0.0711	0.0733	0.000282	0.3771	0.3839	0.000736	0.6797	0.6830	0.001003	0.9355	0.9344	0.001017	1.729	1.729	0.001327
3	0.0210	0.0233	0.000210	0.0157	0.0164	0.000195	0.0068	0.0074	0.000200	0.0266	0.0286	0.000224	0.1500	0.1520	0.000736
4	--	0.0002	0.000027	--	0.0003	0.000060	--	--	0.000102	--	0.0007	0.000129	--	0.0003	0.000634
5	--	--	--	--	--	--	--	--	--	--	--	--	--	--	--
6	0.0585	0.0573	0.000039	0.2109	0.2111	0.000073	0.3088	0.3055	0.000265	0.3662	0.3644	0.000515	0.6278	0.6241	0.000611
7	--	--	0.000001	--	--	0.000001	--	--	0.000002	--	--	0.000002	0.0001	0.0001	0.000001
8	--	0.0503	0.002375	--	0.0837	0.004406	--	0.0534	0.006227	--	0.0052	0.000653	--	0.0344	0.004241
9	0.5932	0.4180	0.002455	0.8144	0.5463	0.004900	0.3606	0.1905	0.009398	0.1423	0.1460	0.010820	0.6606	0.4408	0.003427
10	0.0054	0.0056	0.000469	0.0144	0.0202	0.000247	0.0316	0.0288	0.000171	0.0314	0.0235	0.000213	0.0912	0.0694	0.000049
11	--	--	--	--	--	--	--	--	0.000001	--	--	0.000001	--	--	--
12	0.0062	0.0079	0.000078	0.0191	0.0305	0.000112	0.0100	0.0161	0.000220	0.0001	0.0004	0.000272	0.0178	0.0366	0.000954

Table 2.4.a Modal Response Factors - Internal Structure

Mass j / Mode i	m_6			m_7			m_8			m_9			m_{10}		
	ULTM	CLTM		ULTM	CLTM		ULTM	CLTM		ULTM	CLTM		ULTM	CLTM	
	$\Gamma^u_{yi}\phi_{yij}$	$\Gamma_{yi}\phi_{yij}$	$\Gamma_{yi}\phi_{\theta ij}$	$\Gamma^u_{yi}\phi_{yij}$	$\Gamma_{yi}\phi_{yij}$	$\Gamma_{yi}\phi_{\theta ij}$	$\Gamma^u_{yi}\phi_{yij}$	$\Gamma_{yi}\phi_{yij}$	$\Gamma_{yi}\phi_{\theta ij}$	$\Gamma^u_{yi}\phi_{yij}$	$\Gamma_{yi}\phi_{yij}$	$\Gamma_{yi}\phi_{\theta ij}$	$\Gamma^u_{yi}\phi_{yij}$	$\Gamma_{yi}\phi_{yij}$	$\Gamma_{yi}\phi_{\theta ij}$
1	0.1324	0.1324	--	0.3704	0.3704	--	0.6358	0.6358	--	0.9065	0.9065	--	1.162	1.162	--
2	--	--	--	0.0001	0.0001	--	0.0002	0.0002	--	0.0003	0.0003	--	0.0004	0.0004	--
3	--	--	--	--	--	--	--	--	--	--	--	--	--	--	0.000001
4	--	--	--	--	--	--	--	--	--	--	--	--	--	--	--
5	--	--	--	--	--	--	--	--	--	--	--	--	--	--	--
6	--	--	--	--	--	--	--	--	--	--	--	0.000001	--	--	0.000001
7	0.3169	0.3169	--	0.06521	0.6521	--	0.6582	0.6583	--	0.3234	0.3234	--	0.2058	0.2058	--
8	--	--	0.000004	--	--	0.000001	--	--	0.000002	--	--	0.000005	--	--	0.000008
9	0.0002	0.0002	0.000010	--	0.0001	0.000006	0.0001	--	0.000002	0.0002	0.0001	0.000002	--	--	0.000006
10	--	--	--	--	--	--	--	--	--	--	--	--	--	--	--
11	0.1530	0.1529	--	0.3049	0.3048	--	0.2092	0.2091	--	0.0205	0.0205	--	0.1207	0.1207	--
12	--	--	--	--	--	--	--	--	--	--	--	--	--	--	--

Table 2.4.b Modal Response Factors - Containment Wall

Mass j / Mode i	m_{11}			m_{12}		
	ULTM	CLTM		ULTM	CLTM	
	$\Gamma^{u}_{yi}\psi_{yij}$	$\Gamma_{yi}\phi_{yij}$	$\Gamma_{yi}\phi_{\theta ij}$	$\Gamma^{u}_{yi}\psi_{yij}$	$\Gamma_{yi}\phi_{yij}$	$\Gamma_{yi}\phi_{\theta ij}$
1	0.0001	0.0001	--	0.0003	0.0003	--
2	0.2290	0.2332	0.000282	0.4657	0.4670	0.000282
3	0.4126	0.4180	0.000210	1.194	1.199	0.000210
4	--	0.0005	0.000027	--	0.0026	0.000027
5	--	--	--	--	--	--
6	0.0168	0.0155	0.000039	0.1986	0.1962	0.000039
7	--	--	0.000001	--	--	0.000001
8	--	0.0693	0.002376	--	0.0960	0.002376
9	1.246	0.9648	0.002457	1.2410	0.9381	0.002457
10	0.2069	0.1773	0.000469	0.1424	0.1189	0.000469
11	0.0006	0.0005	--	0.0004	0.0003	--
12	0.1019	0.1433	0.000078	0.0548	0.0766	0.000078

Table 2.4.c: Modal Response Factors - Concrete Vault

Mode	ULTM		CLTM		
	$\sum_j m_j \psi_{yij}^2$	$\sum_j m_j r_j^2 \psi_{\theta ij}^2$	$\sum_j m_j \phi_{yij}^2$	$\sum_j m_j r_j^2 \phi_{\theta ij}^2$	$\sum_j m_j r_j \phi_{\theta ij} \phi_{yij}$
1	1.0	-	1.0	--	--
2	1.0	-	0.9974	0.0026	0.0469
3	1.0	-	0.9972	0.0028	0.0058
4*	-	1.0	0.0038	0.9962	0.0046
5*	-	1.0	--	1.0	--
6	1.0	-	0.9974	0.0026	0.0460
7	1.0	-	1.0	--	--
8*	-	1.0	0.0740	0.9260	0.1412
9	1.0	-	0.7663	0.2337	0.0934
10	1.0	-	0.9302	0.0698	0.0047
11	1.0	-	1.0	--	--
12	1.0	-	0.9787	0.0213	0.0158

Table 2.5: Overall Modal Coupling Parameters

The results of this analysis indicate that the following observations can be made:

1. The twelve modes of vibration taken into consideration consist of nine translational modes and three torsional modes (4, 5 and 8).
2. Comparing the uncoupled frequencies to the corresponding coupled ones shows an increase in some frequencies, a decrease in others and four modes (1, 5, 7 and 11) have identical uncoupled and coupled frequencies. These modes also have identical uncoupled and coupled modal participation factors. Hence one may conclude that these four modes (1, 5, 7 and 11) are not affected by torsional coupling. This conclusion can be drawn directly as these four modes represent the modes of vibration of the symmetrical containment building.
3. Even though the third mode (1st mode of vault vibration) is relatively close to the fourth mode (torsional mode) no major coupling occurs and a similar observation can be made for the seventh mode which is closer to the eighth mode than the ninth. Torsional coupling affects only the lateral modes representing the modes of vibration of the internal structure.
4. The variation of the uncoupled modal response factors versus the coupled values ($\Gamma^{u}_{yi}\psi_{yij} \rightarrow \Gamma_{yi}\phi_{yij}$), for the internal components of the reactor system, is significant for some modes of vibration. The largest variation is associated with the ninth mode. Such variation vanishes for the containment wall (symmetrical structure).
5. The rotational modal response factors ($\Gamma_{yi}\phi_{\theta ij}$) vary significantly through the twelve modes of vibration taken into consideration. The peak values are due to modes eight and nine, and this is true for

all the masses of the mathematical model. These induced modal response factors are most pronounced in the internal structure (m_1,m_2,m_3,m_4 and m_5).

6. The effect of torsional coupling may be investigated by considering the relative values of the uncoupled modal response factors to the coupled modal response factors ($\Gamma^u_{yi}\psi_{yij}/\Gamma_{yi}\phi_{yij}$). These parameter ratios are mass and mode dependent (Tables 2.4.a, 2.4.b and 2.4.c). With the objective of defining the number of modes to be taken into consideration in studying the torsional effect, an overall modal coupling parameter (OMCP) is proposed. The overall modal coupling parameters are mode dependent only (Table 2.5). The variation of the overall modal coupling parameters in addition to the variation of the modal participation factors with the modes of vibration enable one to determine the number of modes which must be taken into consideration in the coupled response analysis.

7. The overall modal coupling parameters give a more complete picture of the effect of torsional coupling on the dynamic characteristics of the example reactor building. Examining these values one may conclude that modes (1, 7 and 11) are uncoupled lateral modes of vibration ($\sum_j m_j\phi^2_{yij}=1.0$) and mode (5) is an uncoupled rotational one ($\sum_j m_j r_j^2\phi^2_{\theta ij}=1.0$). It may be concluded also that strong torsional coupling occurs between the rotational mode 8 and the lateral mode 9; the $(OMCP)_{\theta i}$ associated with these modes of vibration (0.1412 and 0.0934, respectively) are the largest values of the twelve modal coupling parameters determined in this analysis.

CHAPTER III

SEISMIC FLOOR RESPONSE SPECTRA FOR A TORSIONALLY COUPLED REACTOR BUILDING

3.1 Introduction

It is shown in Chapter II that for a torsionally coupled structural system with one axis of symmetry, the lateral and rotational motions are coupled if the centers of mass and rigidity do not coincide and the dynamic properties would be composed of both translational and rotational components. In this chapter, these coupled dynamic properties are used to obtain the overall floor response parameters of interest. For the coupled analysis, the parameters of interest are the lateral floor acceleration at the center of the building and the rotational floor acceleration. These resulting floor accelerations are used to generate the extreme edge floor motions. Each floor motion time history is then used to determine the floor response spectra.

In order to be able to evaluate the effect of torsional coupling on floor response spectra, the uncoupled floor response parameters are also generated. By comparing the coupled floor spectra to the corresponding uncoupled spectra, one may develop guidelines to define situations for which a detailed coupled analysis is required.

3.2 Seismic Response of a Torsionally Coupled Reactor Building

Following the analysis procedure of Section 2.3.2, by introducing the viscous damping factor ζ, expressed as a fraction of critical

damping and assumed to be the same in each mode of vibration, the damped modal equation of motion is written as

$$\ddot{T}_i(t) + 2\zeta\omega_i \dot{T}_i(t) + \omega_i^2 T_i(t) = -\Gamma_{yi} \ddot{u}_{gy}(t) \qquad (3.1)$$

in which

$$\Gamma_{yi} = \{\phi_{yi}\}^T [M]\{1\}$$

is the ith modal participation factor in y-direction.

Equation (3.1) can then be solved by numerical integration (25) to determine the response in mode "i"; the modal responses can then be superimposed using equation (2.22) to determine the overall system response.

For the coupled analysis the response parameter of interest, in this study, are the lateral floor acceleration $\ddot{u}_{yc}(t)$ and the rotational floor acceleration $\ddot{u}_{\theta}(t)$.

These floor acceleration response parameters are due to the contribution of the coupled modes of vibration (i=1,2,...,2n). In order to be able to evaluate the effect of torsional coupling, it is necessary to determine the uncoupled response as well. In the corresponding uncoupled analysis the seismic response is expressed by the uncoupled floor acceleration $\ddot{u}_{yu}(t)$.

The characteristics of the floor motion can be identified by the frequency content and the peak amplitudes. In the coupled analysis the peak amplitude of the lateral and rotational floor motions are directly related to the coupled modal response factors $\Gamma_{yi}\phi_{yij}$ and $\Gamma_{yi}\phi_{\theta ij}$,

respectively. The frequency content of the lateral motion consists of the coupled natural frequencies (ω_i, i=1,2,...,2n) which contribute to the total acceleration response. The rotational motion is induced due to coupling between torsional modes and lateral modes of vibration. The frequency content of such motion consists mainly of one or two frequencies associated with the strong coupling between lateral and torsional motions.

In the uncoupled analysis, the peak amplitudes of the lateral floor motion are associated with the uncoupled modal response factors $\Gamma^u_{yi}\psi_{yij}$. The frequency content, in this case, consists of the uncoupled natural frequencies (ω_{yi}, i=1,2,...,n).

The effect of torsional coupling on floor motions may be expressed by comparing the coupled modal response factors ($\Gamma_{yi}\phi_{yij}$) to the corresponding uncoupled ones ($\Gamma^u_{yi}\psi_{yij}$), which influence the peaks' amplitude, and also by comparing the coupled frequencies (ω_i, i=1,2,...,2n) to the uncoupled ones (ω_{yi}, i=1,2,...,n) which contribute to the frequency content of each motion, respectively.

The influence of torsional coupling on floor motion time histories is better presented by the transformation of such floor motions from the time domain to the frequency domain. The transformation can be conducted by the generation of floor response spectra.

3.3 Generation of Floor Response Spectra

Most commonly, the floor response spectrum is developed using the time history approach. In the coupled analysis, two floor motions are generated: lateral motion and rotational motion. The rotational

floor response spectrum can be obtained by applying the rotational floor motion to a series of torsional single degree of freedom oscillators and plotting their maximum rotational responses as a function of their natural periods for a particular level of damping.

Due to torsional effects, floor response spectra may be generated for more than one location on any floor level.

Considering the edges* as extreme cases, the edge floor spectra are determined using the edge lateral floor motion obtained by

$$\ddot{u}_{ye_{\pm}}(t) = \ddot{u}_{yc}(t) \pm a\,\ddot{u}_{\theta}(t) \qquad (3.2)$$

in which $\ddot{u}_{ye}(t)$ is the edge lateral floor motion, $\ddot{u}_{yc}(t)$ is the centroidal lateral floor motion, $\ddot{u}_{\theta}(t)$ is the rotational floor acceleration and "a" is the horizontal distance from the center of the building to its edge.

In order to evaluate the effect of torsional coupling on lateral floor response spectra, the uncoupled floor response $\ddot{u}_{yu}(t)$ is also used to generate the uncoupled floor spectrum, and the following four cases are investigated:

(a) FRS $\ddot{y}_u$: uncoupled floor response spectrum

(b) FRS $\ddot{y}_c$: centroidal coupled floor response spectrum

(c) FRS $\ddot{y}_{e+}$: (+ve) edge floor response spectrum

(d) FRS $\ddot{y}_{e-}$: (-ve) edge floor response spectrum

3.4 Floor Response Spectra for a Typical CANDU Reactor Building

Using the 1940 El Centro W-E earthquake (normalized to a maximum acceleration of 0.2 g) as input ground motion, and assuming a constant

---

*The positive edge is on the right hand side of the floor plan (see Figure 2.7).

structural damping factor of 0.05, the dynamic response of the uncoupled and coupled mathematical models are computed incorporating the first twelve normal modes. The resulting uncoupled lateral floor motion and the coupled lateral-rotational floor motions are obtained at different floor levels of the reactor building. The corresponding edge lateral floor motions are generated to evaluate the effect of torsion.

These floor motion time histories are then used to develop the floor response spectra. The secondary damping used is assumed to be one percent.

The 1940 El Centro W-E ground response spectrum is shown in Figure 3.1. The lateral floor spectra for the internal structure (m_1, m_2, m_3, m_4 and m_5) are given in Figures 3.2 to 3.6 respectively and the corresponding rotational floor spectra are shown in Figure 3.7.

3.5 Discussion of Results

The results of the analysis conducted on the example reactor building indicate that the following observations can be made:

1. The uncoupled floor spectra peaks are always higher than the coupled spectra ones, except for the period range (0.08 - 0.16) and this is true for all five floor levels of the internal structure (m_1, m_2, m_3, m_4 and m_5). This period range (0.08 - 0.16) is associated predominantly with modes 2, 3 and 4. The variation of the uncoupled and coupled floor spectra ordinates is due to the variation of the corresponding modal response factors ($\Gamma^u_{yi}\psi_{yij}$, $\Gamma_{yi}\phi_{yij}$) and to the frequency change of the two models. It is clear from Table 2.4.a that the coupled model produces larger values of modal response factors for modes 2, 3 and 4. It seems also that coupling does have the effect of broad-

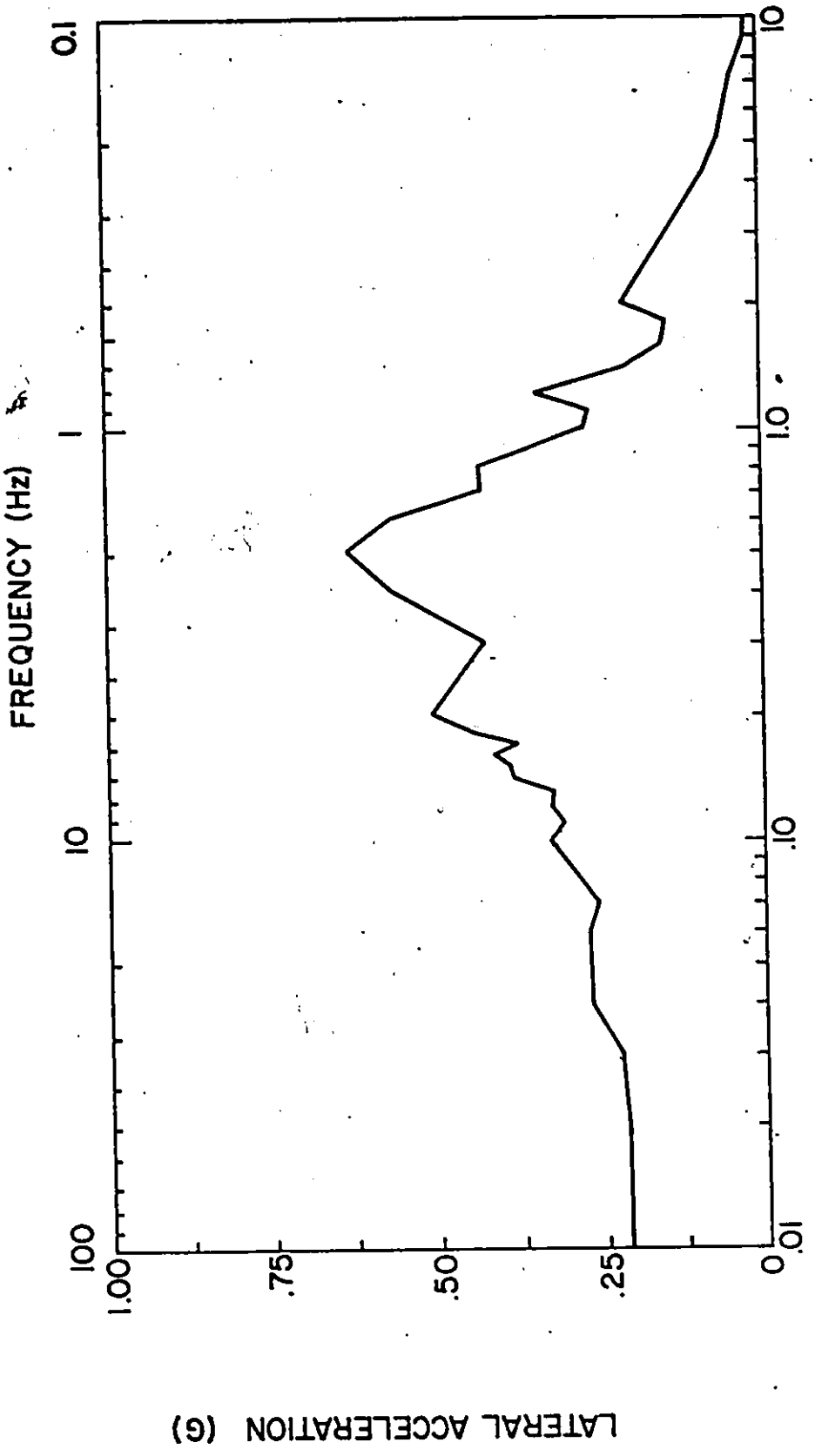

FIG. 3.1 Ground Response Spectrum — 1940 El Centro W-E (5% Damping)

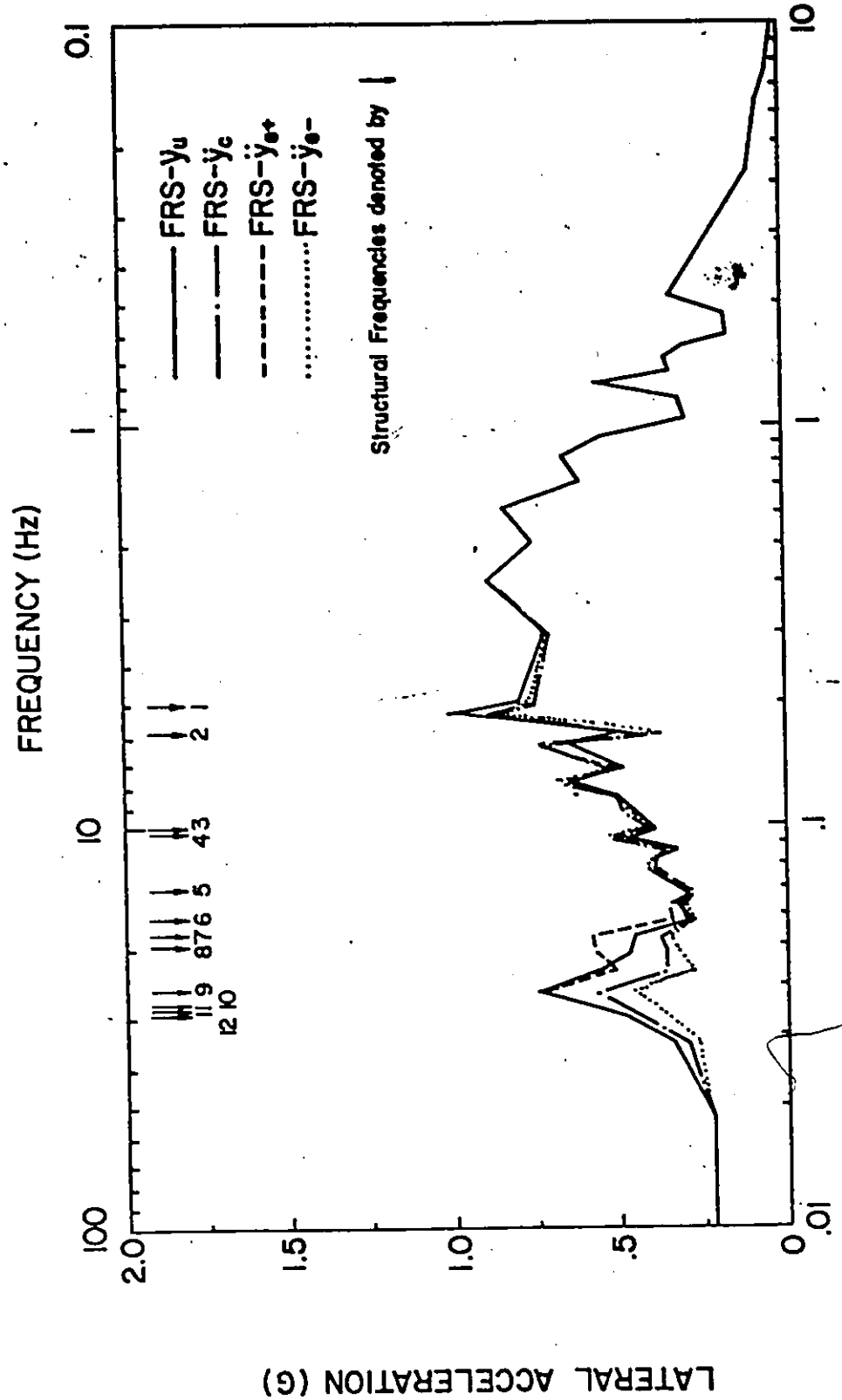

FIG. 3.2 Lateral Floor Response Spectra - Mass M_1 - 1940 El Centro W-E (1% Damping)

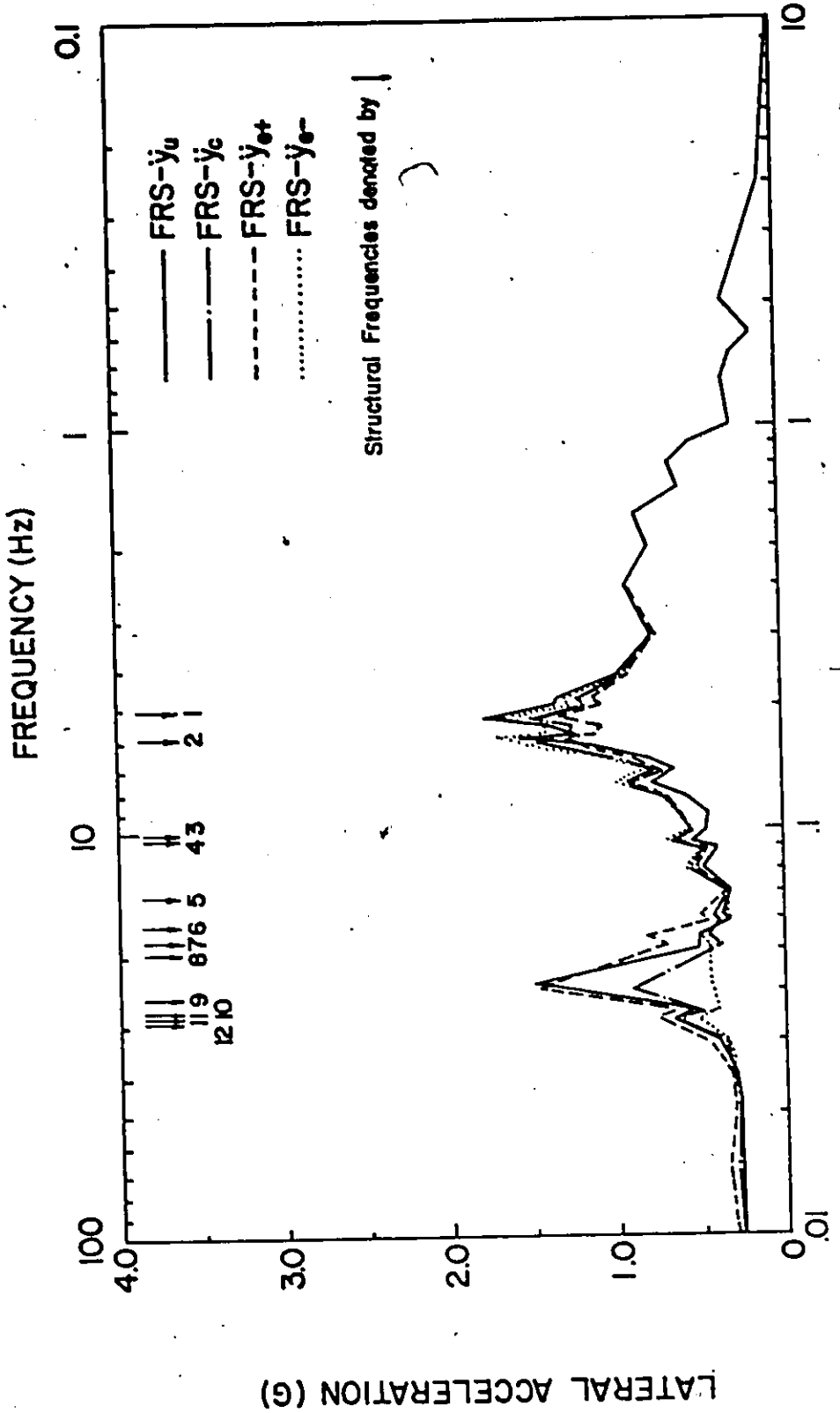

FIG. 3.3 Lateral Floor Response Spectra - Mass M_2 - 1940 El Centro W-E
(1% Damping)

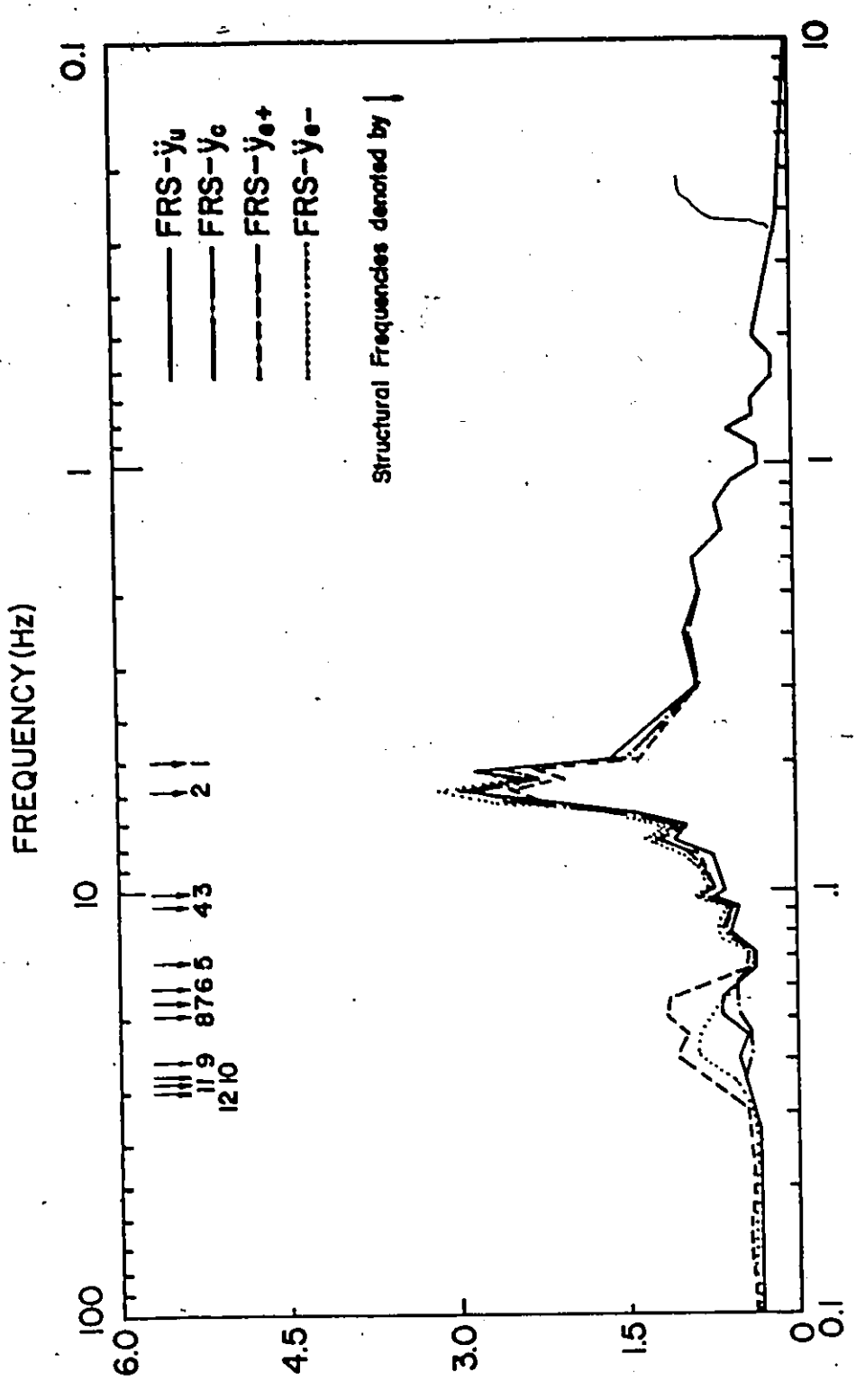

FIG. 3.4 Lateral Floor Response Spectra - Mass M_3 - 1940 El Centro N-E (1% Damping)

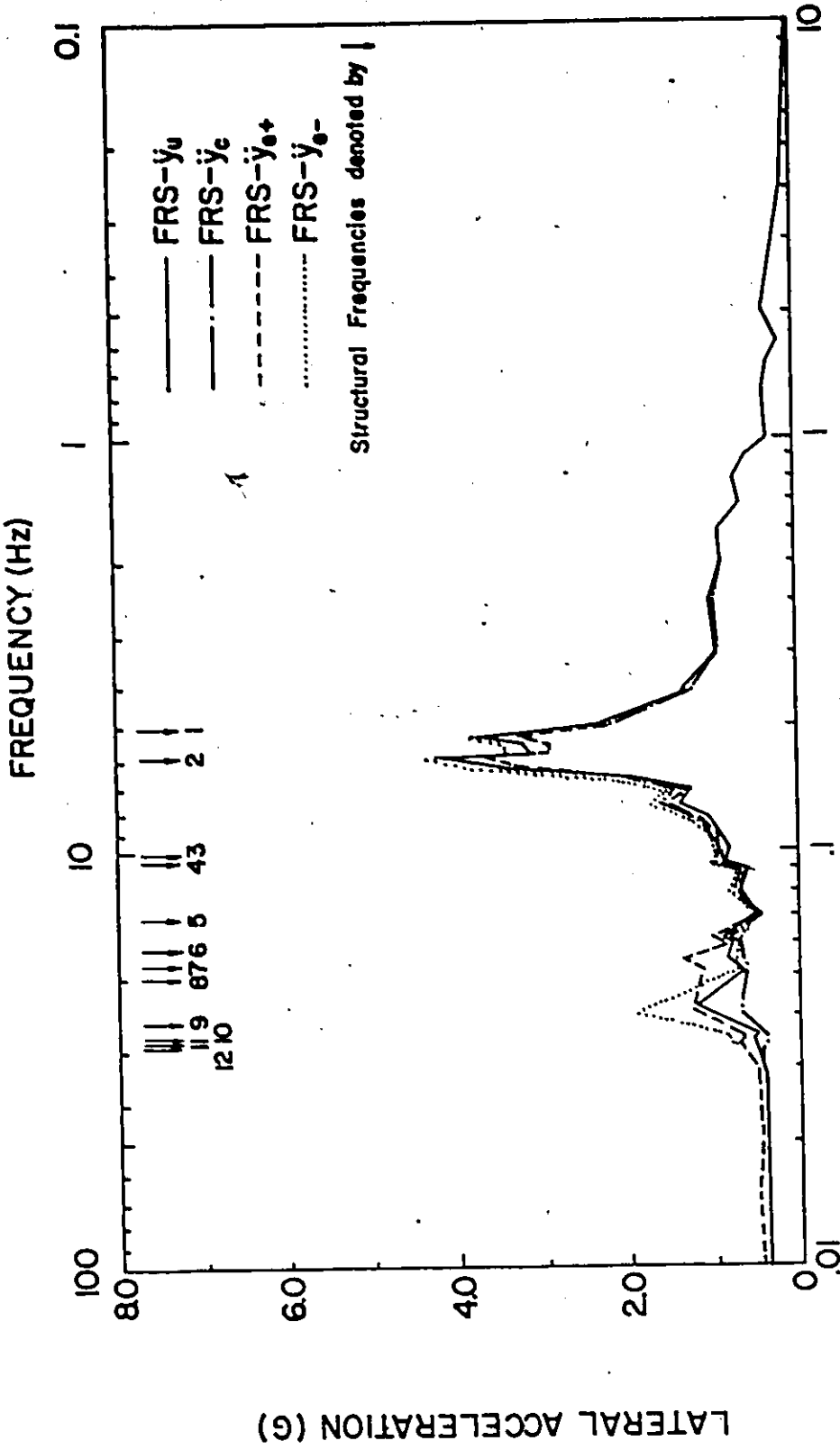

FIG. 3.5 Lateral Floor Response Spectra - Mass M_4 - 1940 El Centro W-E (1% Damping)

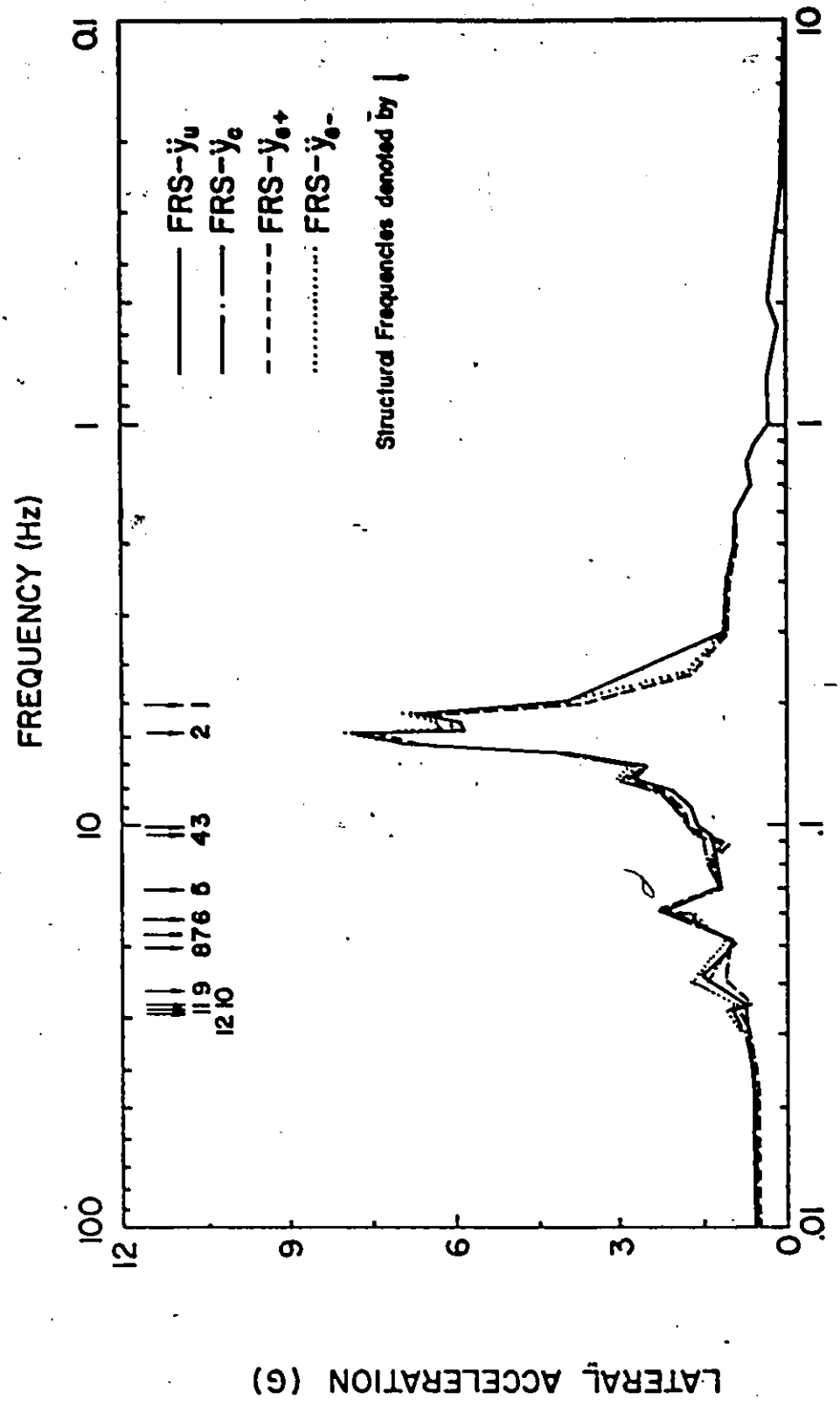

FIG. 3.6 Lateral Floor Response Spectra - Mass M_5 - 1940 El Centro N-E (1% Damping)

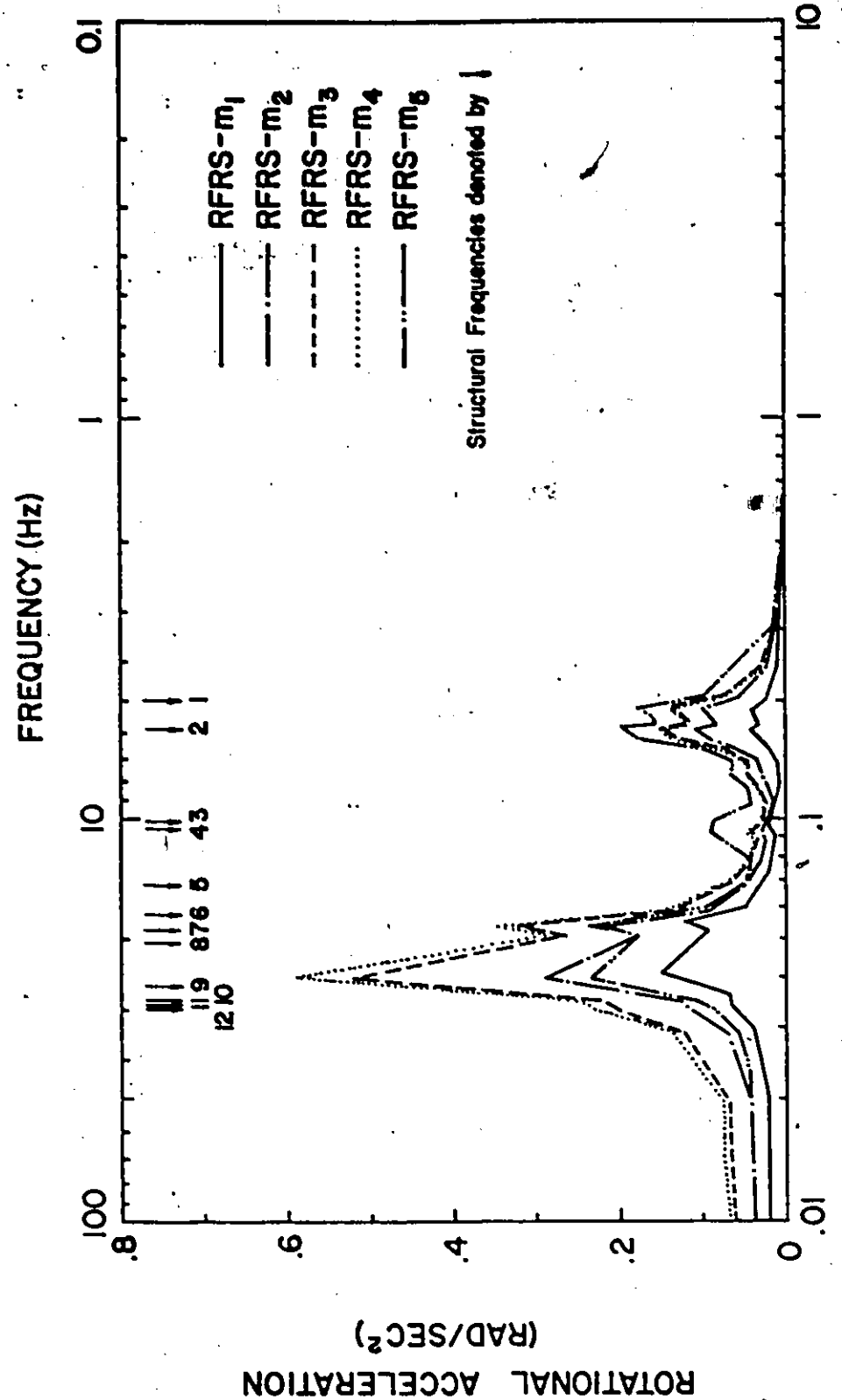

FIG. 3.7 Rotational Floor Response Spectra - 1940 El Centro N-E (1% Damping)

ening the floor response spectra in the frequency range above the first significant mode (second mode of vibration).

2. The peaks of the rotational floor response spectra are associated with the periods contributing large values of rotational modal response factors ($\Gamma_{yi}\phi_{\theta ij}$). Examining Table 2.4.a one may observe that the largest peaks are due to modes 8 and 9 and this is true for all the masses of the internal structure. These floor spectra express the frequency range most affected by torsional coupling and also could be used as dynamic input for some types of equipment which may be sensitive to a rotational input motion.
3. The torsional effect can have some significance on the lateral-floor spectra generated for different locations of equipment within the structure. The equipment response varies not only with respect to its elevation within the structure but also with its lateral location relative to the center of the building. This lateral variation of floor spectra ordinates is due to the induced rotational modal response factors ($\Gamma_{yi}\phi_{\theta ij}$). The largest deviation between the centroidal floor spectra (FRS $\ddot{y}_c$) and the extreme edge floor spectra (FRS $\ddot{y}_{e+}$, FRS $\ddot{y}_{e-}$) occurs, as would be expected, in the range of frequencies corresponding to modes 8 and 9 (this frequency range of strong coupling is obtained from the rotational floor response spectra as well). This is true for the five floor levels of interest, however, it is most pronounced at masses (m_3 and m_4) which produce the largest rotational floor spectra values at this frequency range. For this particular example, the largest variation of lateral floor

response spectrum at the same elevation due to different plan - locations is approximately 1.2 g. This occurs at mass (m_4) at the 9th structural frequency (24.4 Hz) of the coupled lateral-torsional model.

4. The edge floor response spectra values can be higher or lower than the uncoupled floor spectra ordinates depending upon frequency. It is the author's opinion that the asymmetry of a structure should be considered in the development of the floor spectra, and hence, it may be advisable either to develop floor spectra enveloping all floor locations or to generate floor spectra particularly for specific equipment location.

5. The variation of the floor response spectra values due to different lateral location occurs in the frequency range associated with the building natural frequencies and in the high frequency range (relatively rigid equipment) only. No variation is observed in the low frequency range (relatively flexible equipment). Hence, one may conclude that the effect of torsional coupling is mainly contributing to the response of the equipment having natural frequency equal or higher than the predominant natural frequencies of the reactor building (relatively rigid equipment). This conclusion may be drawn by observing the rotational floor response spectra (Figure 3.7) as well.

CHAPTER IV

TORSIONALLY COUPLED REACTOR BUILDING SUBJECTED TO DIFFERENT SEISMIC GROUND MOTIONS

4.1 Introduction

In the previous chapter, the seismic floor response spectra are generated at different floor levels and for more than one location on each floor level, by using the 1940 El Centro W-E as typical earthquake input ground motion, in order to evaluate the asymmetric effect of the reactor building on such floor response spectra.

In this chapter, the floor response spectra are developed for excitation due to several different earthquakes with the objective of evaluating the effect of seismic ground motions with different characteristics on floor response spectra and the influence of such effect on lateral-torsional coupling.

In order to be able to evaluate this effect of seismic ground motion characteristics, a comparison of amplification factors computed at various horizontal locations of the two critical floor levels (m_3 and m_4) is presented. This comparison is made using five different input ground motions:

(a) 1940 El Centro W-E

(b) 1940 El Centro N-S

(c) 1952 Taft N21E

(d) 1971 San Fernando (Wilshire) N-S

(e) AECL Record*

4.2 Seismic Ground Motions

The seismic ground motions considered in this study are chosen to represent different types of motion characteristics. The unsmoothed ground response spectra are shown in Figure 4.1. These spectra are generated for a specific damping ratio of 5 percent. The considerable deviations between the different ground response spectra over the whole frequency range are due to the variation of the frequency content of the seismic ground motions considered. The influence of such variation on the equipment response can be evaluated by generating the floor response spectra associated with each time history ground motion.

4.3 Floor Response Spectra Associated with Different Seismic Ground Motions

Having established five different time-history ground motions, normalized to a maximum acceleration of 0.2 g, for use in development of floor response spectra, the uncoupled and coupled mathematical models of the reactor building are first analysed and time-histories of the two critical floor levels (m_3 and m_4) are determined at the center and at the extreme edges of the building structure. The floor response spectra associated with the floor motion time-histories due to each seismic ground motion are then generated assuming a secondary damping of one percent.

---

*An artificial time history record was supplied by AECL and had been generated in order to yield a response spectrum which closely matches the 2 percent damped design response spectrum (Figure 1.1).

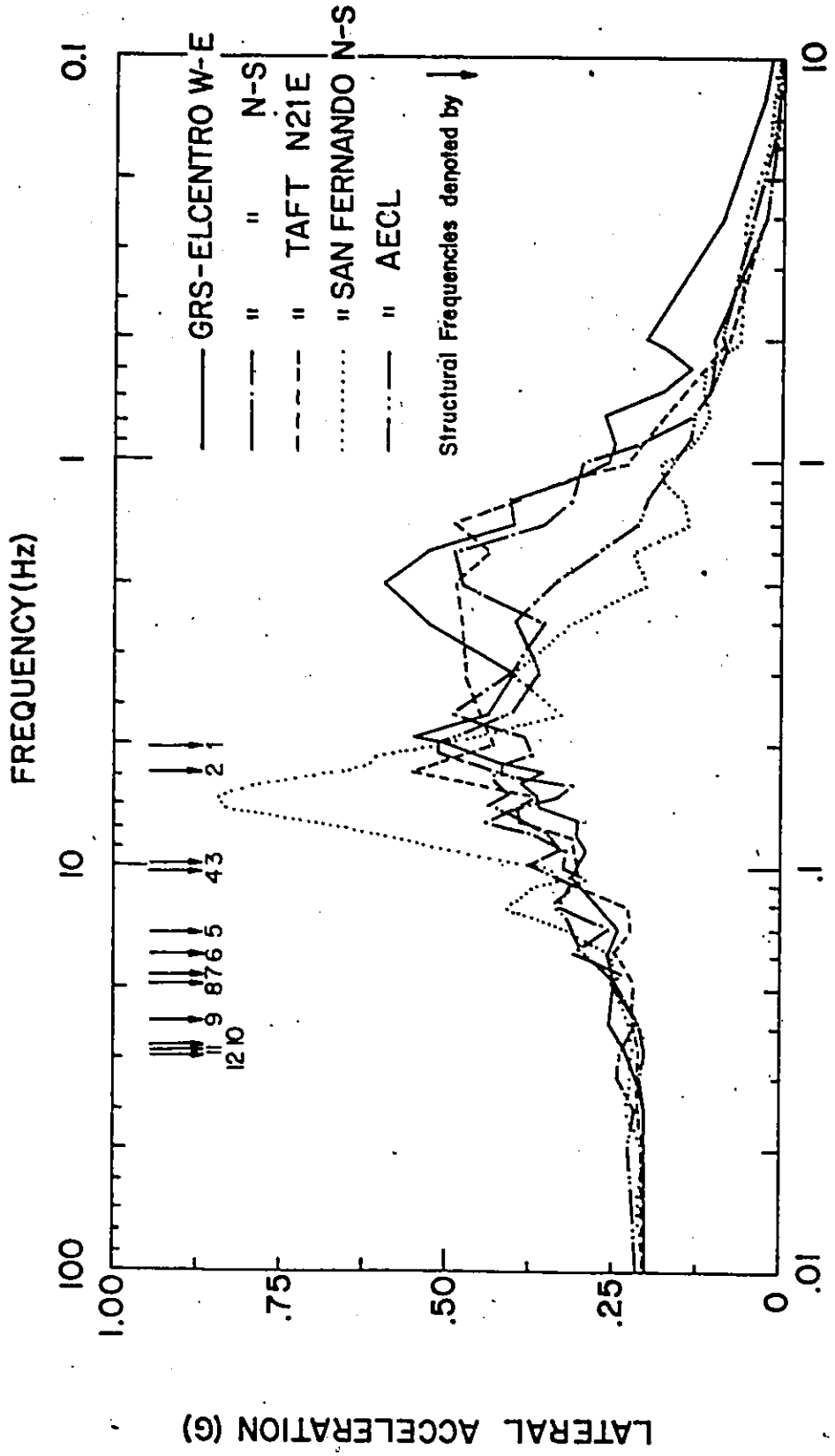

FIG. 4.1 Ground Response Spectra - Different Seismic Ground Motions (5% Damping)

The uncoupled, coupled, (+ve) edge and (-ve) edge lateral floor response spectra of mass m_3 are shown in Figures 4.2 to 4.5, respectively; each figure consists of the floor spectra associated with the five seismic ground motions. Similarly, the lateral floor spectra of mass m_4 are presented in Figures 4.6 to 4.9. The rotational floor response spectra of masses m_3 and m_4 are shown in Figures 4.10 and 4.11, respectively.

In order to evaluate the effect of seismic ground motion characteristics on the equipment response the lateral amplification factors (equipment to structure) and (equipment to ground) are tabulated in Table 4.1.a to 4.8.a, and Table 4.1.b to 4.8.b, respectively. The influence of seismic ground motion characteristics on lateral-torsional coupling effect is presented by introducing the rotational amplification factors (equipment to structure). These rotational amplification factors for masses m_3 and m_4 are given in Tables 4.9 and 4.10, respectively.

4.4 Discussion of Results

The results of the floor response spectra for the typical CANDU reactor building generated using different seismic ground motions indicate that the following observations can be made:

1. The uncoupled floor spectra peaks are always higher than the coupled spectra values except for the period range (0.08 - 0.16) and this is true due to all five seismic ground motions. Similar observations is drawn in Chapter III for all five floor levels due to the 1940 El Centro W-E.
2. The variation of the uncoupled floor response spectra values due to different seismic ground motions is significantly, as would be expected, because these floor spectra are highly affected by the

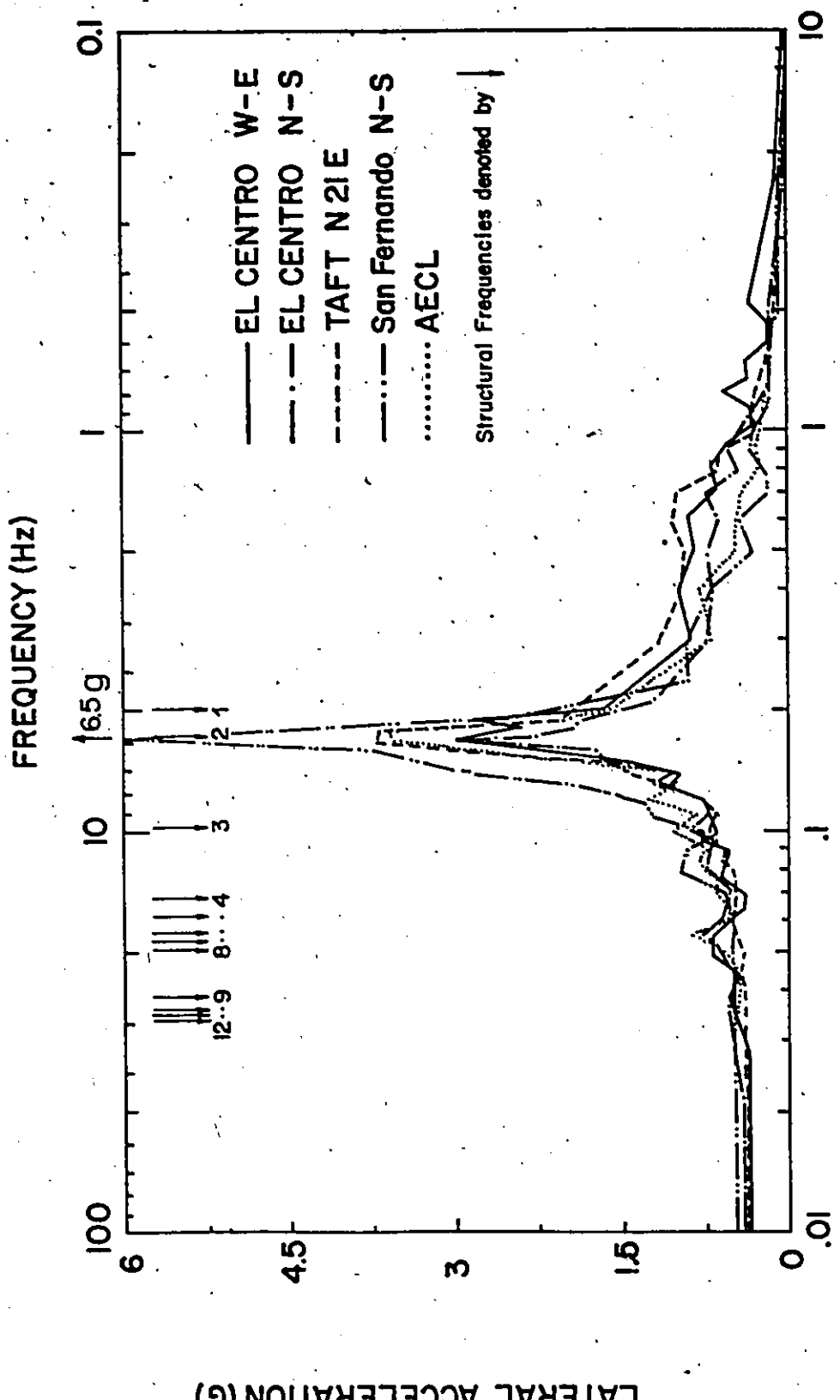

FIG. 4.2 Uncoupled Floor Response Spectra - Mass M_3 - (1% Damping)

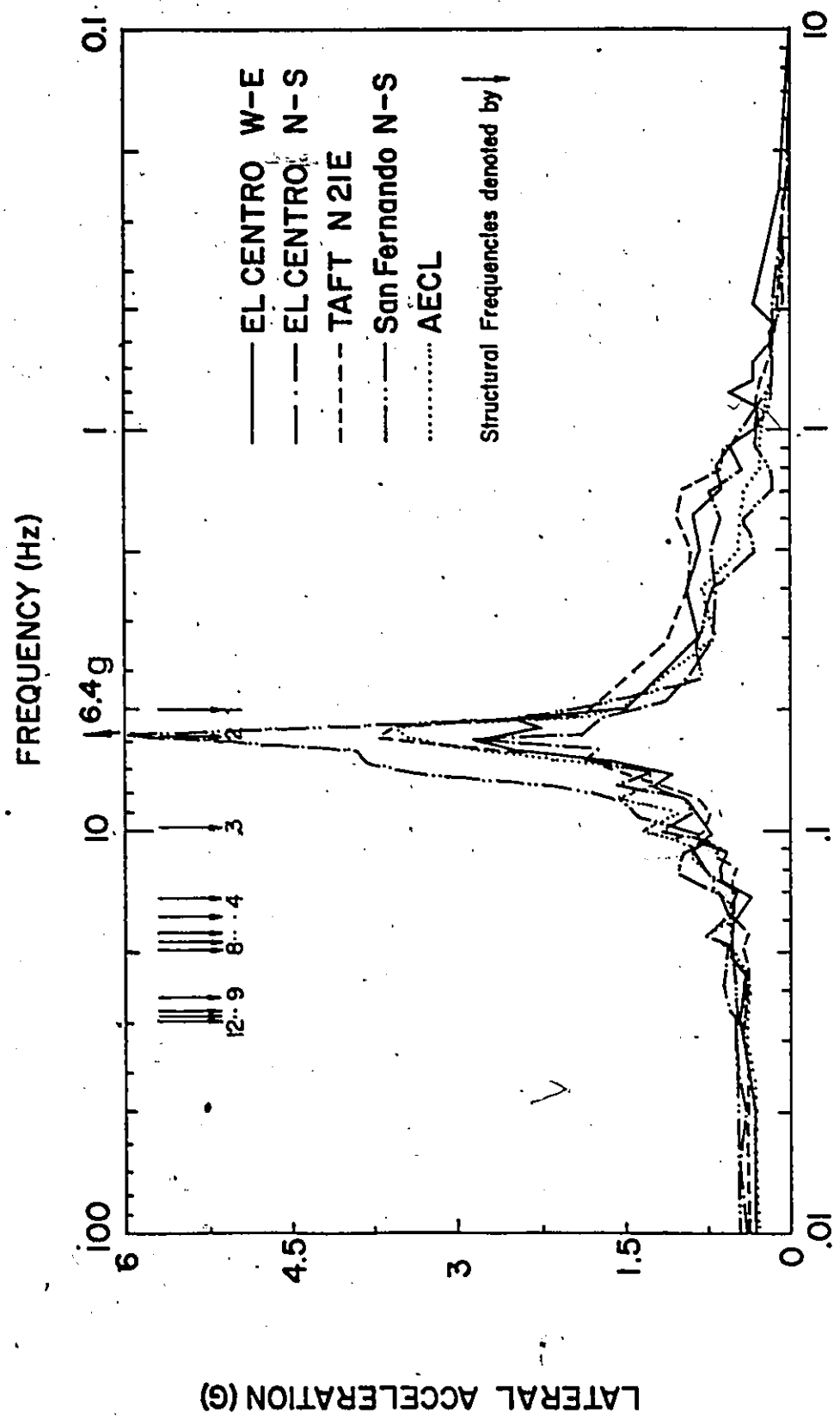

FIG. 4.3 Centroidal Coupled Floor Response Spectra - Mass M_3
(1% Damping)

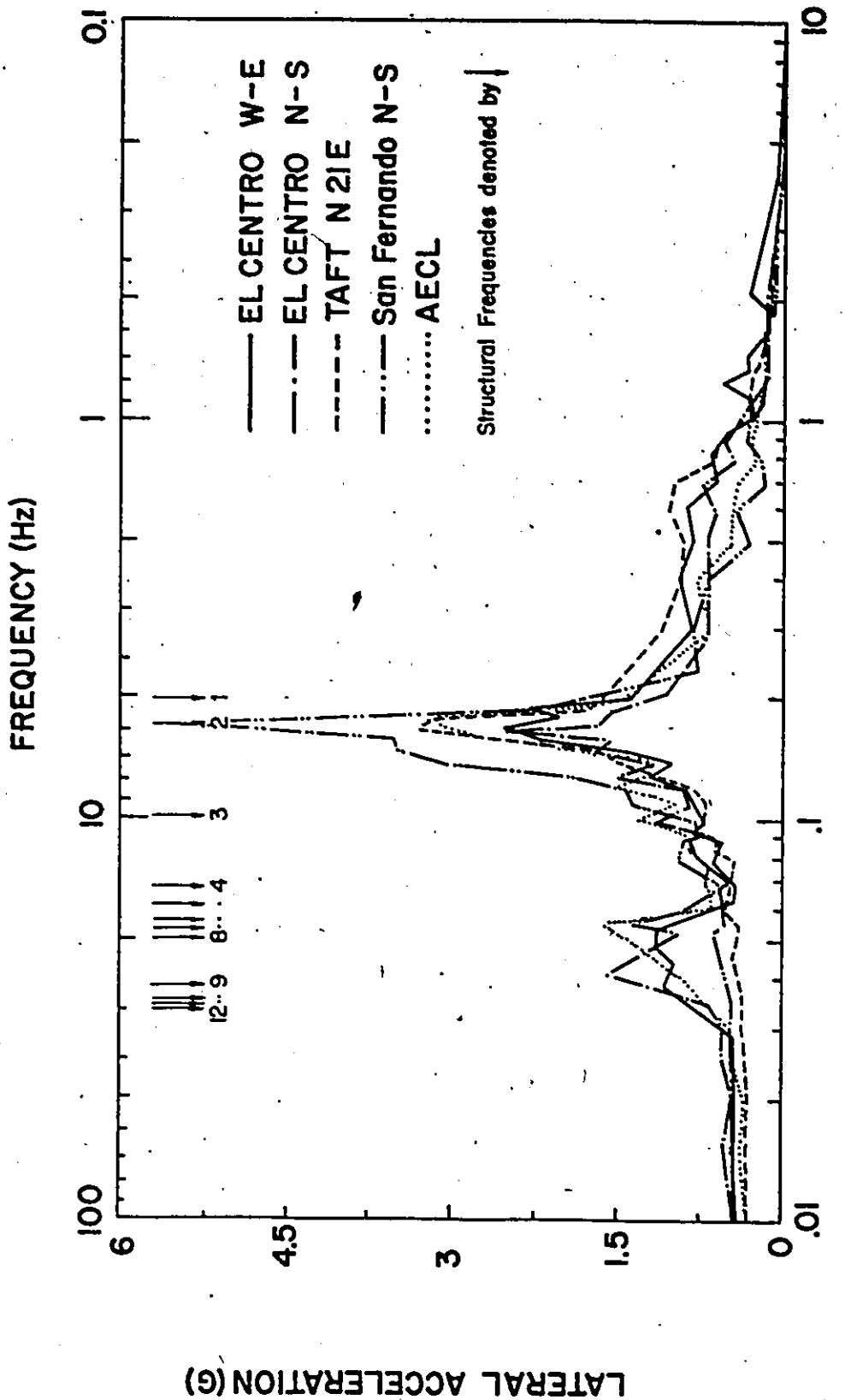

FIG. 4.4 (+ve) Edge Floor Response Spectra - Mass M_3
(1% Damping)

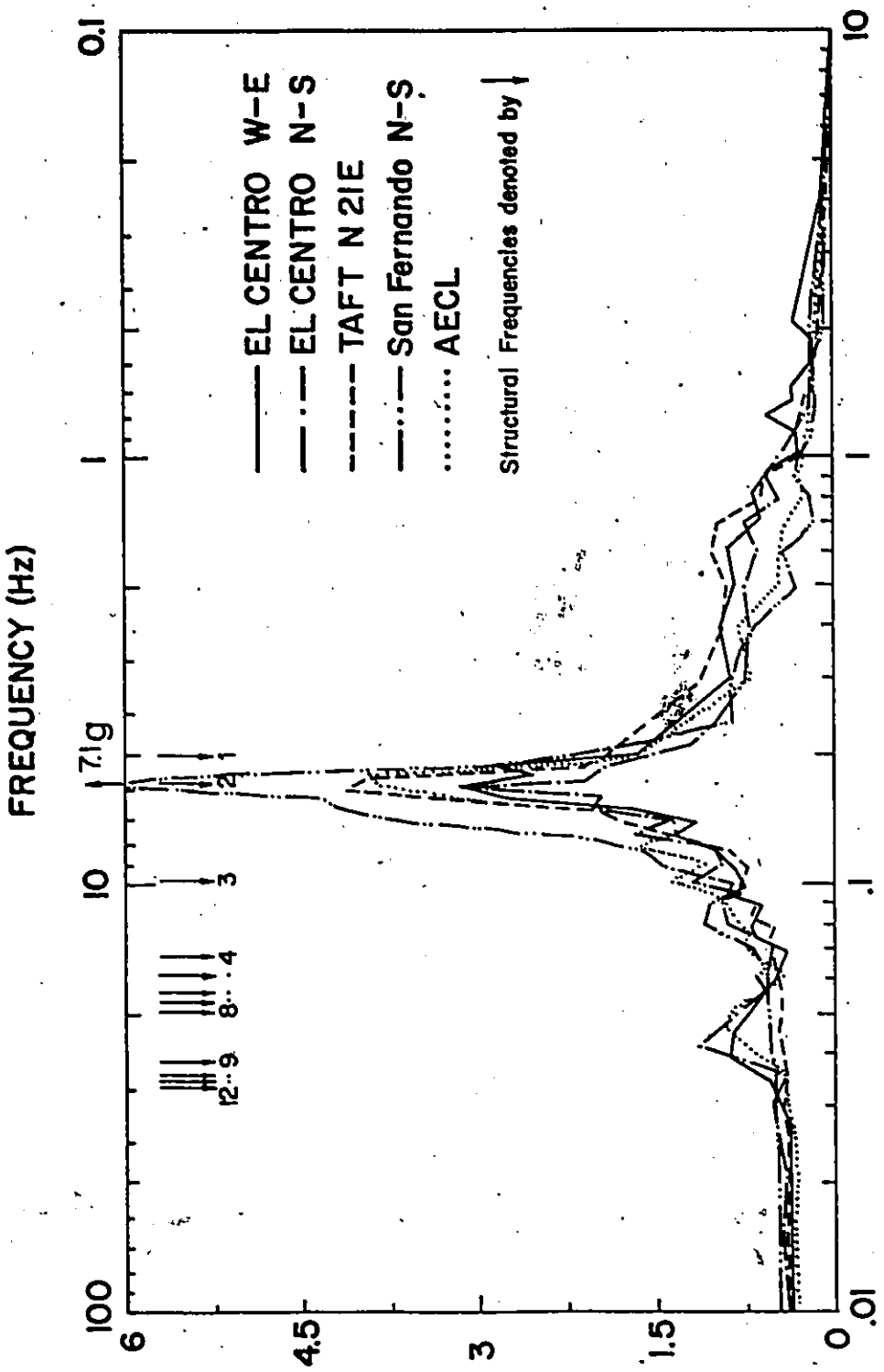

FIG. 4.5 (-ve) Edge Floor Response Spectra - Mass M_3
(1% Damping)

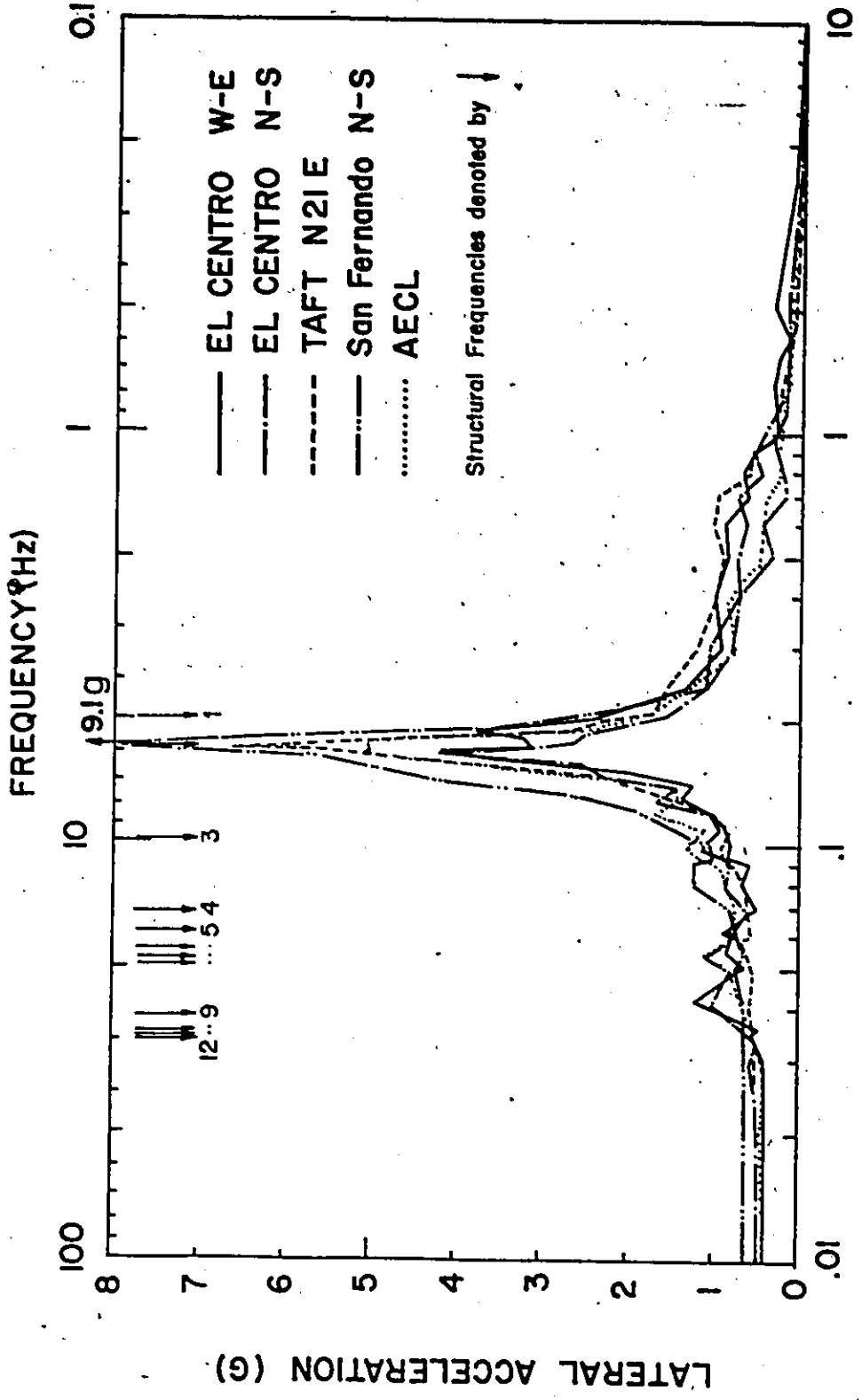

FIG. 4.6 Uncoupled Floor Response Spectra - Mass M_4
(1% Damping)

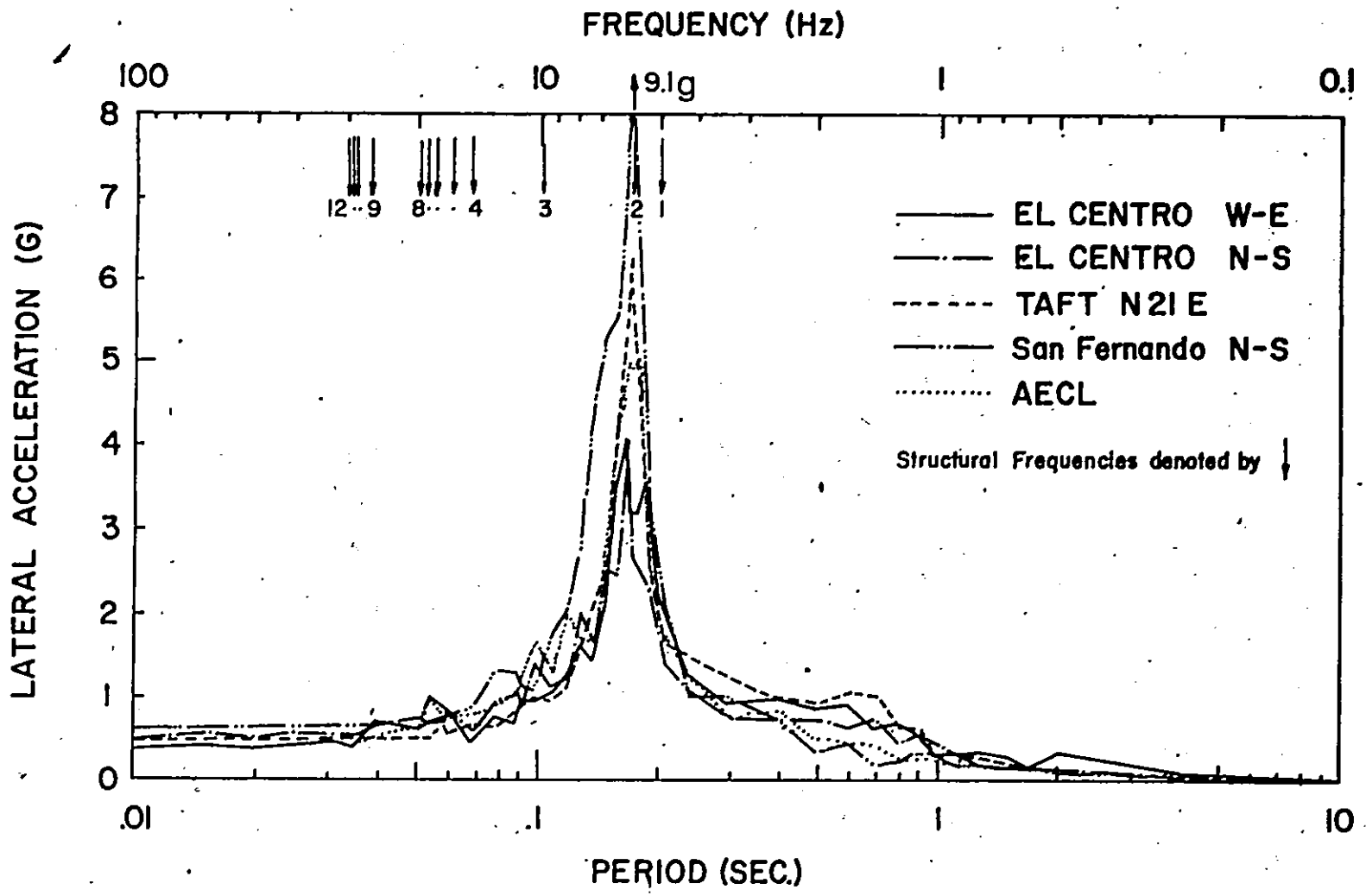

FIG. 4.7 Centroidal Coupled Floor Response Spectra - Mass M_4
(1% Damping)

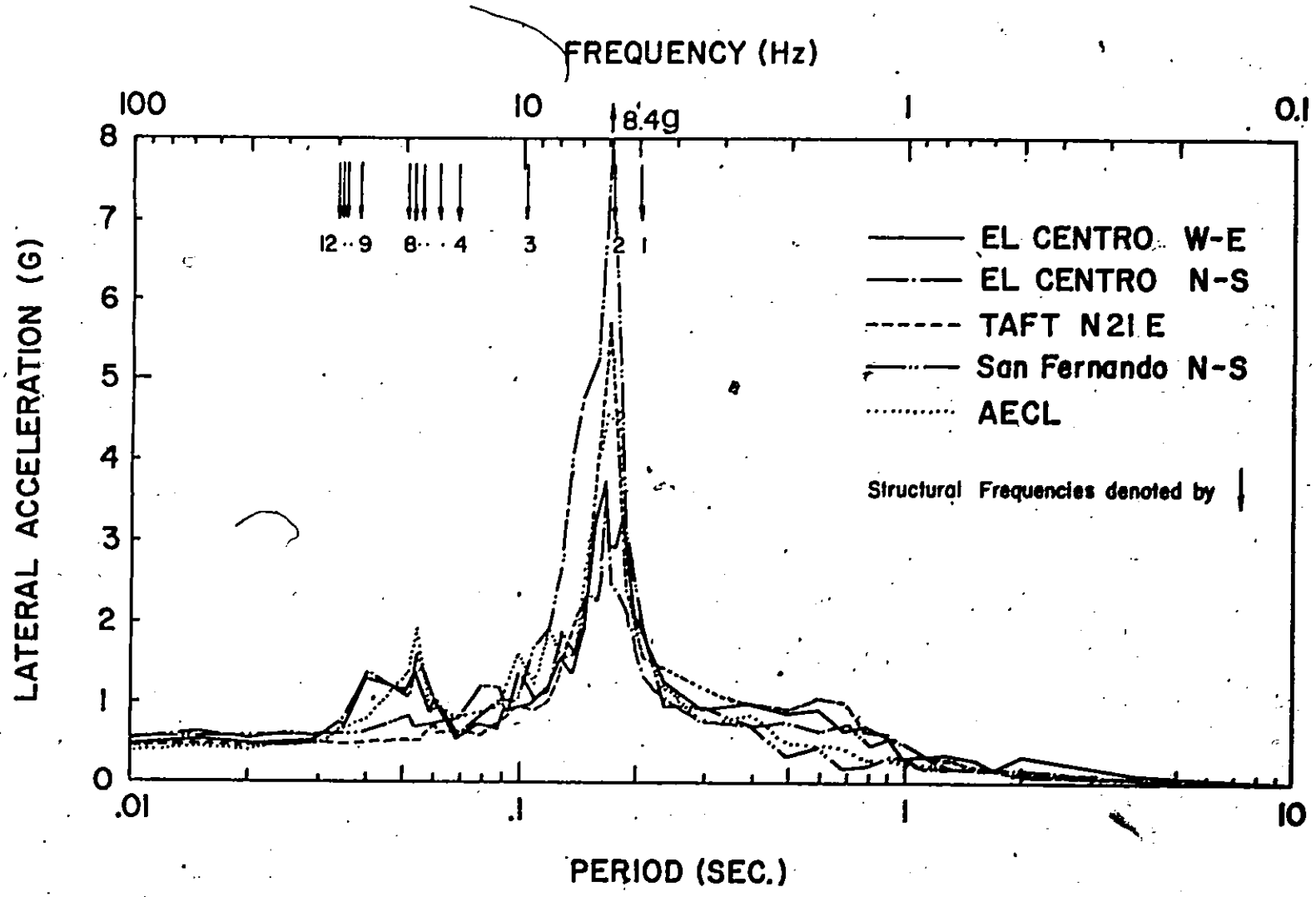

FIG. 4.8 (+ve) Edge Floor Response Spectra - Mass M_4
(1% Damping)

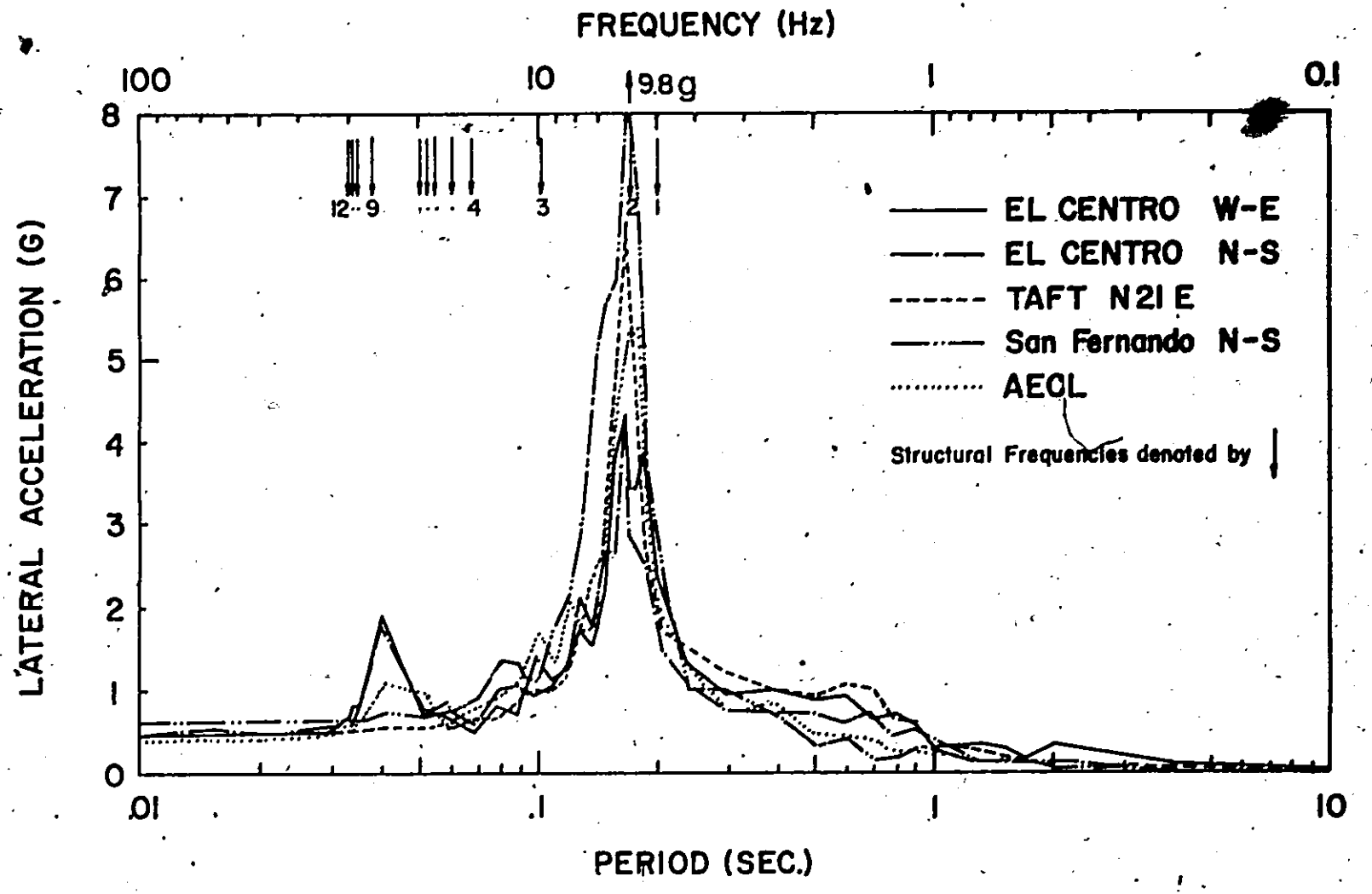

FIG. 4.9 (-ve) Edge Floor Response Spectra - Mass M_4
(1% Damping)

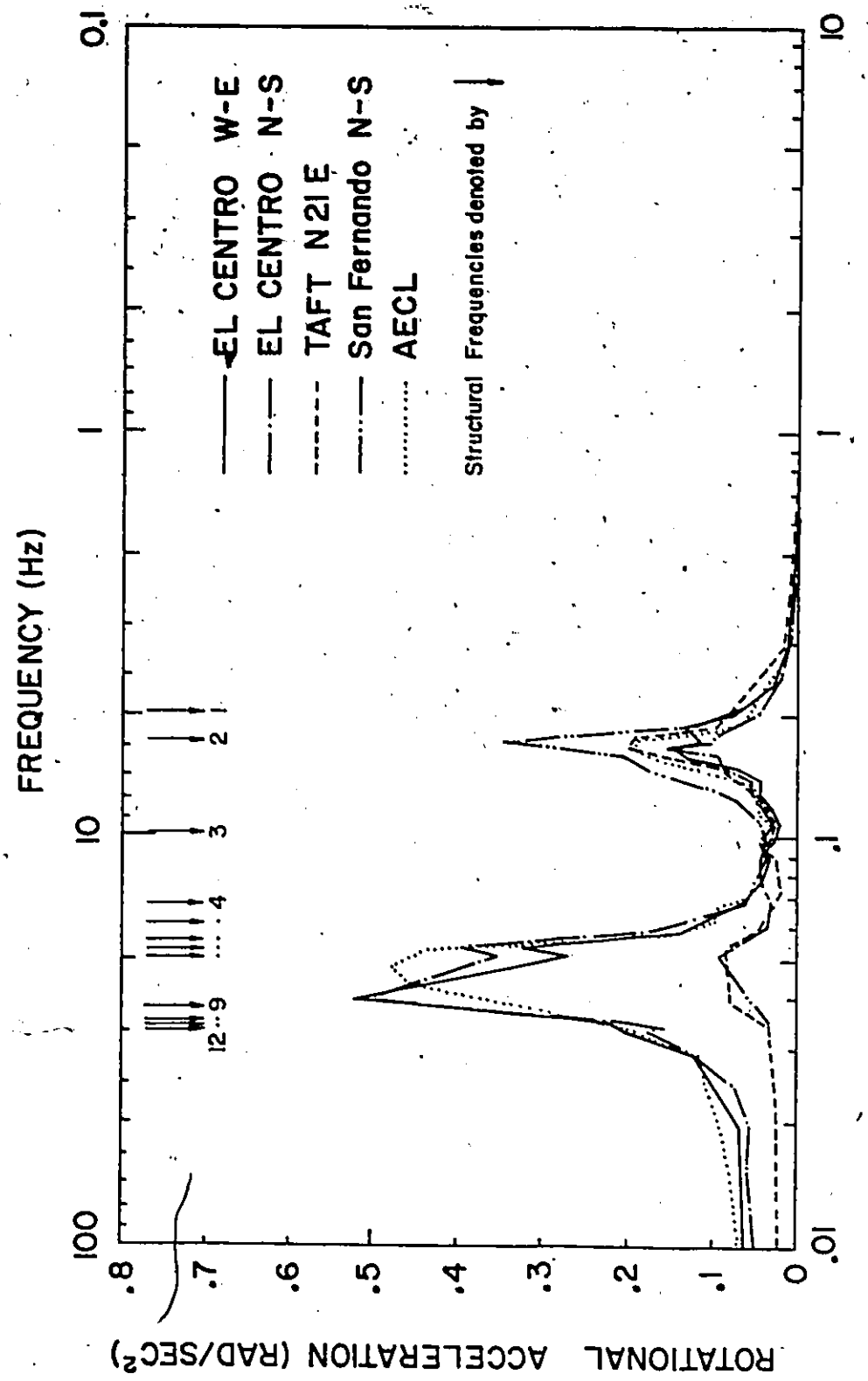

FIG. 4.10 Rotational Floor Response Spectra - Mass M_3
(1% Damping)

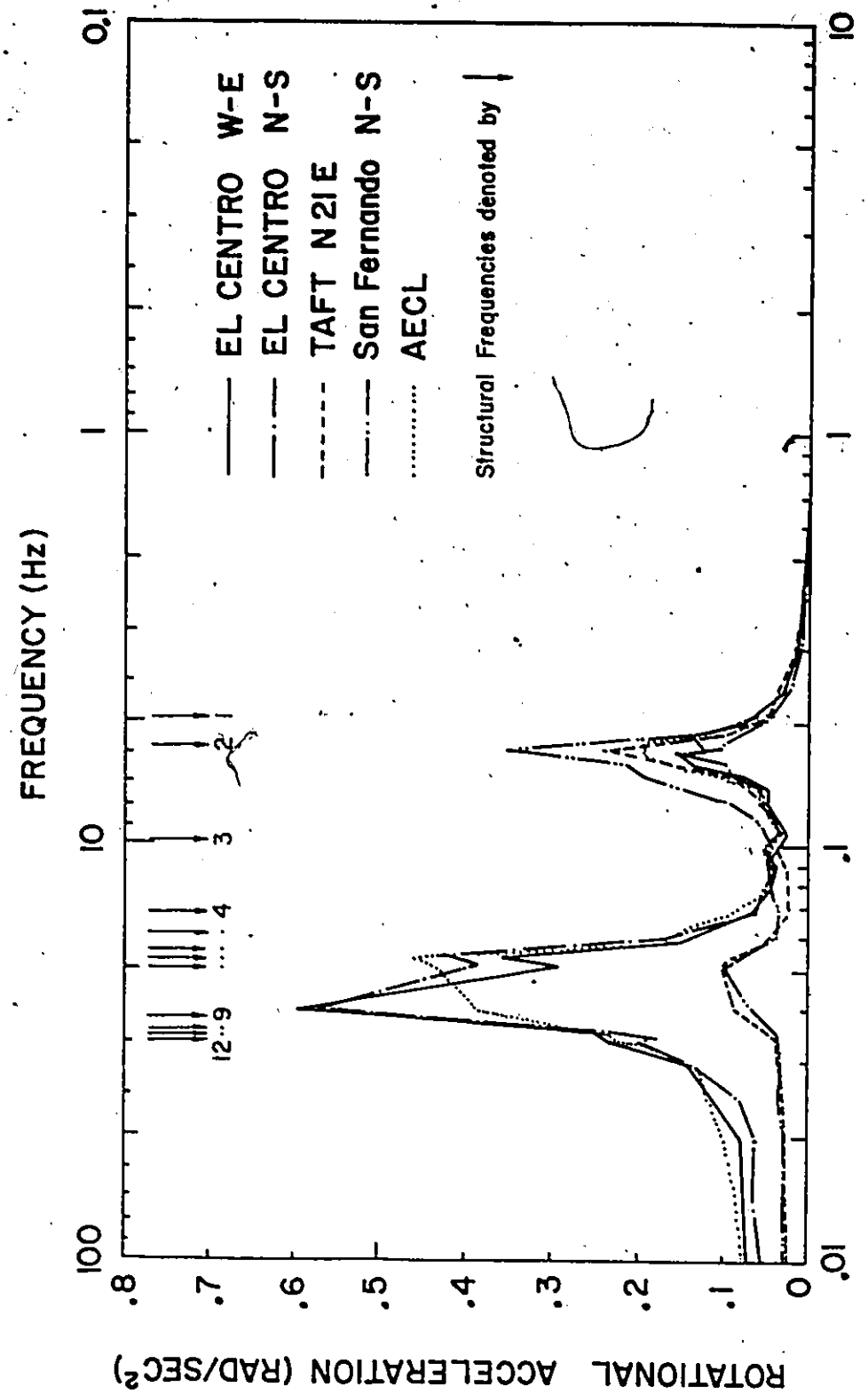

FIG. 4.11 Rotational Floor Response Spectra - Mass M_4
(1% Damping)

Table 4.1.a Uncoupled Amplification Factors (Equipment to Structure) Mass m_3

Building Frequency	5% Structural Damping and 1% Equipment Damping				
	ELCENTRO W-E	ELCENTRO N-S	TAFT N21E	SAN FERNANDO N-S	AECL
1	4.93	3.81	5.50	4.71	4.71
2	8.87	6.13	10.54	14.16	10.33
3	1.92	2.31	1.98	1.67	3.12
4	2.21	1.65	1.97	1.72	2.77
5	1.08	1.32	1.31	1.10	1.90
6	1.70	1.54	1.38	1.05	1.81
7	2.04	2.03	1.28	1.04	2.57
8	2.01	1.65	1.13	1.13	1.67
9	1.57	1.17	1.07	1.07	1.08
10	1.34	1.37	1.06	1.02	1.40
11	1.34	1.43	1.06	1.03	1.36
12	1.34	1.30	1.06	1.04	1.25

Table 4.1.b Uncoupled Amplification Factors (Equipment to Ground) Mass m_3

Building Frequency	5% Structural Damping and 1% Equipment Damping				
	ELCENTRO W-E	ELCENTRO N-S	TAFT N21E	SAN FERNANDO N-S	AECL
1	8.25	7.24	9.65	10.73	7.99
2	14.86	11.65	18.49	32.28	17.52
3	3.21	4.39	3.48	3.81	5.29
4	3.70	3.14	3.45	3.92	4.69
5	1.81	2.51	2.31	2.88	3.22
6	2.85	2.92	2.42	2.52	3.06
7	3.41	3.86	2.25	2.36	4.35
8	3.36	3.14	1.98	2.58	2.84
9	2.62	2.24	1.88	2.43	1.84
10	2.24	2.61	1.87	2.33	2.38
11	2.24	2.72	1.87	2.36	2.30
12	2.24	2.47	1.87	2.36	2.12

Table 4.2.a Centroidal Coupled Amplification Factors (Equipment to Structure) Mass m_3

Building Frequency	5% Structural Damping and 1% Equipment Damping				
	ELCENTRO W-E	ELCENTRO N-S	TAFT N21E	SAN FERNANDO N-S	AECL
1	4.72	3.48	5.14	4.35	5.25
2	8.89	4.86	10.59	14.31	11.95
3	2.28	2.98	2.18	1.83	4.77
4	7.67	1.90	2.44	1.86	3.83
5	1.15	1.24	1.46	1.42	2.44
6	1.68	1.48	1.42	1.20	2.01
7	1.67	1.96	1.03	1.12	2.65
8	1.69	1.44	1.14	1.15	1.74
9	1.26	1.55	1.04	1.07	1.20
10	1.49	1.43	1.08	1.06	1.30
11	1.49	1.36	1.08	1.04	1.34
12	1.49	1.27	1.08	1.04	1.31

Table 4.2.b Centroidal Coupled Amplification Factors (Equipment to Ground) Mass m_3

Building Frequency	5% Structural Damping and 1% Equipment Damping				
	ELCENTRO W-E	ELCENTRO N-S	TAFT N21E	SAN FERNANDO N-S	AECL
1	7.61	6.76	8.92	9.76	7.48
2	14.34	9.44	18.37	32.13	17.01
3	3.68	5.79	3.78	4.10	6.80
4	4.30	3.61	4.23	4.18	5.46
5	1.86	2.41	2.53	3.20	3.47
6	2.70	2.87	2.47	2.70	2.86
7	2.69	3.80	1.78	2.51	3.78
8	2.72	2.80	1.97	2.58	2.48
9	2.03	3.01	1.81	2.41	1.70
10	2.41	2.78	1.88	2.37	1.86
11	2.41	2.65	1.88	2.33	1.90
12	2.41	2.48	1.88	2.34	1.86

Table 4.3.a (+ve) Edge Amplification Factors (Equipment to Structure) Mass m_3

Building Frequency	5% Structural Damping and 1% Equipment Damping				
	ELCENTRO W-E	ELCENTRO N-S	TAFT N21E	SAN FERNANDO N-S	AECL
1	3.64	2.89	5.22	4.31	4.40
2	6.67	3.89	10.48	13.82	9.50
3	1.88	2.62	2.30	1.89	4.12
4	2.15	1.62	2.53	1.83	3.19
5	1.09	1.11	1.52	1.39	2.23
6	1.78	1.88	1.71	1.22	2.30
7	2.96	3.13	1.30	1.26	5.05
8	3.02	2.15	1.32	1.49	3.79
9	2.81	3.69	1.25	1.22	2.64
10	2.05	1.94	1.14	1.08	2.21
11	2.05	1.69	1.14	1.04	2.23
12	2.04	1.51	1.14	1.05	1.93

Table 4.3.b (+ve) Edge Amplification Factors (Equipment to Ground) Mass m_3

Building Frequency	5% Structural Damping and 1% Equipment Damping				
	ELCENTRO N-E	ELCENTRO N-S	TAFT N21E	SAN FERNANDO N-S	AECL
1	6.98	6.25	8.13	8.90	6.94
2	12.80	8.41	16.32	28.54	15.06
3	3.60	5.65	3.58	3.90	6.53
4	4.13	3.50	3.95	3.77	5.06
5	2.09	2.39	2.37	2.87	3.53
6	3.41	4.06	2.66	2.52	3.64
7	5.68	6.77	2.03	2.60	8.00
8	5.79	4.65	2.05	3.07	6.00
9	5.39	7.98	1.95	2.51	4.19
10	3.93	4.19	1.78	2.23	3.50
11	3.93	3.65	1.78	2.14	3.54
12	3.93	3.27	1.78	2.18	3.06

Table 4.4.a (-ve) Edge Amplification Factors (Equipment to Structure) Mass m_3

Building Frequency	5% Structural Damping and 1% Equipment Damping				
	ELCENTRO W-E	ELCENTRO N-S	TAFT N21E	SAN FERNANDO N-S	AECL
1	4.52	3.69	5.07	4.39	4.74
2	8.69	5.31	10.67	14.74	11.20
3	2.09	3.00	2.08	1.78	4.17
4	2.47	1.99	2.36	1.90	3.46
5	1.11	1.30	1.41	1.45	2.26
6	1.46	1.40	1.20	1.19	1.60
7	1.75	1.47	1.15	1.17	1.72
8	2.09	1.78	1.16	1.18	2.41
9	2.46	2.89	1.12	1.14	2.12
10	1.49	1.34	1.04	1.04	1.36
11	1.49	1.06	1.04	1.03	1.20
12	1.49	1.04	1.04	1.03	1.14

Table 4.4.b (-ve) Edge Amplification Factors (Equipment to Ground) Mass m_3

Building Frequency	5% Structural Damping and 1% Equipment Damping				
	ELCENTRO W-E	ELCENTRO N-S	TAFT N21E	SAN FERNANDO N-S	AECL
1	8.27	7.27	9.70	10.64	8.03
2	15.88	10.47	20.43	35.73	18.97
3	3.81	5.92	3.98	4.30	7.07
4	4.51	3.93	4.51	4.60	5.86
5	2.02	2.57	2.70	3.52	3.83
6	2.66	2.76	2.31	2.89	2.71
7	3.20	2.90	2.20	2.84	2.92
8	3.83	3.52	2.21	2.85	4.08
9	4.50	5.69	2.14	2.76	3.60
10	2.73	2.63	1.99	2.52	2.31
11	2.73	2.10	1.99	2.53	2.03
12	2.73	2.06	1.99	2.50	1.93

Table 4.5.a Uncoupled Amplification Factors (Equipment to Structure) Mass m_4

Building Frequency	5% Structural Damping and 1% Equipment Damping				
	ELCENTRO N-E	ELCENTRO N-S	TAFT N21E	SAN FERNANDO N-S	AECL
1	6.27	3.84	4.78	4.64	5.19
2	8.17	7.00	14.06	15.34	12.84
3	2.09	2.43	1.95	1.72	3.44
4	2.22	1.72	1.89	1.69	2.96
5	1.31	1.25	1.26	1.33	1.89
6	2.29	1.70	1.18	1.14	2.11
7	2.20	2.28	1.22	1.07	2.87
8	1.72	1.69	1.13	1.22	2.07
9	3.15	2.14	1.19	1.07	1.72
10	1.25	1.23	1.09	1.03	1.32
11	1.46	1.12	1.08	1.03	1.34
12	1.27	1.04	1.04	1.04	1.29

Table 4.5.b Uncoupled Amplification Factors (Equipment to Ground) Mass m_4

Building Frequency	5% Structural Damping and 1% Equipment Damping				
	ELCENTRO N-E	ELCENTRO N-S	TAFT N21E	SAN FERNANDO N-S	AECL
1	12.01	9.18	11.23	13.80	10.09
2	15.66	16.75	33.06	45.66	24.93
3	4.01	5.82	4.59	5.12	6.67
4	4.26	4.12	4.44	5.02	5.74
5	2.51	3.00	2.95	3.97	3.66
6	4.39	4.06	2.78	3.40	4.10
7	4.23	5.46	2.88	3.17	5.57
8	3.30	4.05	2.65	3.63	4.02
9	6.04	5.12	2.79	3.18	3.34
10	2.39	2.94	2.57	3.07	2.56
11	2.80	2.68	2.55	3.07	2.59
12	2.44	2.49	2.46	3.11	2.50

Table 4.6.a Centroidal Coupled Amplification Factors (Equipment to Structure) Mass m_4

Building Frequency	5% Structural Damping and 1% Equipment Damping				
	ELCENTRO W-E	ELCENTRO N-S	TAFT N21E	SAN FERNANDO N-S	AECL
1	6.03	3.60	4.44	4.30	5.06
2	8.59	5.52	13.39	15.20	12.98
3	2.51	2.89	2.08	1.78	4.39
4	2.58	1.90	1.88	1.85	3.46
5	1.25	1.19	1.38	1.43	2.04
6	2.27	1.57	1.15	1.23	2.04
7	1.82	2.06	0.99	1.13	2.61
8	1.65	1.52	1.05	1.19	1.74
9	1.88	1.37	1.01	1.08	1.38
10	1.06	1.09	1.02	1.03	1.10
11	1.01	1.12	1.04	1.03	1.10
12	1.15	1.11	1.05	1.04	1.13

Table 4.6.b Centroidal Coupled Amplification Factors (Equipment to Ground) Mass m_4

Building Frequency	5% Structural Damping and 1% Equipment Damping				
	ELCENTRO W-E	ELCENTRO N-S	TAFT N21E	SAN FERNANDO N-S	AECL
1	11.17	8.71	10.33	12.92	9.52
2	15.92	13.36	31.11	45.59	24.41
3	4.65	7.00	4.85	5.33	8.25
4	4.79	4.61	4.37	5.56	6.45
5	2.32	2.89	3.20	4.29	3.83
6	4.21	3.81	2.68	3.70	3.84
7	3.37	4.99	2.31	3.40	4.90
8	3.06	3.68	2.43	3.57	3.26
9	3.48	3.31	2.34	3.24	2.59
10	1.96	2.64	2.38	3.10	2.06
11	1.88	2.71	2.41	3.09	2.07
12	2.14	2.69	2.44	3.11	2.12

Table 4.7.a (+ve) Edge Amplification Factors (Equipment to Structure) Mass m_4

Building Frequency	5% Structural Damping and 1% Equipment Damping				
	ELCENTRO W-E	ELCENTRO N-S	TAFT N21E	SAN FERNANDO N-S	AECL
1	4.79	3.05	4.54	4.37	4.87
2	6.72	4.60	13.37	15.24	12.19
3	2.11	2.57	2.18	1.83	4.34
4	2.05	1.64	1.91	1.86	3.31
5	1.2	1.08	1.43	1.44	2.11
6	2.31	1.90	1.39	1.27	2.59
7	3.09	2.99	1.17	1.24	5.18
8	2.58	1.98	1.17	1.50	3.68
9	2.91	2.60	1.15	1.13	2.14
10	1.50	1.56	1.07	1.05	1.79
11	1.66	1.40	1.09	1.04	1.78
12	1.55	1.33	1.09	1.05	1.60

Table 4.7.b (+ve) Edge Amplification Factors (Equipment to Ground) Mass m_4

Building Frequency	5% Structural Damping and 1% Equipment Damping				
	ELCENTRO W-E	ELCENTRO N-S	TAFT N21E	SAN FERNANDO N-S	AECL
1	10.46	8.18	9.71	12.03	8.95
2	14.69	12.31	28.61	41.92	22.41
3	4.61	6.87	4.66	5.04	7.98
4	4.47	4.40	4.08	5.12	6.08
5	2.62	2.88	3.06	3.97	3.88
6	5.04	5.08	2.97	3.50	4.76
7	6.75	8.01	2.50	3.42	9.52
8	5.64	5.30	2.49	4.12	6.75
9	6.36	6.97	2.46	3.09	3.93
10	3.29	4.17	2.30	2.90	3.30
11	3.63	3.74	2.33	2.87	3.28
12	3.37	3.55	2.34	2.89	2.94

Table 4.8.a (-ve) Edge Amplification Factors (Equipment to Structure) Mass m_4

Building Frequency	5% Structural Damping and 1% Equipment Damping				
	ELCENTRO W-E	ELCENTRO N-S	TAFT N21E	SAN. FERNANDO N-S	AECL
1	5.17	3.74	4.36	4.24	4.85
2	7.45	5.85	13.39	15.08	12.70
3	2.05	2.90	2.01	1.74	4.10
4	2.24	1.99	1.86	1.84	3.33
5	1.07	1.23	1.33	1.41	1.99
6	1.48	1.45	1.06	1.19	1.69
7	1.63	1.54	1.10	1.17	1.76
8	1.57	1.62	1.07	1.08	2.33
9	4.14	3.64	1.12	1.19	2.67
10	1.75	1.58	1.04	1.04	1.74
11	1.77	1.27	1.01	1.02	1.60
12	1.49	1.17	1.05	1.02	1.34

Table 4.8.b (-ve) Edge Amplification Factors (Equipment to Ground) Mass m_4

Building Frequency	5% Structural Damping and 1% Equipment Damping				
	ELCENTRO W-E	ELCENTRO N-S	TAFT N21E	SAN FERNANDO N-S	AECL
1	11.89	9.24	10.95	13.83	10.08
2	17.16	14.44	33.61	49.25	26.41
3	4.71	7.16	5.04	5.67	8.53
4	5.15	4.90	4.67	6.00	6.92
5	2.47	3.03	3.35	4.61	4.13
6	3.40	3.57	2.67	3.90	3.51
7	3.76	3.80	2.77	3.82	3.66
8	3.62	3.99	2.69	3.52	4.85
9	9.52	9.00	2.81	3.88	5.56
10	4.02	3.90	2.61	3.40	3.62
11	4.08	3.15	2.54	3.33	3.33
12	3.44	2.89	2.65	3.33	2.78

Table 4.9 Rotational Amplification Factors (Equipment to Structure) Mass m_3

Building Frequency	5% Structural Damping and 1% Equipment Damping				
	ELCENTRO W-E	ELCENTRO N-S	TAFT N21E	SAN FERNANDO N-S	AECL
1	1.23	1.10	3.93	3.58	0.97
2	1.88	2.04	9.39	14.00	2.86
3	0.45	0.92	1.56	1.52	0.70
4	0.68	0.78	1.76	1.63	0.55
5	1.06	1.21	1.19	1.29	1.40
6	1.93	3.00	2.30	1.45	2.23
7	5.21	7.93	3.81	3.16	6.45
8	4.28	70.3	4.00	3.63	7.09
9	8.40	10.01	3.69	2.30	4.90
10	3.55	4.01	1.45	1.30	2.94
11	3.34	3.12	1.45	1.28	2.94
12	3.25	3.52	1.45	1.23	2.94

Table 4.10 Rotational Amplification Factors (Equipment to Structure) Mass m_4

Building Frequency	5% Structural Damping and 1% Equipment Damping				
	ELCENTRO W-E	ELCENTRO N-S	TAFT N21E	SAN FERNANDO N-S	AECL
1	1.12	0.99	2.97	3.48	0.84
2	1.73	1.86	10.99	13.73	2.58
3	0.47	0.95	1.62	1.55	0.73
4	0.68	0.79	1.43	1.63	0.59
5	1.01	1.10	1.04	1.24	1.25
6	1.90	2.90	2.35	1.45	2.30
7	5.08	7.69	4.26	3.25	6.18
8	4.17	6.87	4.61	3.75	5.82
9	8.56	10.22	3.81	2.44	5.15
10	3.59	4.05	1.88	1.35	3.10
11	3.39	3.18	1.59	1.33	3.01
12	3.32	3.61	1.63	1.27	2.61

frequency content of the applied seismic ground motion. The largest amplification factors are associated with the second building frequency, and the maximum value of these amplification factors is due to the 1971 San Fernando (Wilshire) N-S earthquake record with a narrow band ground response spectra (Figure 4.1). The San Fernando ground spectrum peak is found to be matching the second building frequency.

3. The rigid equipment amplification values are much lower than the flexible* values because structural response does not produce significantly amplified floor motions for periods less than 0.03 seconds. For flexible equipment the variation of the amplification factors due to different seismic ground motions is large. For rigid equipment such variation is minimized. This observation is true for the uncoupled, coupled, (+ve) edge and (-ve) edge amplification values.
4. The peaks of the rotational floor response spectra are associated with the periods contributing large values of rotational modal response factors ($\Gamma_{yi}\phi_{\theta ij}$) as natural modes 8 and 9 (Chapter III) or with the periods conducting large values of ground spectral accelerations as the period 0.173 sec (second building mode) for the 1971 San Fernando (Wilshire) N-S earthquake record. This observation is drawn by examining Figures 4.10 and 4.11.
5. The torsional coupling effect of the lower frequency range (5→10 Hz) is more pronounced due to San Fernando, Taft and AECL records, however the torsional coupling effect in the higher frequency

---

*The term "flexible" applies to flexibly-mounted rigid equipment as well as to rigidly-mounted flexible equipment with a period of 0.03 seconds or greater.

range (20→30 Hz) appears only due to El Centro W-E, El Centro N-S and AECL seismic ground motions. The torsional coupling and its influence on the floor response spectra are affected by the shape of the ground response spectrum, i.e., by the frequency content of the applied seismic ground motion.

6. The (+ve) and (-ve) edge spectral acceleration values associated with the higher frequency range (20→30 Hz) are more pronounced due to El Centro W-E, El Centro N-S and AECL seismic ground motions. This observation is made by examining Figures 4.4, 4.5, 4.8 and 4.9 (showing the (+ve) and (-ve) edge lateral floor spectra) and it can be drawn, also, from Figures 4.10 and 4.11 (showing the rotational floor response spectra).

7. The amplification factors (equipment to structure), shown in Tables 4.1.a to 4.8.a, vary significantly for the different cases of study but they are far below the maximum amplification factor $(\frac{1}{2\zeta})$ which may be developed during harmonic steady state vibration. In this particular study, the maximum amplification factor observed has a value of 15.34 in the extreme case of San Fernando earthquake record (a narrow band spectrum matching the predominant frequency of the reactor building) compared to a steady state value of 50 for a secondary damping ratio of 1%. This maximum value occurs at mass m_4 and is associated with the second mode of vibration of the uncoupled model. The minimum value for the same mass of the uncoupled model (and matching the same frequency) has a value of 7.0 in the case of El Centro N-S. The amplification factor is doubled due to different seismic ground motions.

8. Similar to the amplification factors (equipment to structure) developed, due to the lateral response, the rotational amplification factors (equipment to structure) exist, due to the rotational response. The rotational amplification factors, shown in Tables 4.9 and 4.10, have a maximum value of 14.0 (corresponding to mass m_3 and associated with mode 2) in the case of the San Fernando earthquake record, and a minimum value of 1.88 (for the same mass and matching the same frequency) in the case of El Centro W-E. The rotational amplification variation may be as high as 7 times due to different seismic ground motions.

CHAPTER V

GENERATION OF LATERAL AND ROTATIONAL FLOOR RESPONSE SPECTRA BY AN ALTERNATIVE APPROACH

5.1 Introduction

In addition to the time-history analysis technique there are some simplified procedures for the construction of floor response spectra. A brief description of these methods is presented in Section 1.2 of Chapter 1. None of these methods considers the rotational floor response spectra.

It is the purpose of this chapter to investigate a deterministic method to generate the lateral and rotational floor spectra by using an alternative definition of floor response spectra based on a theoretical formulation. It is shown that the spectral values obtained by filtering the ground motion first through the structure and the resulting lateral-rotational motions through simple oscillators are equal to the maximum lateral-rotational responses of the structure developed when the order of filtration is reversed. Based on this preceeding concept a deterministic method is presented to construct the lateral and rotational floor response spectra using the response spectrum technique.

5.2 Theoretical Formulation

The equations of motion for a lumped mass coupled lateral-torsional system, with one axis of symmetry, subjected to base ground excitation $\ddot{u}_{gy}(t)$ are given in equation (2.24).

The expression for the relative displacements of equation (2.24) may be obtained from Duhamel's integral (43)

$$\underset{2n\times 1}{\begin{Bmatrix} \underline{u}_y(t) \\ \underline{u}_\theta(t) \end{Bmatrix}} = -\int_0^t \underset{2n\times 2n}{\begin{bmatrix} \\ \underline{G}(t_1) \\ \\ \end{bmatrix}} \underset{2n\times 2n}{\begin{bmatrix} [M] & [0] \\ [0] & [M] \end{bmatrix}} \underset{2n\times 1}{\begin{Bmatrix} \underline{1} \\ \underline{0} \end{Bmatrix}} \ddot{u}_{gy}(t-t_1)dt_1 \tag{5.1}$$

in which $[\underline{G}(t)]$ is the impulse response function matrix. The expression for the relative velocities may be obtained by differentiating equation (5.1); the resulting equation takes the form

$$\underset{2n\times 1}{\begin{Bmatrix} \dot{\underline{u}}_y(t) \\ \dot{\underline{u}}_\theta(t) \end{Bmatrix}} = -\int_0^t \underset{2n\times 2n}{\begin{bmatrix} \\ \dot{\underline{G}}(t_1) \\ \\ \end{bmatrix}} \underset{2n\times 2n}{\begin{bmatrix} [M] & [0] \\ [0] & [M] \end{bmatrix}} \underset{2n\times 1}{\begin{Bmatrix} \underline{1} \\ \underline{0} \end{Bmatrix}} \ddot{u}_{gy}(t-t_1)dt_1 \tag{5.2}$$

A further differentiation will give the absolute acceleration vector

$$\underset{2n\times 1}{\begin{Bmatrix} \ddot{\underline{u}}_y(t) \\ \ddot{\underline{u}}_\theta(t) \end{Bmatrix}} = \underset{2n\times 1}{\begin{Bmatrix} \ddot{\underline{u}}_y(t) \\ \ddot{\underline{u}}_\theta(t) \end{Bmatrix}} + \underset{2n\times 1}{\begin{Bmatrix} \underline{1} \\ \underline{0} \end{Bmatrix}} \ddot{u}_{gy}(t)$$

$$= -\int_0^t \underset{2n\times 2n}{\begin{bmatrix} \\ \ddot{\underline{G}}(t_1) \\ \\ \end{bmatrix}} \underset{2n\times 2n}{\begin{bmatrix} [M] & [0] \\ [0] & [M] \end{bmatrix}} \underset{2n\times 1}{\begin{Bmatrix} \underline{1} \\ \underline{0} \end{Bmatrix}} \ddot{u}_{gy}(t-t_1)dt_1 \tag{5.3}$$

In the above differentiation the following properties of the impulse response matrix are used (43)

$$\underset{t\to 0}{\lim} \underset{2n\times 2n}{[\underline{G}(t)]} = \underset{2n\times 2n}{[\underline{0}]}, \qquad \underset{t\to 0}{\lim} \underset{2n\times 2n}{[\dot{\underline{G}}(t)]} = \underset{2n\times 2n}{[\underline{M}]^{-1}} \tag{5.4}$$

The absolute acceleration of the ith degree-of-freedom may then be obtained from equation (5.3) as

$$\begin{Bmatrix} \ddot{z}_{yi}(t) \\ \ddot{z}_{\theta i}(t) \end{Bmatrix} = -\int_0^t \begin{bmatrix} \sum_{j=1}^{n} \ddot{g}_{ij}(t_1)m_j \\ \sum_{K=n+1}^{2n} \ddot{g}_{iK}(t_1)m_{K-n} \end{bmatrix} \ddot{u}_{gy}(t-t_1)dt_1 \qquad (5.5)$$

in which $g_{ij}(t)$ and $g_{iK}(t)$ are the i,jth and i,Kth elements of $[\underset{2n\times 2n}{G}(t)]$.

The response spectra are defined as the maximum responses of a simple oscillator over a range of values of its natural period and damping, subjected to a prescribed base motion. Considering the response spectra of the lateral and rotational motion, the equations of motion of the two simple oscillators are

$$\ddot{A} + 2\beta\omega\dot{A} + \omega^2 A = -\ddot{z}_{yi}(t) \qquad (5.6.a)$$

$$\ddot{B} + 2\beta\omega\dot{B} + \omega^2 B = -\ddot{z}_{\theta i}(t) \qquad (5.6.b)$$

where β is the percentage of critical damping and ω is the natural frequency of the oscillator.

The lateral and rotational acceleration response spectra $S_y^i(\beta,\omega)$ and $\tilde{S}_\theta^i(\beta,\omega)$ may be given as

$$S_y^i(\beta,\omega) = \max\left[-\int_0^t \ddot{g}(t_1)\ddot{z}_{yi}(t-t_1)dt_1\right] \qquad (5.7.a)$$

$$\tilde{S}_\theta^i(\beta,\omega) = \max\left[-\int_0^t \ddot{g}(t_1)\ddot{z}_{\theta i}(t-t_1)dt_1\right] \qquad (5.7.b)$$

where g(t) is the impulse response function of the simple oscillators described in equations (5.6.a) and (5.6.b). Substituting equation (5.5) into equations (5.7.a) and (5.7.b) yields

$$S_y^i(\beta,\omega) = \max\left[\int_0^t \ddot{g}(t_1)\int_0^{t-t_1}\sum_{j=1}^{n}\ddot{g}_{ij}(t_1)m_j\,\ddot{u}_{gy}(t-t_1-t_2)dt_2dt_1\right] \tag{5.8.a}$$

$$\tilde{S}_\theta^i(\beta,\omega) = \max\left[\int_0^t \ddot{g}(t_1)\int_0^{t-t_1}\sum_{K=n+1}^{2n}\ddot{g}_{iK}(t_1)m_{K-n}\,\ddot{u}_{gy}(t-t_1-t_2)dt_2dt_1\right] \tag{5.8.b}$$

For a given oscillator damping and frequency, equations (5.8.a) and (5.8.b) define the magnitude of a spectral absolute lateral and rotational acceleration, respectively.

For an alternative description of this quantity consider the identical lateral oscillator being subjected to the prescribed ground motion directly. The equation of motion of this simple oscillator becomes

$$\ddot{A}^0 + 2\beta\omega\dot{A}^0 + \omega^2 A^0 = -\ddot{u}_{gy}(t) \tag{5.9}$$

and the absolute acceleration of the simple oscillator $\ddot{v}^0(t)$ will be

$$\ddot{v}^0(t) = -\int_0^t \ddot{g}(t_1)\ddot{u}_{gy}(t-t_1)dt_1 \tag{5.10}$$

Now, consider the coupled structural system of equation (2.18) being excited by a base motion which is identical to $\ddot{v}^0(t)$ (the absolute acceleration of the single oscillator) the equations of motion take the form

$$\begin{bmatrix}[M] & [0]\\ [0] & [M]\end{bmatrix}\begin{Bmatrix}\ddot{\underline{u}}_y^0\\ \ddot{\underline{u}}_\theta^0\end{Bmatrix} + \begin{bmatrix}[K_{yy}] & [K_{y\theta}]\\ [K_{y\theta}]^T & [K_{\theta\theta}]\end{bmatrix}\begin{Bmatrix}\underline{u}_y^0\\ \underline{u}_\theta^0\end{Bmatrix} = -\begin{Bmatrix}[M]\{1\}\ddot{v}^0(t)\\ 0\end{Bmatrix} \tag{5.11}$$

The absolute accelerations become

$$\begin{Bmatrix} \ddot{z}^0_{yi} \\ \ddot{z}_{\theta i} \end{Bmatrix} = -\int_0^t \begin{Bmatrix} \sum_{j=1}^{n} \ddot{g}_{ij}(t_1)m_j \\ \sum_{K=n+1}^{2n} \ddot{g}_{iK}(t_1)m_{K-n} \end{Bmatrix} \ddot{v}^0(t-t_1)dt_1 \qquad (5.12)$$

Substituting equation (5.10) into equation (5.12) one obtains

$$\begin{Bmatrix} \ddot{z}^0_{yi}(t) \\ \ddot{z}^0_{\theta i}(t) \end{Bmatrix} = \int_0^t \begin{Bmatrix} \sum_{j=1}^{n} \ddot{g}_{ij}(t_1)m_j \\ \sum_{K=n+1}^{2n} \ddot{g}_{iK}(t_1)m_{K-n} \end{Bmatrix} \int_0^{t-t_1} \ddot{g}(t_2)\ddot{u}_{gy}(t-t_1-t_2)dt_2dt_1 \qquad (5.13)$$

Changing the order of the integration and taking its maximum value results in

$$\max[\ddot{z}^0_{yi}(t)] = \max\left[\int_0^t \ddot{g}(t_2) \int_0^{t-t_2} \sum_{j=1}^{n} \ddot{g}_{ij}(t_1)m_j \, \ddot{u}_{gy}(t-t_2-t_1)dt_1dt_2\right] \qquad (5.14.a)$$

$$\max[\ddot{z}^0_{\theta i}(t)] = \max\left[\int_0^t \ddot{g}(t_2) \int_0^{t-t_2} \sum_{K=n+1}^{2n} \ddot{g}_{iK}(t_1)m_{K-n} \, \ddot{u}_{gy}(t-t_2-t_1)dt_1dt_2\right] \qquad (5.14.b)$$

Comparing equations (5.8.a) and (5.8.b) with (5.14.a) and (5.14.b) respectively, yields

$$S^i_y(\beta,\omega) = \max[\ddot{z}^0_{yi}(t)] \qquad (5.15.a)$$

$$\tilde{S}^i_\theta(\beta,\omega) = \max[\ddot{z}^0_{\theta i}(t)] \qquad (5.15.b)$$

That is, for a given simple oscillator (with specific damping and natural frequency) the corresponding spectral lateral and rotational accelerations of the structural response of the ith degree-of-freedom, when the structural system is subjected to a prescribed ground motion, is equal to the maximum absolute lateral and rotational acceleration of that degree-of-freedom when the system is excited by a support motion which is obtained by filtering the prescribed ground motion through the simple lateral oscillator.

5.3 Estimation of Lateral-Rotational Floor Response Spectra

The procedure to generate the lateral-rotational floor response spectra is to use as input to the structure the secondary spectra (43); this set of secondary spectra is developed in two steps: the first step is to filter the prescribed ground motion through simple oscillators having natural periods corresponding to the periods at which the floor spectral values are to be calculated. The percentage damping value assigned to the simple oscillators will be equal to that of the desired floor spectra e.g. equipment level of damping. The second step is to determine the response spectra of each filtered motion by standard techniques (40). To compute the maximum responses of the structure using the secondary spectra, the structure itself is first decomposed into its coupled lateral-rotational modes of vibration. The maximum absolute lateral acceleration, for mode "i", may be given by

$$R_{yij} = \Gamma_{yi} S_i^s \phi_{yij} \tag{5.16.a}$$

and the maximum relative rotational acceleration, for mode "i", may be written in the form

$$\tilde{R}_{\theta iK} = \Gamma_{yi} S_{ir}^s \tilde{\phi}_{\theta iK} \tag{5.16.b}$$

in which Γ_{yi} is the lateral modal participation factor of the ith mode of vibration and may be written as

$$\Gamma_{yi} = \frac{\sum_{j=1}^{n} m_j \phi_{yij}}{\sum_{j=1}^{n} m_j (\phi_{yij})^2 + \sum_{K=n+1}^{2n} m_{K-n} (\tilde{\phi}_{\theta iK})^2} \tag{5.17}$$

S_i^s is the secondary acceleration required to generate the lateral floor response spectrum for mode "i" and $S_{ir}^{s\,*}$ is the relative secondary spectral acceleration required to generate the induced rotational floor response spectrum for mode "i", and ϕ_{yij} and $\phi_{\theta iK}$ are the ith coupled lateral-rotational mode shapes of mass "j" of the structure. Note that the percentage damping value assigned to the secondary spectra is equal to that of the reactor building structure (ζ).

An estimate of the maximum response is determined by combining the modal maxima according to the relation (28)

$$R_{yj} = \sqrt{\sum_{i=1}^{2n} \bar{R}_{yij}^2 + \sum_{i=1}^{2n}\sum_{\ell=1}^{2n} R_{yij}\, R_{y\ell j}/(1+\epsilon_{i\ell}^2)} \qquad i \neq \ell \quad (5.18.a)$$

$$\tilde{R}_{\theta K} = \sqrt{\sum_{i=1}^{2n} \bar{\tilde{R}}_{\theta iK}^2 + \sum_{i=1}^{2n}\sum_{\ell=1}^{2n} \tilde{R}_{\theta iK}\, \tilde{R}_{\theta \ell K}/(1+\epsilon_{i\ell}^2)} \qquad i \neq \ell \quad (5.18.b)$$

where

$$\epsilon_{i\ell} = \frac{\sqrt{1-\zeta^2}}{\zeta}\ \frac{\omega_i - \omega_\ell}{\omega_i + \omega_\ell}$$

The first term in equations (5.18.a) and (5.18.b) represents the more commonly used combination rule: square-root-of-the-sum-of-the-squares of the modal maxima. The second term is important under certain conditions, in particular when two of the natural frequencies of the structure are close. As this is often the case for structures with coupled lateral-torsional motions in their modes of vibration,

---

*$S_{ir}^s = S_i^s - ZPA^s$ (ZPA^s is the zero period acceleration of the Secondary Response Spectra).

the second term has to be considered as well. For obtaining the system response, an acceptable method (8,55) which is derived from the relation given in equation (5.18.a) is to take the absolute sum (ABS) of the response of the closely-spaced modes and combine this sum with other remaining modal responses using the square root of the sum of the squares (SRSS) rule. The closely spaced modes should be divided into groups that include all modes having frequencies lying between the lowest frequency in the group and a frequency 10 percent higher (55). The most probable system responses R_{yj} and $\tilde{R}_{\theta K}$ are given by

$$R_{yj} = \sqrt{\sum_{i=1}^{2n} \bar{R}_{yij}^2 + 2 \sum |R_{yij} R_{y\ell j}|} \qquad i \neq \ell \qquad (5.19.a)$$

$$\tilde{R}_{\theta j} = \sqrt{\sum_{i=1}^{2n} \bar{\tilde{R}}_{\theta iK}^2 + 2 \sum |\tilde{R}_{\theta iK} \tilde{R}_{\theta \ell K}|} \qquad i \neq \ell \qquad (5.19.b)$$

where the second summation shall be performed on all (i) and (ℓ) modes whose frequencies are closely spaced to each other.

5.4 Numerical Example — CANDU 600 Reactor Building

Consider the coupled lateral-torsional model of the typical CANDU reactor building described in Figure 2.8.b. The W-E component of the 1940 El Centro earthquake is used as the prescribed input motion.

The floor spectral accelerations at eight arbitrary periods (T=0.03,0.06,0.09,0.12,0.15,0.18,0.21 and 0.24 sec) are selected for comparison purposes. Hence, the input ground motion is filtered through eight lateral oscillators having respective natural periods of 0.03, 0.06, 0.09, 0.12, 0.15, 0.18, 0.21 and 0.24 sec. A damping ratio of 1% identical to that of the target floor spectra is assigned to all oscillators. From

the resulting motions, the secondary response spectra are generated for the 5% damping of the reactor building. Note that for each filtered motion, the secondary spectral acceleration ordinarily required are only those corresponding to the structure periods and modal damping values; therefore, the secondary spectra need not be generated for the whole period spectrum. The secondary spectral accelerations corresponding to the example structure periods are tabulated in Table 5.1.a and 5.1.b.

Once the secondary spectra are obtained and the coupled lateral-rotational mode shapes of the reactor building have been determined, the response spectrum method can be applied and the maximum system absolute lateral and rotational* accelerations are then computed. The modal maxima may be combined using equations (5.19.a) and (5.19.b).

The modal maxima of the first 12 modes of vibration are combined, for masses (m_3, m_4 and m_5) and the comparisons between the spectral lateral-rotational accelerations computed by the alternative approach and those determined by the conventional time history modal analysis are shown in Figures 5.1 to 5.3.

5.5 Discussion of Results

The results obtained in this chapter indicate that the following conclusions and recommendations can be made.

1. The procedure described in Section 5.3 to estimate the floor response spectra is more economical than a time-history analysis. The reactor building under consideration has 6 significant modes and it is desired, generally, to compute 50 floor spectral points for each of 12 locations

*The relative rotational accelerations are considered absolute values, as the rotational ground motion is not within the scope of this study.

Table 5.1.a: Secondary Spectral Acceleration (g) Required to Generate LFRS

Structural Period (sec)	$S_{33.3}$ Hz $S_{0.03}$ sec	$S_{16.6}$ Hz $S_{0.06}$ sec	$S_{11.1}$ Hz $S_{0.09}$ sec	$S_{8.3}$ Hz $S_{0.12}$ sec	$S_{6.6}$ Hz $S_{0.15}$ sec	$S_{5.5}$ Hz $S_{0.18}$ sec	$S_{4.7}$ Hz $S_{0.21}$ sec	$S_{4.1}$ Hz $S_{0.24}$ sec	Structural Frequency (Hz)
0.2022	0.5097	0.5373	0.5726	0.7887	1.4103	2.7300	6.3547	2.6764	4.95
0.1729	0.3760	0.3953	0.4976	0.8741	2.0196	3.9336	2.7202	1.5361	5.78
0.1002	0.3191	0.4933	1.1344	1.2725	1.0955	0.8705	1.1087	0.9014	9.98
0.0936	0.3352	0.4959	1.5513	1.0287	1.0328	0.8268	1.0676	0.8784	10.68
0.0704	0.2918	0.8837	0.5956	0.6819	0.8246	0.7410	0.9594	0.8236	14.20
0.0616	0.3324	1.8165	0.4485	0.6011	0.7842	0.7165	0.9315	0.8075	16.25
0.0548	0.3365	1.0177	0.4079	0.5616	0.7517	0.7052	0.9180	0.7977	18.24
0.0521	0.3413	0.7881	0.3992	0.5465	0.7385	0.6970	0.9127	0.7937	19.18
0.0410	0.4754	0.4682	0.3666	0.5066	0.6882	0.6763	0.8914	0.7803	24.40
0.0361	0.5229	0.4389	0.3424	0.4960	0.6776	0.6702	0.8842	0.7756	27.77
0.0349	0.5842	0.4257	0.3369	0.4934	0.6764	0.6686	0.8826	0.7746	28.69
0.0340	0.6069	0.4127	0.3330	0.4916	0.6757	0.6675	0.8815	0.7738	29.40
ZPA	0.2307	0.3333	0.2912	0.4608	0.6519	0.6507	0.8627	0.7606	ZPA

Table 5.1.b: Relative Secondary Spectral Acceleration (g) Required to Generate RFRS

	Structural Period (sec)	$S_{33.3}$ Hz $S_{0.03}$ sec	$S_{16.6}$ Hz $S_{0.06}$ sec	$S_{11.1}$ Hz $S_{0.09}$ sec	$S_{8.3}$ Hz $S_{0.12}$ sec	$S_{6.6}$ Hz $S_{0.15}$ sec	$S_{5.5}$ Hz $S_{0.18}$ sec	$S_{4.7}$ Hz $S_{0.21}$ sec	$S_{4.1}$ Hz $S_{0.24}$ sec	Structural Frequency (Hz)
1	0.2022	0.2790	0.2040	0.2814	0.3279	0.7584	2.0793	5.492	1.9158	4.95
2	0.1729	0.1453	0.0620	0.2064	0.4133	1.3677	3.2829	1.8575	0.7755	5.78
3	0.1002	0.0884	0.1600	0.8432	0.8117	0.4436	0.2198	0.2460	0.1408	9.98
4	0.0936	0.1045	0.1626	1.2601	0.5679	0.3809	0.1761	0.2049	0.1178	10.68
5	0.0707	0.0611	0.5504	0.3044	0.2211	0.1727	0.0903	0.0967	0.0630	14.20
6	0.0616	0.1017	1.4832	0.1573	0.1403	0.1323	0.0658	0.0688	0.0469	16.25
7	0.0548	0.1058	0.6844	0.1167	0.1008	0.0999	0.0545	0.0553	0.0371	18.24
8	0.0521	0.1106	0.4548	0.1080	0.0857	0.0866	0.0463	0.0500	0.0331	19.18
9	0.0410	0.2447	0.1349	0.0754	0.0458	0.0363	0.0256	0.0287	0.0197	24.40
10	0.0361	0.2922	0.1056	0.0512	0.0352	0.0257	0.0195	0.0215	0.0150	27.74
11	0.0349	0.3535	0.0924	0.0457	0.0326	0.0245	0.0179	0.0199	0.0140	28.69
12	0.0340	0.3762	0.0794	0.0418	0.0308	0.0238	0.0168	0.0188	0.0132	29.40

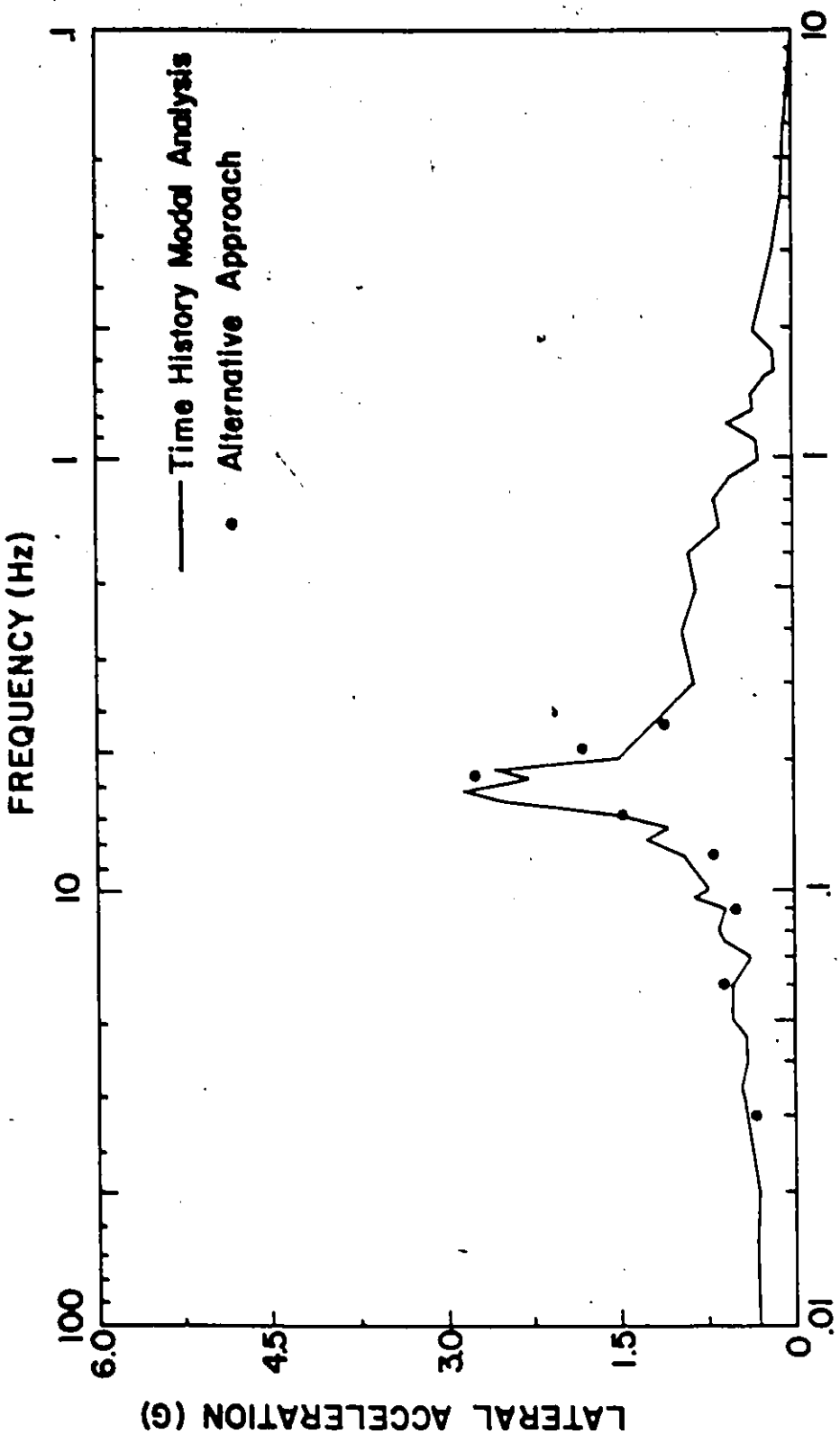

FIG. 5.1.a LFRS Mass m_3 - Comparison of Results

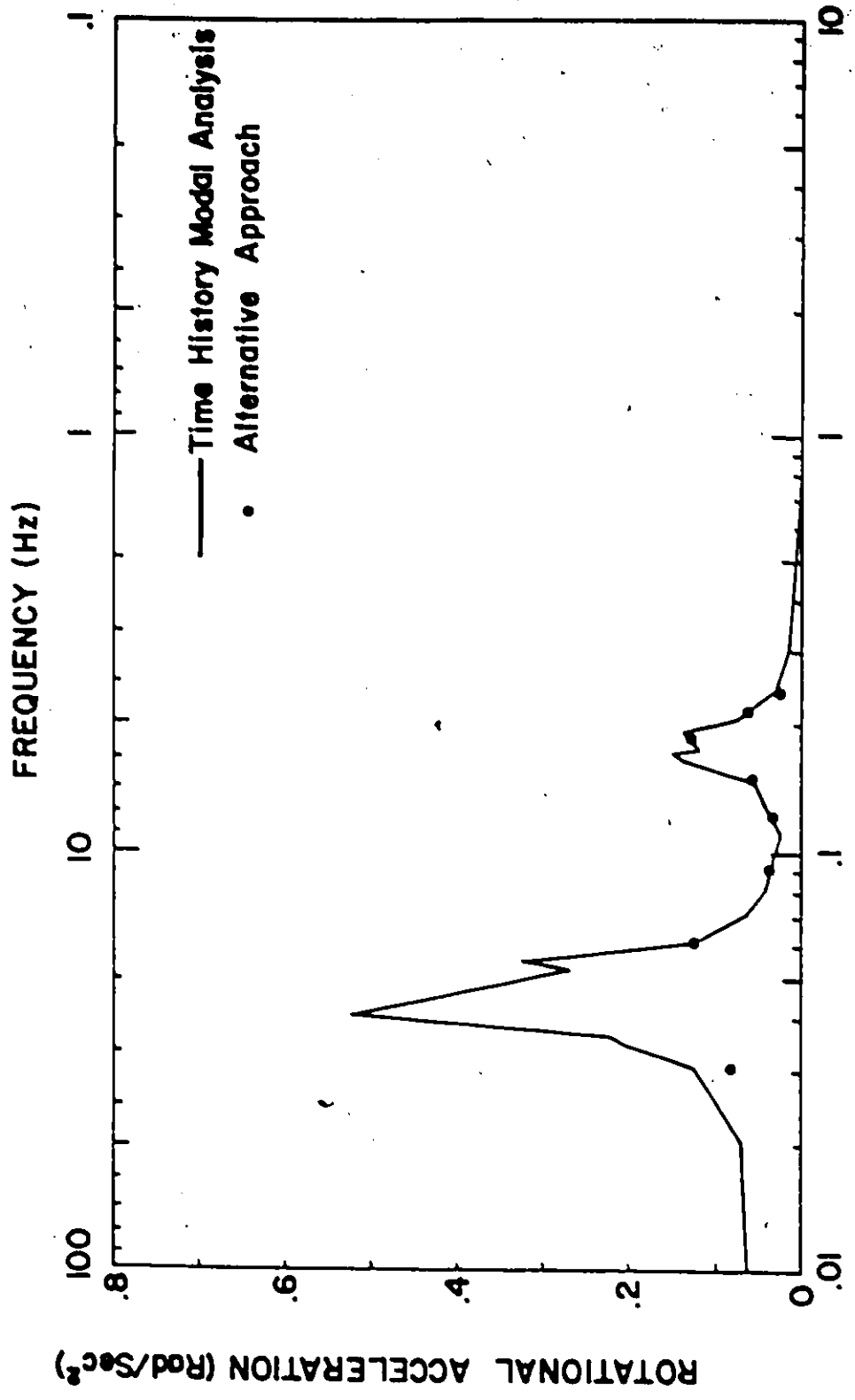

FIG. 5.1.b RFRS Mass - m_3 - Comparison of Results

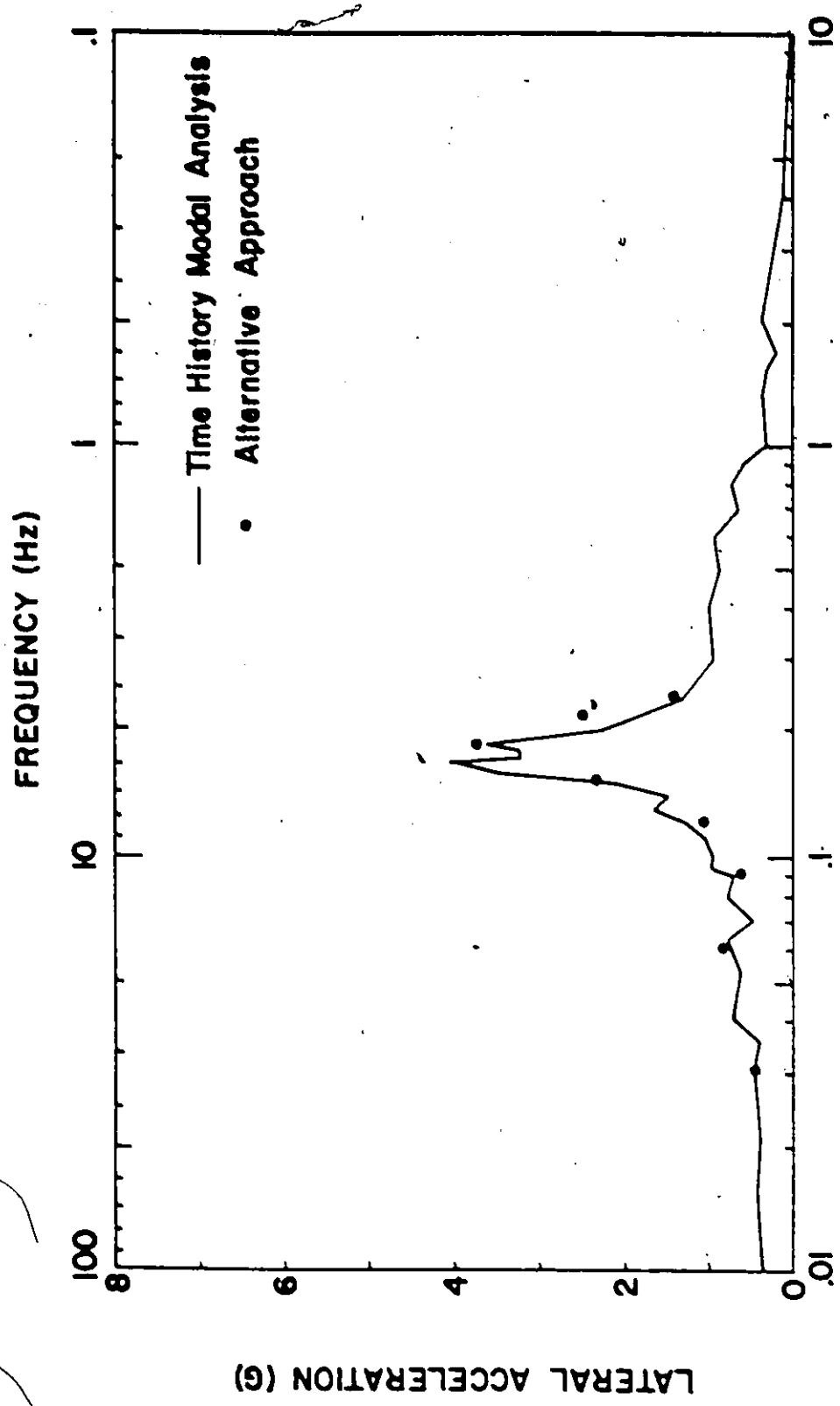

FIG. 5.2.a LFRS Mass m_4 – Comparison of Results

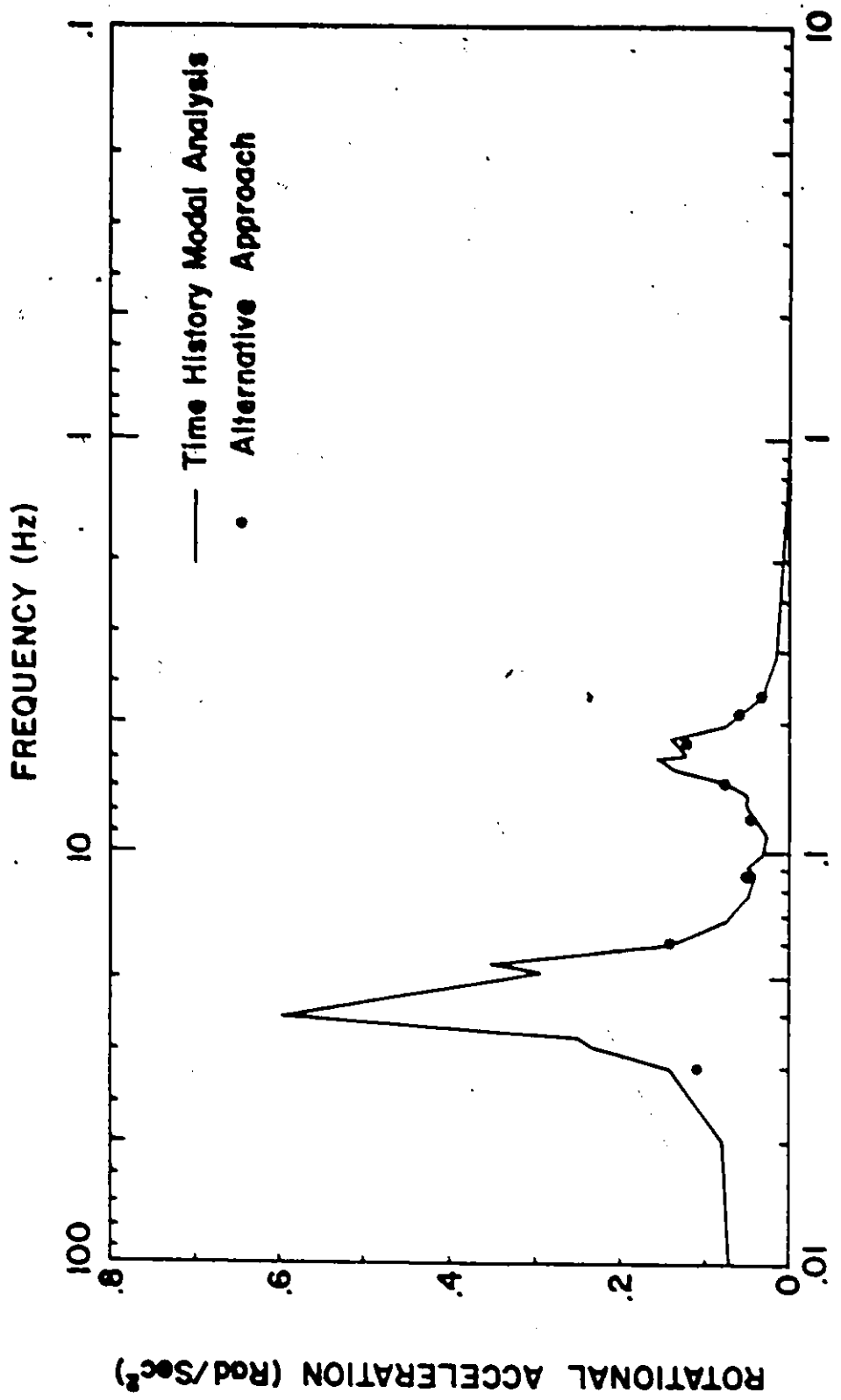

FIG. 5.2.b RFRS Mass m_4 - Comparison of Results

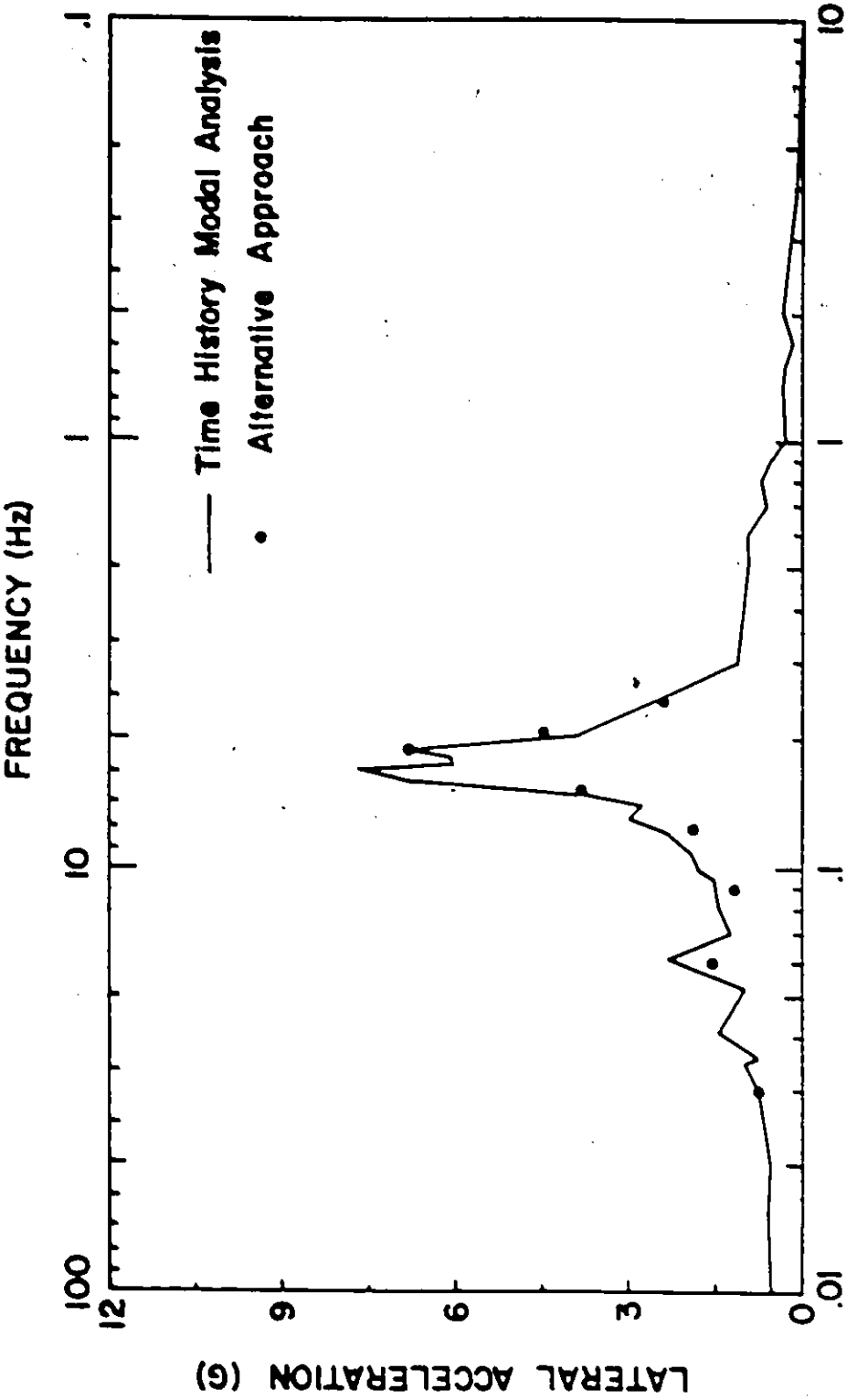

FIG. 5.3.a LFRS Mass m_8 - Comparison of Results

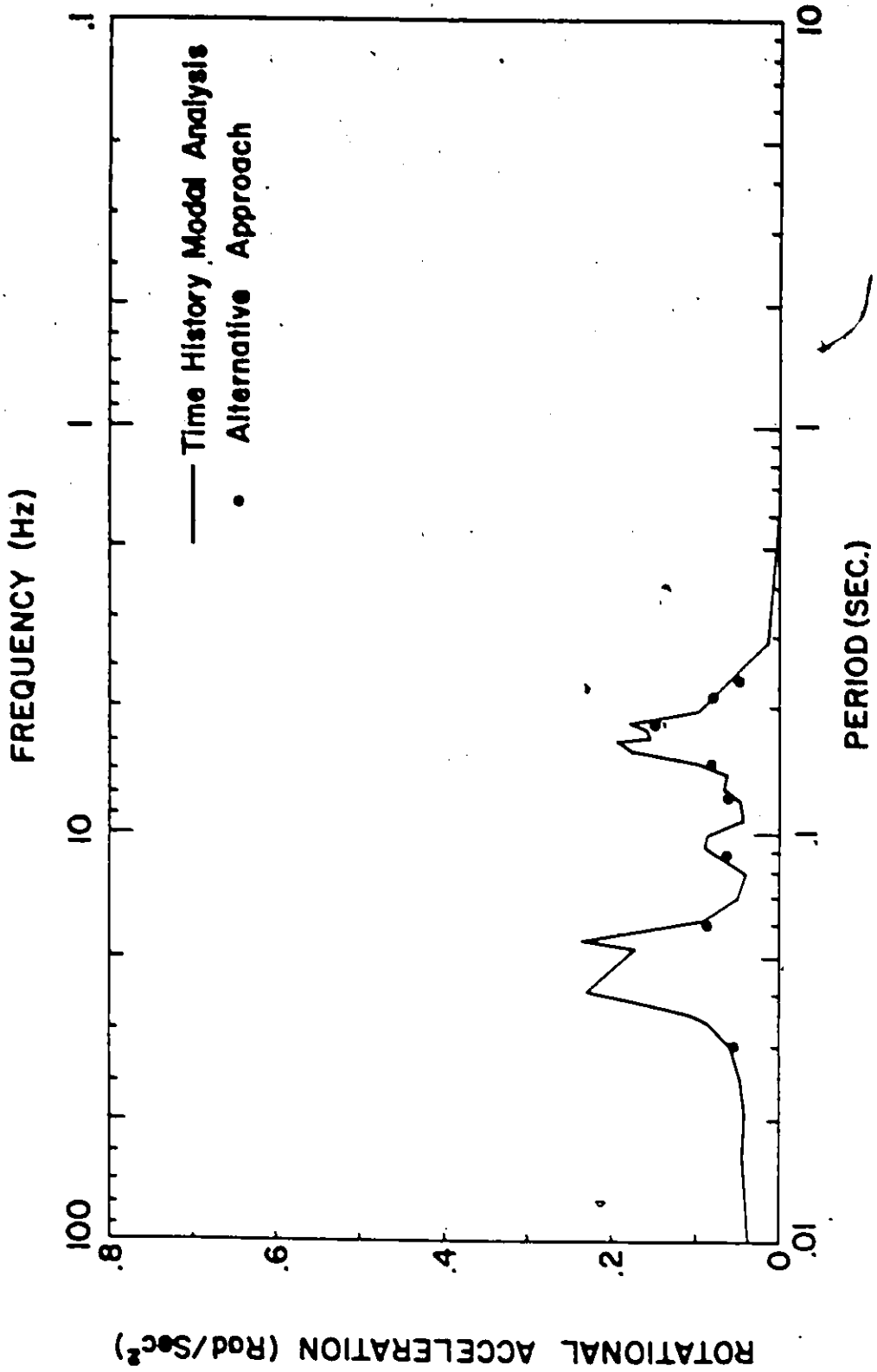

FIG. 5.3.b RFRS Mass m_8 - Comparison of Results

in the reactor building (12 mass levels). Taking as the bases for comparison the number of integrations of single DOF systems required in order to generate the spectra curves for a given damping, the time-history analysis would entail 6 modal and 50×12 spectral integrations for a total of 606 integrations. In the proposed procedure, one needs 50 integrations to produce the filtered motions and 50×6 integrations to evaluate the secondary spectra at the structural frequencies, giving a total of 350 integrations. Then the percentage savings for the proposed procedure may conveniently be of the order of 40%. Taking into consideration the effect of lateral location as well and generating the spectra at each of 3 horizontal locations (center, (+ve) edge and (-ve) edge) for the 12 mass levels will increase the time-history set of integrations only and as a result the percentage savings for the deterministic method may be as high as 80%.

2. It must be emphasized that for the procedure outlined herein, the base input is secondary response spectra rather than an acceleration time-history. This distinction is important because whereas it is impossible to describe one accelerogram representing all known earthquakes, it is possible to develop a set of secondary response spectra enveloping, with a high probability level, all their major characteristics. One way to obtain these generalized secondary spectra is to combine statistically a number of individual spectra derived from

the filtered records of known past earthquakes and by taking into consideration the soil conditions, distance from the epicenter, etc., of the recorded data. The resulting secondary spectra would then be representative of any known real earthquake with an appropriate scaling factor.

3. The only approximation involved in the proposed alternative approach to generate the floor response spectra is in the computation of maximum responses from a given secondary response spectrum. This, of course, may be diminished as more sophisticated methods of combining modal maxima are developed.
4. A similar procedure may be developed to include the effect of torsional ground motion which can be considered as a desirable subject for future research.

CHAPTER VI

EFFECT OF ESTIMATED TORSIONAL GROUND MOTION ON LATERAL AND ROTATIONAL FLOOR RESPONSE SPECTRA

6.1 Introduction

In the previous chapters, lateral-torsional coupling and its influence on the seismic response of reactor systems have been investigated and lateral-rotational floor response spectra are generated for several cases of study using one lateral component of seismic ground motion.

In this last chapter, a separate investigation is presented where a rotational time history ground motion is generated in addition to the recorded lateral component; these two time history motions, i.e., lateral and rotational, are used as input motions applied at the base of a torsionally coupled reactor building and the coupled lateral-rotational floor responses are determined.

Each floor motion time history is then used as input to a series of damped single degree of freedom systems in order to determine the floor response spectra. The response results are analysed to study the influence of the estimated torsional ground motion on both the lateral and rotational floor response spectra of such a structure.

6.2 Torsional Ground Motion - Review of Previous Investigations

In 1969, Newmark (37) offered observations concerning torsion that could arise in symmetrical buildings from earthquake ground motions; he developed an approach for determing the effective eccentricity which simulates the torsional effect in a response spectrum analysis of a sym-

metrical structure. This approach considered the effect of building size, wave propagation velocity, and dynamic characteristics of the structure.

Another approach to evaluate the torsional effect has been presented by Dijulio and Hart (11, 21). In their approach, torsional response spectra have been obtained by solving the equation of motion of torsional response. The torsional ground acceleration is obtained by differentiating the recorded translational ground accelerations in two perpendicular horizontal directions.

Following the ideas of Newmark, a complete record of torsional ground motion was generated by Nathan and MacKenzie (35) using the two translational components of an earthquake record. The approximate spectra developed by Newmark are generally confirmed.

In 1976, Shibata et al (47) presented a short report summarizing the results of the observation of torsional ground motions using a newly developed moving-coil-type torsional motion pickup. To enable valid conclusions to be reached for design purposes, the authors indicate the need to continue such observations for many years.

More recently, Valathur and Shah (57) presented an approach to analyse structures for torsional effects arising from each of the two perpendicular horizontal excitations. Each component of horizontal motion is divided into two parts based on wave propagation velocity and building dimension. The two time-history motions (i.e., translational and torsional) are then used as input motions to the structure.

Recently, a computational scheme was presented by Tso and Hsu (53) to construct torsional spectra due to the rotational component of

seismic ground motions. The rotational component of ground motion is estimated from the measured earthquake acceleration records, assuming the surface ground motions at a site can be considered as a superposition of two independent non-dispersible waves propagating along perpendicular principal directions. Newmark's torsional spectrum for the 1940 El Centro earthquake is compared and found to underestimate the torsional effect by as much as 50 percent.

The torsional spectrum by Nathan and MacKenzie (35) is also compared with Tso and Hsu (53) spectrum and is found to underestimate the torsional response for short period structures and overestimate the torsional response for long period structures.

6.3 Estimation of Rotational Ground Motion

Based on these previous investigations a rotational time history ground motion may be generated in addition to the recorded lateral component. The two approaches by Nathan et al (35) and Tso et al (53) are selected as two different bases for the determination of the rotational time history ground motion of interest.

The limits of validity of Nathan's technique are based on the following assumptions:

1. The seismic motion consists of waves of constant shape travelling at constant horizontal velocity.
2. The plan dimension of the building in the direction of wave travel is much smaller than one wave length.
3. The presence of the building does not alter the wave shape.
4. The rotation of the base is equal to the rotation of the ground.

Following the technique of Nathan and MacKenzie (35), the rotational component would be given by

$$\ddot{u}_{g\theta}(t) = \frac{1}{2}\left[\frac{\ddot{u}_{gy}(t-X/c) - \ddot{u}_{gy}(t)}{X} - \frac{\ddot{u}_{gx}(t-Y/c) - \ddot{u}_{gx}(t)}{Y}\right] \quad (6.1)$$

in which X and Y are the plan dimensions of the building, $\ddot{u}_{gx}$ and $\ddot{u}_{gy}$ are the two lateral components of a given seismic ground motion in the horizontal direction and c is the constant shear wave velocity.

Using the north-south and east-west components of the 1940 El Centro earthquake records and assuming a shear wave velocity of 300 m/sec (984 ft/sec), the rotational input motion for a circular building (typical CANDU reactor) having a diameter of 45 m (148 ft) is generated.

The determination of the rotational component of a seismic ground motion by Tso's technique is based upon the following assumptions:

1. The surface ground motions are treated as a superposition of two non-dispersive propagating waves.
2. The spatial derivatives is approximated by the difference of ground motions at neighbouring points, since the wave form will not change from point to point (similar to Nathan's assumption).
3. The ground motions at any arbitrary point 0 are the result of a planar shear wave travelling from the epicenter towards the point 0.
4. The epicentral direction makes an angle ϕ with respect to the recording axis. This epicentral direction is determined by joining the instrument site to the epicenter of the earthquake.

Based on the computational scheme illustrated by Tso and Hsu (53), the rotational velocity $\dot{u}_{g\theta}(t)$ would be given by

$$\dot{u}_{g\theta}(t) = \frac{1}{2c} [\ddot{u}_{gx}(t) \sin\phi - \ddot{u}_{gy}(t) \cos\phi] \qquad (6.2)$$

where ϕ is the angle between the epicentral direction and the recording axis. The rotational acceleration $\ddot{u}_{g\theta}(t)$ may be computed by differentiation of the estimated rotational velocity $\dot{u}_{g\theta}(t)$.

Using the north-south component of the 1940 El Centro record as the x component with an angle ϕ of 26° (53) and assuming a shear wave velocity of 300 m/sec (984 ft/sec), the rotational acceleration time history is found.

In comparing the above two approaches considered, it should be noted that Nathan (35) has taken into consideration the width of the building and the validity of his method is based on the ratio between the building width and the shear wave velocity. According to the application of Newmark's spectrum (basis of Nathan's technique), the response should be inversely proportional to the shear wave velocity. The spectra determined by Nathan show the inverse relationship breaking down for natural periods below 0.5 sec, and again at periods in excess of 2 sec; the reason for this discrepancy is not justified.

In contrast to Nathan, Tso (53) has considered the ground motions, acting at a point, to be the result of a travelling planar shear wave from the epicenter of the earthquake to the instrument site. The torsional spectrum computed by Tso (53) is a conservative estimate of the effect of the rotational component of ground motions for the following reasons:

1. The time history records are assumed to be the result of horizontally propagating waves, but in reality, they are the result of a combination of both vertical and horizontal propagating waves.

2. The rotational component of ground motion is computed based on the assumption that the rotation caused by each of the non-dispersive waves propagating along the principal directions can be treated independently. The resulting rotational effect is taken as the sum of the rotational effects associated with each propagating wave. However, the phase interaction between the waves would reduce the rotational component and hence the torsional spectra as computed.
3. Considering the ground motion acting at a point represents an upper limit case of study.

Each of these time histories is applied to a series of damped torsional single degree-of-freedom oscillators and their maximum responses are plotted to obtain the torsional ground response spectra. Figure 6.1 shows the torsional ground spectra for the two techniques. The damping used is assumed to be 5 percent of the critical damping.

6.4 Mathematical Formulation of Structural Response

The equations of motion for a lumped mass coupled lateral-torsional system subjected to both lateral and rotational base ground excitations $\ddot{u}_{gy}(t)$ and $\ddot{u}_{g\theta}(t)$, respectively, may be expressed as

$$\begin{bmatrix} [M] & [0] \\ [0] & [M] \end{bmatrix} \begin{Bmatrix} \ddot{\underline{u}}_y \\ \ddot{\underline{u}}_\theta \end{Bmatrix} + \begin{bmatrix} [K_{yy}] & [K_{y\theta}] \\ [K_{y\theta}]^T & [K_{\theta\theta}] \end{bmatrix} \begin{Bmatrix} \underline{u}_y \\ \underline{u}_\theta \end{Bmatrix} = -\begin{Bmatrix} [M]\{1\}\ddot{u}_{gy}(t) \\ [M]\{r\}\ddot{u}_{g\theta}(t) \end{Bmatrix} \quad (6.3)$$

The above parameters are defined previously in Section 2.3.1.

The response of the structure to ground motions may be estimated by the modal superposition method. A major part of the computational effect required for such an analysis is expended in the computation of vibration frequencies and mode shapes which requires the

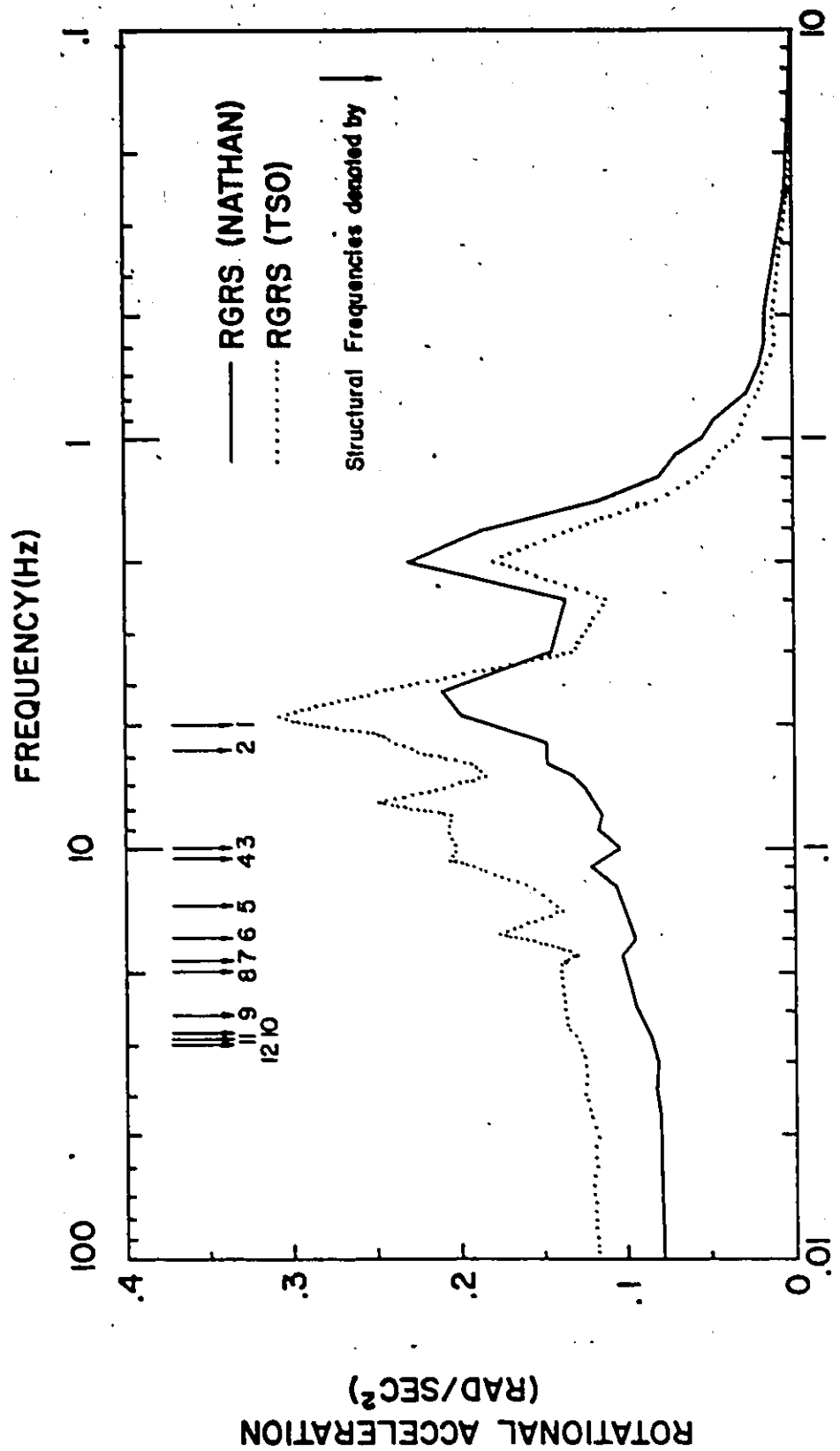

FIG. 6.1 Rotational Ground Response Spectra - 1940 El Centro (5% Damping)

solution of the eigenvalue problem mentioned in Section 2.3.1. Substitution of equations (2.22) and (2.23) into equation (6.3) yields for the ith mode of vibration

$$\begin{bmatrix} [M] & [0] \\ [0] & [M] \end{bmatrix} \begin{Bmatrix} \underline{\phi}_{yi} \\ \underline{\tilde{\phi}}_{\theta i} \end{Bmatrix} \ddot{T}_i(t) + \omega_i^2 \begin{bmatrix} [M] & [0] \\ [0] & [M] \end{bmatrix} \begin{Bmatrix} \underline{\phi}_{yi} \\ \underline{\tilde{\phi}}_{\theta i} \end{Bmatrix} T_i(t) = \begin{Bmatrix} [M]\{1\}\ddot{u}_{gy}(t) \\ [M]\{r\}\ddot{u}_{g\theta}(t) \end{Bmatrix} \tag{6.4}$$

Premultiplying equation (6.4) by $\{\underline{\phi}_{yi}\}^T\{\underline{\tilde{\phi}}_{\theta i}\}^T$ and using the orthogonality-normality relationship given in equation (2.28), equation (6.4) takes the form

$$\ddot{T}_i(t) + \omega_i^2 T_i(t) = -\{\phi_{yi}\}^T[M]\{1\}\ddot{u}_{gy}(t) - \{\tilde{\phi}_{\theta i}\}^T[M]\{r\}\ddot{u}_{g\theta}(t) \tag{6.5}$$

Introducing the modal viscous damping and rewritting the above equation in a convenient form gives

$$\ddot{T}_i(t) + 2\zeta\omega_i \dot{T}_i(t) + \omega_i^2 T_i(t) = -\Gamma_{yi}\ddot{u}_{gy}(t) - \Gamma_{\theta i}\ddot{u}_{g\theta}(t) \tag{6.6}$$

in which

$$\Gamma_{yi} = \{\phi_{yi}\}^T[M]\{1\} \tag{6.7.a}$$

$$\Gamma_{\theta i} = \{\tilde{\phi}_{\theta i}\}^T[M]\{r\} \tag{6.7.b}$$

Γ_{yi} and $\Gamma_{\theta i}$ are the ith modal participation factors in y direction and θ direction, respectively. Equation (6.6) is the combination of two equations of motion in the ith normal mode

$$\ddot{D}_i(t) + 2\zeta\omega_i \dot{D}_i(t) + \omega_i^2 D(t) = -\Gamma_{yi}\ddot{u}_{gy}(t) \tag{6.8.a}$$

$$\ddot{F}_i(t) + 2\zeta\omega_i \dot{F}_i(t) + \omega_i^2 F(t) = -\Gamma_{\theta i}\ddot{u}_{g\theta}(t) \tag{6.8.b}$$

in which

$$T_i(t) = D_i(t) + F_i(t) \qquad (6.9)$$

Equations (6.8.a) and (6.8.b) can then be solved by numerical integration (25) to determine the response in mode "i", the modal responses can then be superimposed to determine the overall system response. In this case of study, the coupled modal response factors associated with the lateral response parameter $\ddot{u}_{yj}$ of mass m_j are $(\Gamma_{yi}\phi_{yij}, \Gamma_{\theta i}\phi_{yij})$ and those associated with the rotational response parameter $\ddot{u}_{\theta j}$ are $(\Gamma_{\theta i}\tilde{\phi}_{\theta ij}, \Gamma_{yi}\tilde{\phi}_{\theta ij})$. The two terms $\Gamma_{\theta i}\phi_{yij}$ and $\Gamma_{yi}\tilde{\phi}_{\theta ij}$ are induced due to lateral-torsional coupling. The term $\Gamma_{\theta i}\tilde{\phi}_{\theta ij}$ is a direct measure of the rotational response due to rotational input motion analogy to the term $\Gamma_{yi}\phi_{yij}$ associated with the lateral response due to lateral input motion.

6.5 Numerical Example - CANDU 600 Reactor Building

Consider the coupled lateral-torsional model of the typical CANDU reactor building described in Figure 2.8.b. The W-E component of the 1940 El Centro earthquake is used as the prescribed lateral input motion and the time history rotational motions estimated by both Nathan's and Tso's techniques are used as the prescribed torsional input motions.

Applying the lateral and rotational input motions to the reactor building and using the time history modal analysis, the floor motions of each mass are determined: the modal damping is assumed to be 5% of the critical damping. The floor response spectra for mass m_3 (selected for comparison purposes) are generated using a secondary damping of 1%.

In order to be able to evaluate the effect of torsional ground motion, the rotational floor response spectra of mass m_3, obtained by applying the lateral and rotational input motions, are compared to the corresponding rotational spectrum induced by torsional coupling only. This comparison is shown in Figure 6.2.

The centroidal, (+ve) edge and (-ve) edge lateral floor response spectra of mass m_3, associated with the double input motions, are shown in Figure 6.3.

It seems that the centroidal floor response spectrum is not affected by the torsional ground motion regardless of whether Nathan's or Tso's motion is used.

The effect of torsional ground motion on the extreme edge floor spectra values is investigated by the comparison shown in Figures 6.4 and 6.5. The results of this investigation indicate that the following observations can be made:

1. The estimated torsional ground motion has a major effect on the rotational floor response spectrum. The peaks of the rotational spectrum are associated with the predominant torsional modes of vibration [4, 5 and 8] excited by the torsional ground motion, in addition to the contribution of the torsional coupling effect studied in the previous chapters.
2. The torsional coupling effect is concentrated in the frequency range associated with the strongly coupled natural frequencies. However, the torsional ground motion has an influence on the whole frequency range; such influence is due to the frequency content of the torsional ground motion considered in the analysis.

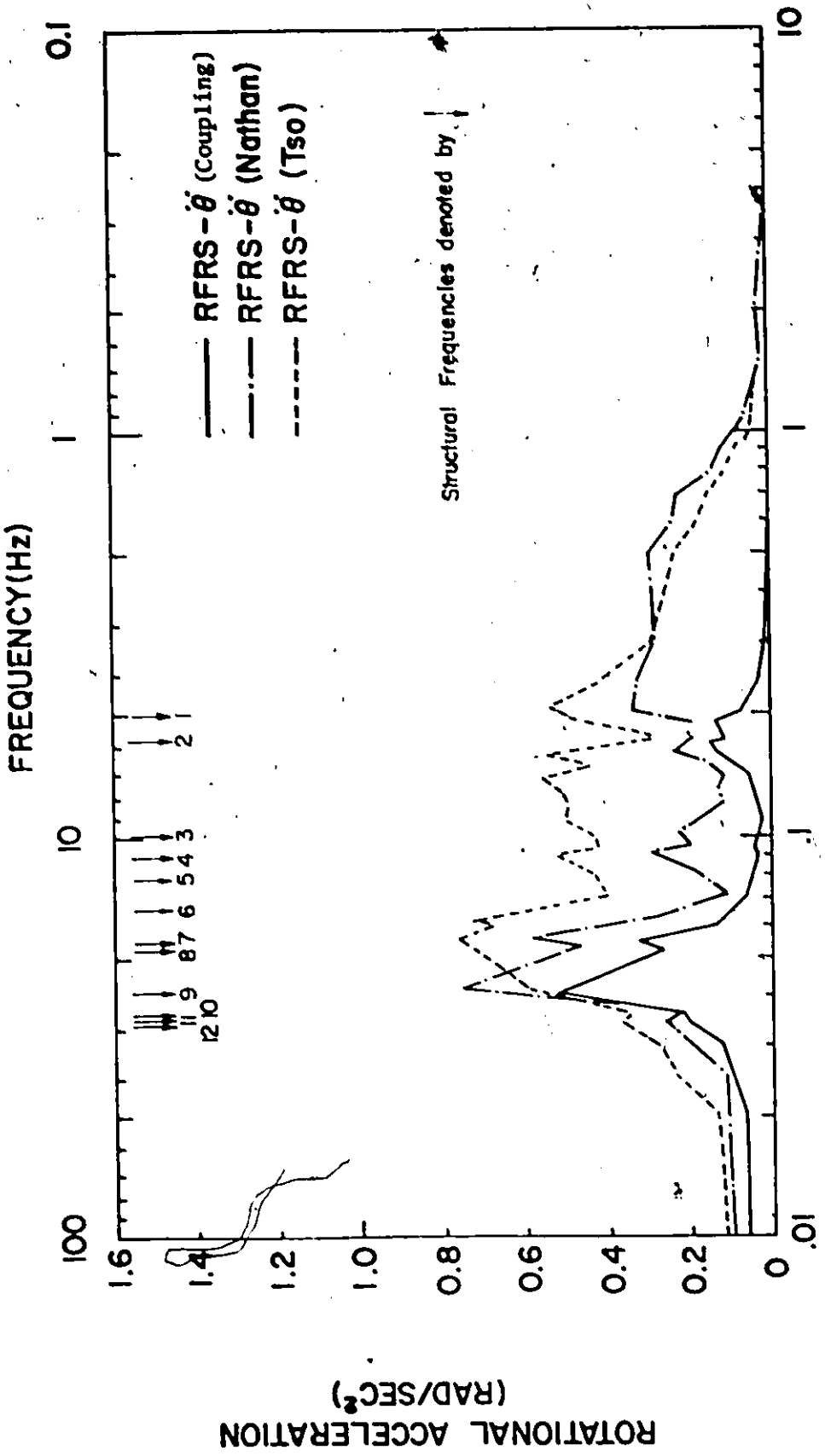

FIG. 6.2 Rotational Floor Response Spectra - Mass M_3 - 1940 El Centro (1% Damping)

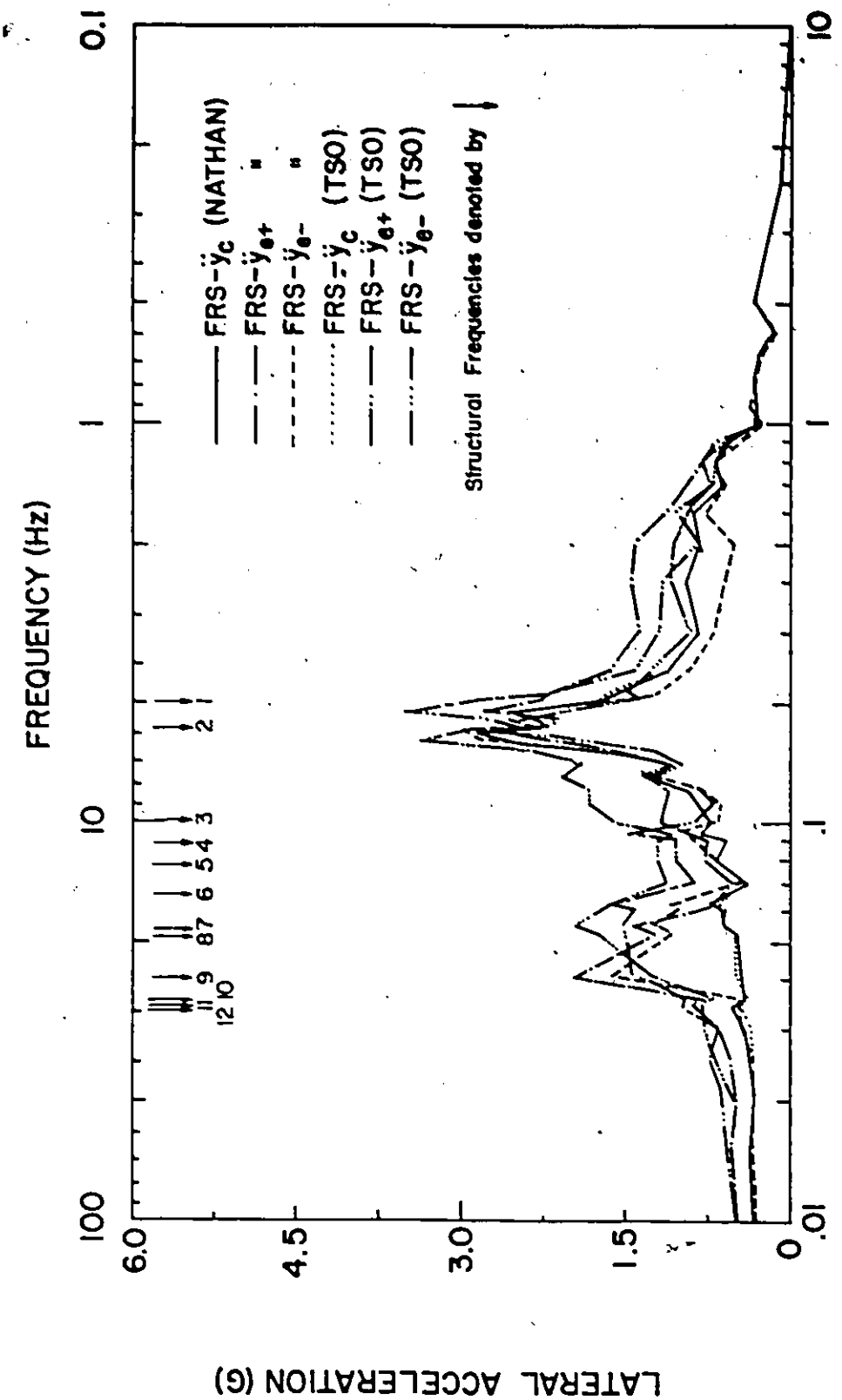

FIG. 6.3 Lateral Floor Response Spectra - Mass M_3 - 1940 El Centro - Lateral-Rotational Ground Motion (1% Damping)

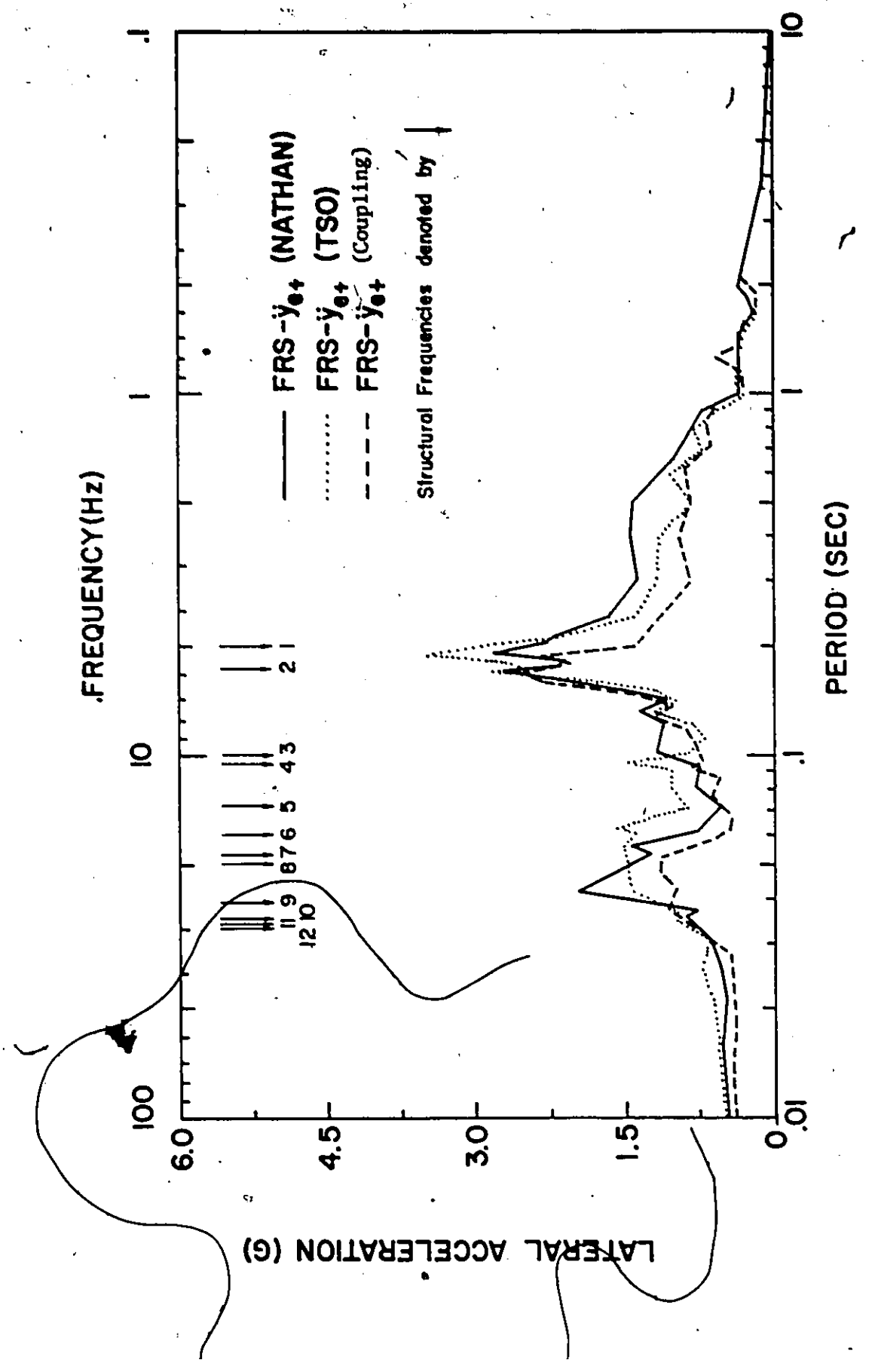

FIG. 6.4 (+ve) Edge Floor Response Spectra - Mass M_4
(1% Damping)

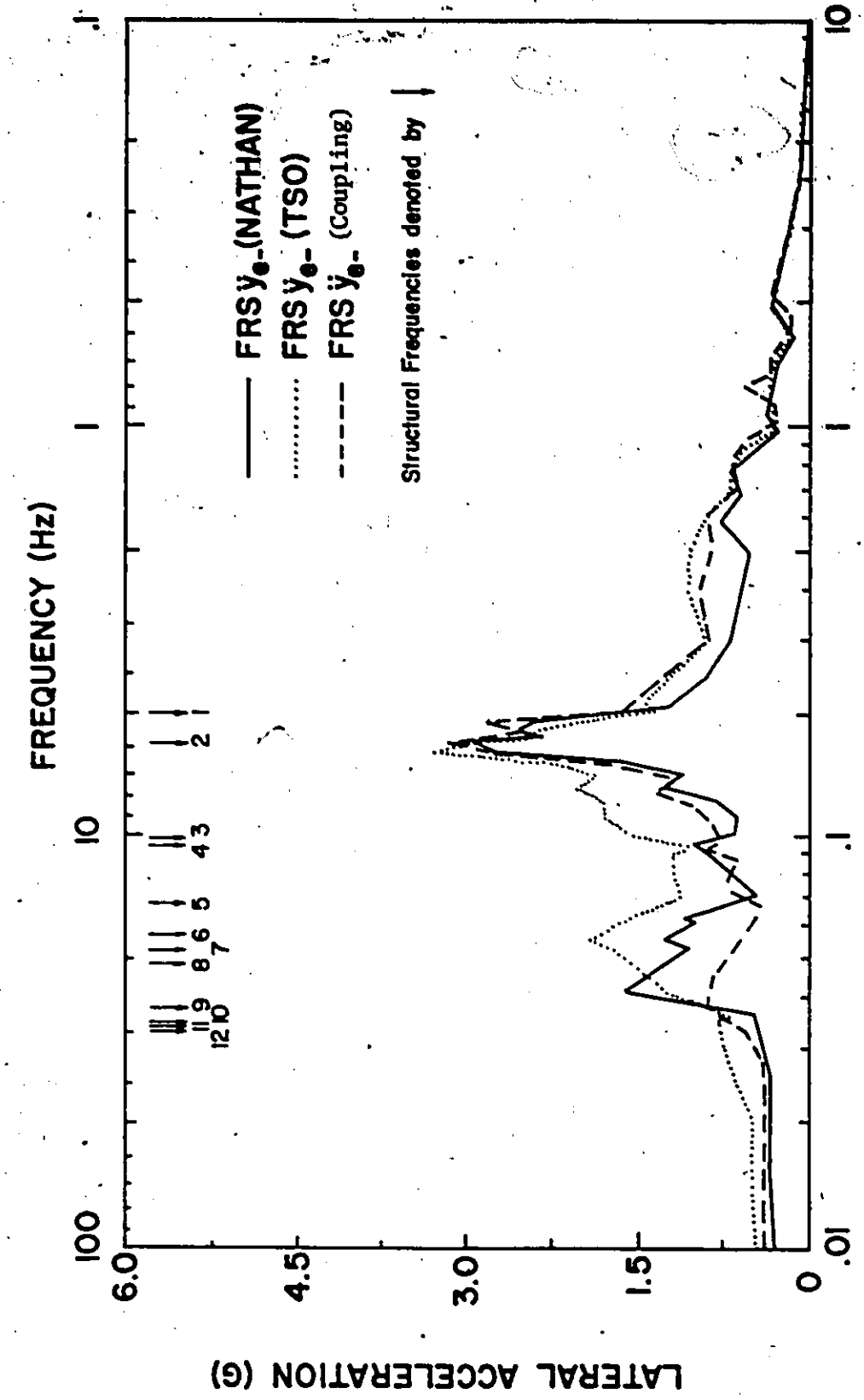

FIG. 6.5 (-ve) Edge Floor Response Spectra - Mass M_3
(1% Damping)

3. The edge lateral floor response spectra are strongly affected by taking into consideration the torsional ground motion effect. The contribution of the rotational floor motion in this case is significantly large.
4. The lateral variation of floor spectra ordinates is due not only to the induced rotational modal response factors ($\Gamma_{yi}\phi_{\theta ij}$) resulting from torsional coupling, but also to the rotational modal response factors ($\Gamma_{\theta i}\phi_{\theta ij}$) associated with the rotational response due to torsional ground motion. For this particular example, the largest variation of lateral floor response spectrum at the same elevation due to different plan locations is approximately 1.55 g. This occurs at the 9th structural frequency (24.4 Hz) for mass m_3.
5. The peaks of the edge floor spectra are associated with the frequency range corresponding to the predominant torsional natural frequencies of the structure as well as those of lateral predominance and also the range corresponding to the frequency content of both lateral and estimated rotational ground motions.

CHAPTER VII

CONCLUSIONS AND RECOMMENDATIONS

A research programme has been set up to study the effect of torsional coupling in the seismic response of reactor structures and components. In this programme a detailed study of the torsional coupling phenomena is presented, a mathematical model for a torsionally coupled reactor building is developed and a coupled analysis is investigated. Due to torsional coupling, the reactor building induces two dynamic inputs to the internal components; and hence lateral and rotational floor response spectra have to be determined. The concept of the rotational floor response spectra is developed and examined in this thesis.

Uncoupled and coupled floor response spectra are generated for excitation due to several different earthquakes and the floor spectra are analysed to consider the influence of the torsional coupling on the various response parameters.

A deterministic method is presented to construct the lateral-rotational floor response spectra without a detailed time history analysis. And, finally, the influence of an estimated torsional ground motion on both lateral and rotational floor response spectra is studied.

The results of this investigation indicate that the following conclusions and recommendations can be made:

7.1 General Conclusions

1. Coupling between lateral and torsional motions induces torsional response and in general reduces the lateral response.

2. The maximum responses (lateral and torsional) in a torsionally coupled system may be related to the maximum response (lateral) in the corresponding uncoupled system through simple interaction equations (single mass model).
3. The reactor building model represents the interaction of three different components: 1) internal structure, 2) containment wall, and 3) concrete vault. Torsional coupling is induced due to the eccentricities between the centers of mass and rigidity of the internal structure. As the internal structure rests on the same foundation of the containment wall and the dynamic response of each is affected by the presence of the other, the effect of torsional coupling may be transferred to the overall system. In this particular case of study (reactor building with fixed base) the torsional coupling is mainly affecting the internal structure. Such torsional effect is more pronounced in the higher frequency range (20 Hz → 30 Hz).
4. The torsional effect has some significance on the lateral floor spectra generated for different locations of equipment within the structure. The equipment response varies not only with respect to its elevation within the structure but also with its lateral location relative to the center of the building. It is the author's opinion that the asymmetry of a structure should be considered in the development of the floor spectra, and hence, it may be advisable either to develop floor spectra enveloping all floor locations or to generate floor spectra particularly for specific equipment location.
5. The concept of the rotational floor response spectra is a direct analogy to the floor response spectra concept which has been widely described in the literature.

6. The variation of the floor response spectra values generated using different earthquake records is significant , as would be expected, because these floor spectra are highly affected by the frequency content of the applied seismic ground motion. The variation of the rotational amplification factors is much higher than that of the lateral amplifications.
7. In addition to the time history analysis technique, a deterministic method is presented to generate the lateral and rotational floor response spectra by an alternative approach. The proposed method is based on a theoretical formulation and the only approximation involved in the alternative approach is in the computation of the maximum responses. This, of course, may be diminished as more sophisticated methods of combining modal maxima are developed.
8. The estimated torsional ground motion has major effect on the rotational floor response spectra. As a result, the edge lateral floor spectra are strongly affected especially at the frequency range corresponding to the torsional natural frequencies of the structure and also at the range corresponding to the frequency content of the estimated rotational ground motion.

7.2 Detailed Conclusions

1. The coupled dynamic properties depend only on the two dimensionless parameters:
   a) ω_θ/ω_y: the ratio of natural frequencies for uncoupled torsional and lateral motions of the corresponding uncoupled system.
   b) e/r: the ratio of eccentricity between centers of mass and rigidity to the mass radius of gyration.

2. The effect of torsional coupling depends strongly on (ω_θ/ω_y). If (ω_θ/ω_y) is too small the coupling depends on (e/r) and if (ω_θ/ω_y) is too large the coupling vanishes.
3. It is clear from the above conclusion that torsional coupling decreases by increasing the ratio (ω_θ/ω_y), i.e., by increasing the relative torsional stiffness of the structure to its lateral stiffness.
4. The concept of the rotational modal participation factor is a straight forward analogy to the well known concept of the lateral modal participation factor. A mathematical expression has been presented.
5. To express the degree of torsional coupling in any mode "i" a proposed overall modal coupling parameter $(OMCP)_{\theta i}$ is presented. The mathematical expression includes the mass, the mass radius of gyration and the coupled lateral-torsional mode shapes. The interaction of these parameters is governed by the summation over j (j=1,2,...,n, where n is the number of masses) to produce a mode-dependent coupling parameter.
6. The centroidal coupled floor response spectra values are usually smaller than the uncoupled ordinates, with several exceptions. Edge floor response spectra values can be higher or lower than the uncoupled ordinates depending upon frequency and degree of torsional coupling.
7. In the alternative approach, to generate the floor response spectra, it is shown that the spectral values, obtained by filtering the prescribed ground motion first through the structure and the resulting lateral-rotational motions through simple oscillators, are equal to the maximum lateral-rotational responses of the structure developed when the order of filtration is reversed.

7.3 Recommendations and Research Needs

1. The response phenomenon in the case of coupled lateral-torsional behaviour is much more complex than for the planar case. It seems that coupling decreases the peak floor response spectra value but does have the effect of broadening the floor spectra in the frequency range above the first significant mode. The reason for this observation escapes the author. It may be appropriate to do some additional studies in this area.
2. The effect of lateral-torsional coupling induced by the asymmetry of the internal structure and transferred to the overall reactor system through the base slab, may be more pronounced by taking into consideration the soil-structure interaction. Research in this direction is needed.
3. The estimation of torsional ground motion is based on a very limited set of data and by including many assumptions; the validity for more confident situations will require substantial analytical studies and experimental verifications.
4. A procedure, similar to the alternative approach to generate the floor response spectra without a time history analysis, may be developed to include the effect of torsional ground motion which can be considered as a desirable subject for future research.

REFERENCES

1. Aziz, T.S., and Duff, C.G., "Mass Coupling Effects in the Dynamic Analysis of Nuclear Power Plant Systems", The Joint ASME/CSME Pressure Vessels and Piping Conference, Montreal, Canada, June 25-30, 1978.

2. Aziz, T.S., and Duff, C.G., "Decoupling Criteria for Seismic Analysis of Nuclear Power Plant Systems", The Joint ASME/CSME Pressure Vessels and Piping Conference, Montreal, Canada, June 25-30, 1978.

3. Bathe, K.J., Wilson, E.L., and Peterson, F.E., "SAP IV - A Structural Analysis Programme for Static and Dynamic Response of Linear Systems", EERC Report No. 73-11, University of California, Berkeley, June 1973, revised April 1974.

4. Baruch, M., Gluck, J., and Mendelson, E., "Normal Modes for Non-symmetric Multi-storey Structures", Proceedings of Institution of Civil Engineer, Vol. 50, February 1972.

5. Bergstrom, R., Chu, S., and Small, R., "Seismic Analysis of Nuclear Power Plant Structures", Journal of the Power Division, ASCE, Vol. 97, No. P02, March 1971, pp. 367-393.

6. Biggs, J.M., and Roesset, J.M., "Seismic Analysis of Equipment Mounted on a Massive Structure, Seismic Design for Nuclear Power Plant", R.J. Hansen, editor, the M.I.T. Press, Cambridge, Massachusetts, 1970.

7. Biggs, J.M., "Seismic Response Spectra for Equipment Design in Nuclear Power Plants", Proceedings of the First International Conference on Structural Mechanics in Reactor Technology, Vol. 5, Part K, Berlin, Germany, September 1971.

8. Canadian Standards Associations, "Design Procedures for Seismic Qualification of CANDU Nuclear Power Plants", CSA Standard No. 289.3, Draft, February 1978.

9. Chen, C., "A Seismic Design of Asymmetric Structures and the Equipment Contained", Proceedings of the First International Conference on Structural Mechanics in Reactor Technology, Vol. 5, K4/4, Berlin, Germany, September 1971.

10. Chen, C., "Comments on Floor Response Spectra", Proceedings of the Second International Conference on Structural Mechanics in Reactor Technology, K4/3, Berlin, Germany, 1973.

11. Dijulio, R.M., and Hart, G.C., "Torsional Response of Buildings", UCLA Technical Report No. UCLA-ENG-7373, University of California, Los Angeles, California, December 1973.

12. Duff, C.G., "Simplified Method for Development of Earthquake Ground and Floor Response Spectra for Nuclear Power Plant Design", Proceedings of the Second Canadian Conference on Earthquake Engineering Research, Hamilton, Ontario, June 1975.

13. Duff, C.G., "Earthquake Response Spectra for Nuclear Power Plants using Graphical Methods", Proceedings of the Specialist Meeting on the Anti-Seismic Design of Nuclear Power Plant Installations, Paris, France, December 1975.

14. Duff, C.G., and Biswas, J.K., "Floor Response Spectra from Spectrum Compatible Motions", Proceedings of the Fourth International Conference on Structural Mechanics in Reactor Technology, K4/12, San Francisco, U.S.A., August 1977.

15. Fischer, E.G., "Seismic Qualification of Systems, Structures, Equipment and Components", Nuclear Engineering and Design, Vol. 46, 1978, pp. 151-167.

16. Gluck, J., "Lateral Load Analysis of Asymmetric Multi-storey Structures", Journal of the Structural Division, ASCE, Vol. 96, No. ST2, February 1970, pp. 317-333.

17. Gluck, J., and Gallert, M., "Three Dimensional Lateral Load Analysis of Multi-storey Structures", International Association for Bridge and Structural Engineering, 1972, pp. 77-80.

18. Hadjian, A.H., "Earthquake Forces on Equipment in Nuclear Power Plants", Journal of the Power Division, ASCE, Vol. 97, No. P03, July 1971, pp. 649-665.

19. Hadjian, A.H., "Some Problems with the Calculations of Seismic Forces on Equipment", Speciality Conference on Structural Design of Nuclear Power Plant Facilities, Vol. II, Chicago, Illinois, December 1973.

20. Hadjian, A.H., "On the Decoupling of Secondary Systems for Seismic Analysis", 6th World Conference on Earthquake Engineering, India, January 1977.

21. Hart, G.C., Dijulio, R.M., and Lew, M., "Torsional Response of High-Rise Buildings", Journal of the Structural Division, ASCE, Vol. 101, No. ST2, February 1975, pp. 397-417.

22. Heidebrecht, A.G., "Dynamic Analysis of Asymmetric Wall-Frame Buildings", Proceedings of the ASCE National Structural Engineering Convention, New Orleans, Louisiana, April 1975.

23. Hoerner, J.B., "Modal Coupling and Earthquake Response of Tall Buildings", Report No. EERL 71-07, Earthquake Engineering Research Laboratory, California Institute of Technology, Pasadena, California, May 1971.

24. Howard, G., Ibanez, P., and Smith, C., "Seismic Design of Nuclear Power Plant - An Assessment", Nuclear Engineering and Design, Vol. 38, 1976, pp. 385-461.

25. Ishac, M.F., "Dynamic Response of Asymmetric Shear Wall-Frame Building Structures", Thesis submitted in partial fulfilment of the requirements for the degree of Master of Engineering, McMaster University, Hamilton, Ontario, Canada, December 1975.

26. Jeanpierre, F., and Livolant, M., "Direct Calculation of Floor Response Spectra from the Fourier Transform of Ground Movement - Application to the Superphenix Fast Reactor Project", Nuclear Engineering and Design, Vol. 41, 1977, pp. 45-51.

27. Johnson, J., and Kennedy, R., "Earthquake Response of Nuclear Power Facilities", ASCE Fall Convention and Exhibit, San Francisco, October 17-21, 1977.

28. Kan, C.L., and Chopra, A.K., "Coupled Lateral Torsional Response of Buildings to Ground Shaking", Report No. 76-13, Earthquake Engineering Research Center, University of California, Berkeley, California, May 1976.

29. Kan, C.L., and Chopra, A.K., "Elastic Earthquake Analysis of Torsionally Coupled Multi-storey Buildings", Earthquake Engineering and Structural Dynamics, Vol. 5, 1977, pp. 395-412.

30. Kapur, K.K., and Shao, L.C., "Generation of Seismic Floor Response Spectra for Equipment Design", Transactions of the Speciality Conference on Structural Design of Nuclear Power Plant Facilities, Vol. I, ASCE, Chicago, Illinois, December 1973.

31. Keintzel, E., "On the Seismic Analysis of Unsymmetrical Storied Buildings", Proceedings of the 5th World Conference on Earthquake Engineering, Rome, 1977.

32. Mendelson, E., and Baruch, M., "Earthquake Response of Non-symmetric Multi-Storey Structures", The Structural Engineer, Vol. 51, 1973, pp. 61-70.

33. Mizuno, N., et al, "Seismic Response Analysis of Nuclear Reactor Buildings Under Constructuion of Soil-Structure Interaction with Torsional Behaviour", Proceedings of the Fourth International Conference on Structural Mechanics in Reactor Technology, K2/16, San Francisco, U.S.A., August 1977..

34. Muller, F., and Keintzel, E., "Approximate Analysis of Torsional Effects in the New German Seismic Code DIN 4149", Proceedings on the 6th European Conference on Earthquake Engineering, Yugoslavia, September 1978.

35. Nathan, N.D., and MacKenzie, J.R., "Rotational Components of Earthquake Motion", Canadian Journal of Civil Engineering, Vol. 2, 1975, pp. 430-436.

36. National Building Code of Canada 1977, National Research Council of Canada, Ottawa, Canada.

37. Newmark, N.M., "Torsion in Symmetrical Buildings", Proceedings of the Fourth World Conference on Earthquake Engineering, Vol. 2, Santiago, Chile, 1969.

38. Newmark, N.M., "Earthquake Response Analysis of Reactor Structures", Nuclear Engineering and Design, Vol. 20, 1972, pp. 303-322.

39. Newmark, N.M., Blume, J.A., and Kapur, K.K., "Design Response Spectra for Nuclear Power Plants", Journal of the Power Division, ASCE, Vol. 99, No. P02, November 1973, pp. 287-303.

40. Nigam, N.C., and Jennings, P.C., "Programme SPECEQ, A Digital Calculation of Response Spectra from Strong Motion Earthquake Records", NISEE Computer Applications, California Institute of Technology, Pasadena, California, June 1968.

41. Peters, K.A., Schmitz, D., and Wagner, U., "Determination of Floor Response Spectra on the Basis of the Response Spectrum Method", Nuclear Engineering and Design, Vol. 44, 1977, pp. 255-262.

42. Roberts, C.N., and Shipway, G.D., "Seismic Qualification - Philosophy and Methods", Journal of the Power Division, ASCE, Vol. 102, No. P01, January 1976, pp. 113-120.

43. Selcuk Atalik, T., "An Alternative Definition of Instructure Response Spectra", Earthquake Engineering and Structural Dynamics, Vol. 6, pp. 71-78, 1978.

44. Scanlan, R., and Sachs, K., "Earthquake Time Histories and Response Spectra", Journal of the Engineering Mechanics Division, ASCE, Vol. 100, No. EM4, August 1974, pp. 635-655.

45. Scavuzzo, R.J., and Lam, P.C., "Effect of Torsional Excitation on Equipment Seismic Loads", Proceedings of the Third International Conference on Structural Mechanics in Reactor Technology, K714, London, U.K., 1975.

46. Sharpe, R.L., "System Aspects of Seismic Design for Nuclear Plants", Journal of the Power Division, PO1, May 1973.

47. Shibata, H., Shigota, T., Sone, A., "On Some Results of Observation of Torsional Ground Motions and their Response Analysis", Bull., ERS, No. 10, 1976.

48. Stoykovich, M., "Methods of Determining Floor Design Response Spectra", ASCE-ASME Symposium, Pittsburgh, April 1972.

49. Stoykovich, M., "Criteria for Seismic Analysis of Nuclear Plant Structures and Substructures", Nuclear Engineering and Design, Vol. 27, 1974, pp. 106-120.

50. Takemori, Y., et al., "Analytical Procedure in Aseismic Design of Nuclear Power Facilities", ASCE Fall Convention and Exhibit, San Francisco, Obtober 17-21, 1977.

51. Tsai, N., "Spectrum-Compatible Motions for Design Purposes", Journal of the Engineering Mechanics Division, ASCE, Vol. 98, No. EM2, April 1972, pp. 345-356.

52. Tsai, N., and Tseng, W., "Standardized Seismic Design Spectra for Nuclear Plant Equipment", Nuclear Engineering and Design, Vol. 45, 1978, pp. 481-488.

53. Tso, W.K., and Hsu, T.J., "Torsional Spectrum for Earthquake Motions", Earthquake Engineering and Structural Dynamics, Vol. 5, 1978, pp. 375-382.

54. U.S. Nuclear Regulatory Commission, "Design Response Spectra for Seismic Design of Nuclear Power Plants", Regulatory Guide 1.60, December 1973.

55. U.S. Nuclear Regulatory Commission, "Combining Modal Responses and Spatial Components in Seismic Response Analysis", Regulatory Guide 1.92, February 1976.

56. U.S. Nuclear Regulatory Commission, "Development of Floor Design Response Spectra for Seismic Design of Floor-Supported Equipment or Components", Regulatory Guide 1.122, September 1976.

57. Valathur, M., and Shah, H., "Torsional Seismic Response of Symmetrical Structures", Journal of the Power Division, ASCE, Vol. 103, No. PO1, July 1977.

APPENDICES

APPENDIX I

NOTATIONS

a_{ys}, a_{zs}	- wall component eccentricities
a	- dimensionless parameter
$A_{A/C}$	- shear area in direction A/C
A,B,D,F	- function determining the variation with time
f	- frequency (Hz)
e, e_R, e_M	- eccentricities
GA_{ys}	- translational shear stiffnesses
$GJ_s, \overline{GJ}$	- St. Venant torsional stiffnesses
[G]	- impulse response function matrix
$I_{B/D}$	- moment of inertia about BD axis
IM_T	- mass moment of inertia
K_y	- translational stiffness
K_θ, K_ϕ	- rotational stiffness
$[K], [K_{yy}], [K_{\theta\theta}], [K_{y\theta}]$	- stiffness matrices
m	- single mass
[M]	- mass matrix
OMCP	-overall modal coupling parameter
r	- mass radius of gyration $\sqrt{\frac{IM_T}{m}}$
$T_i(t)$	- function determining the temporal variation of the response corresponding to the ith mode of vibration
t	- time variable in seconds

$u_y, \tilde{u}_\theta$	- lateral and normalized rotational displacement functions
$\ddot{u}_{gy}(t), \ddot{u}_{g\theta}(t)$	- lateral and rotational ground motions
X, Y	- dimensions of building
$\alpha_{yi}, \tilde{\alpha}_{\theta i}$	- coupled lateral-rotational mode shapes
β, ζ	- fraction of critical damping
$\phi_{yij}, \tilde{\phi}_{\theta ij}$	- lateral and torsional mode shapes, for mode i and mass j
ω_y, ω_θ	- the uncoupled natural frequencies
ω_1, ω_2	- the coupled natural frequencies
ω_i	- the ith natural frequency of the free coupled vibration in radians per second
$\lambda \left(= \frac{\omega_\theta}{\omega_y} \right)$	- ratio of an uncoupled torsional frequency to the uncoupled lateral frequency
$\Gamma_i, \Gamma_{yi}, \Gamma_{\theta i}$	- modal participation factors

APPENDIX II

DERIVATIONS OF MATHEMATICAL RELATIONSHIPS

A.2.1 One Storey Torsionally Coupled System

Let M and R be the centers of mass and rigidity respectively. The equations of motion governing the coupled model shown in Figure 2.1 are

$$m\ddot{u}_y = F(t) - K_y(u_y - eu_\theta) \tag{A.2.1.1}$$

$$I_M\ddot{u}_\theta = T(t) - K_\theta \cdot u_\theta + K_y(u_y - eu_\theta)e \tag{A.2.1.2}$$

Rewriting the above equations in normalized matrix form yields

$$\begin{bmatrix} m & 0 \\ 0 & m \end{bmatrix}\begin{Bmatrix} \ddot{u}_y \\ \ddot{\tilde{u}}_\theta \end{Bmatrix} + \begin{bmatrix} K_y & -\frac{e}{r}K_y \\ -\frac{e}{r}K_y & \tilde{K}_\theta \end{bmatrix}\begin{Bmatrix} u_y \\ \tilde{u}_\theta \end{Bmatrix} = \begin{Bmatrix} F(t) \\ \frac{T}{r}(t) \end{Bmatrix} \tag{A.2.1.3}$$

in which

$$r^2 = \frac{I_M}{m}, \quad \tilde{u}_\theta = ru_\theta \quad , \quad \tilde{K}_\theta = \frac{K_\theta}{r^2} + \frac{e^2}{r^2}\cdot K_y$$

The corresponding eigenvalue problem takes the form

$$\begin{bmatrix} 1\frac{\omega^2}{\omega_y^2} & -\frac{e}{r} \\ -\frac{e}{r} & \lambda^2\frac{e^2}{r^2} - \frac{\omega^2}{\omega_y^2} \end{bmatrix}\begin{Bmatrix} \alpha_y \\ \tilde{\alpha}_\theta \end{Bmatrix} = 0 \tag{A.2.1.4}$$

in which

$$\omega_\theta^2 = \frac{K_\theta}{I_M} \quad , \quad \omega_y^2 = \frac{K_y}{m} \quad , \quad \lambda^2 = \frac{\omega_\theta^2}{\omega_y^2}$$

It is clear from equation (A.2.1.3) that the frequency ratio $\frac{\omega_i^2}{\omega_y^2}$ and the mode shapes depend only on the two dimensionless parameters: λ, $\frac{e}{r}$. Solving the characteristic equation governing the non-trivial solution of equation A.2.1.2 gives

$$\left(\frac{\omega_i}{\omega_y}\right)^2 = \frac{a + \lambda^2}{2} \mp \left[\left(\frac{a + \lambda^2}{2}\right)^2 - \lambda^2\right]^{\frac{1}{2}} \qquad i=1,2 \qquad \text{(A.2.1.5)}$$

where $a = \left(1 + \frac{e^2}{r^2}\right)$.

A.2.2 Interaction Equation

The squares of the maximum normalized acceleration responses may be expressed by

$$\ddot{\bar{u}}_y^2 = \sum_{i=1}^{2} \ddot{\bar{u}}_{yi}^2 + 2\, a_{12}\, \ddot{\bar{u}}_{y1}\, \ddot{\bar{u}}_{y2} \qquad \text{(A.2.2.1)}$$

$$\ddot{\tilde{u}}_\theta^2 = \sum_{i=1}^{2} \ddot{\tilde{u}}_{\theta i}^2 + 2\, a_{12}\, \ddot{\tilde{u}}_{\theta 1}\, \ddot{\tilde{u}}_{\theta 2} \qquad \text{(A.2.2.2)}$$

where

$$a_{12} = \frac{1}{1 + \varepsilon_{12}^2} \quad , \quad \varepsilon_{12} = \frac{\sqrt{1 - \zeta^2}}{\zeta}\, \frac{\omega_1 - \omega_2}{\omega_1 + \omega_2}$$

Then

$$\ddot{\bar{u}}_y^2 + \ddot{\tilde{u}}_\theta^2 = S_1 + 2S_2 \qquad \text{(A.2.2.3)}$$

where

$$S_1 = \sum_{i=1}^{2} \ddot{\bar{u}}_{yi}^2 + \sum_{i=1}^{2} \ddot{\tilde{u}}_{\theta i}^2 \qquad \text{(A.2.2.4)}$$

$$S_2 = a_{12}(\ddot{\bar{u}}_{y1}\, \ddot{\bar{u}}_{y2} + \ddot{\tilde{u}}_{\theta 1}\, \ddot{\tilde{u}}_{\theta 2}) \qquad \text{(A.2.2.5)}$$

The two types of idealized response spectrum are treated separately in the following subsections.

A.2.2.1 The Case of Flat Acceleration Spectrum

Substitution of equations (2.14.a) and (2.14.b) into equation (A.2.2.4) gives

$$S_1 = \sum_{i=1}^{2} \alpha_{yi}^2 \, (\alpha_{yi}^2 + \tilde{\alpha}_{\theta i}^2) \qquad \text{(A.2.2.6)}$$

But the normalization given by equation (2.14) specifies that

$$\alpha_{yi}^2 + \tilde{\alpha}_{\theta i}^2 = 1 \qquad \text{(A.2.2.7)}$$

Therefore

$$S_1 = \sum_{i=1}^{2} \alpha_{yi}^2 \qquad \text{(A.2.2.8)}$$

The orthogonality condition for the mode shapes may be expressed by

$$\begin{bmatrix} \alpha_{y1} & \alpha_{y2} \\ \tilde{\alpha}_{\theta 1} & \tilde{\alpha}_{\theta 2} \end{bmatrix} \begin{bmatrix} \alpha_{y1} & \tilde{\alpha}_{\theta 1} \\ \alpha_{y2} & \tilde{\alpha}_{\theta 2} \end{bmatrix} = \begin{bmatrix} 1 & 0 \\ 0 & 1 \end{bmatrix} \qquad \text{(A.2.2.9)}$$

and hence

$$S_1 = 1 \qquad \text{(A.2.2.10)}$$

Substitution of equations (2.14.a) and (2.14.b) into equation (A.2.2.5) gives

$$S_2 = a_{12} \, \alpha_{y1} \, \alpha_{y2} (\alpha_{y1} \, \alpha_{y2} + \tilde{\alpha}_{\theta 1} \, \tilde{\alpha}_{\theta 2}) \qquad \text{(A.2.2.11)}$$

But by the orthogonality of the modes

$$\alpha_{y1}\,\alpha_{y2} + \tilde{\alpha}_{\theta 1}\,\tilde{\alpha}_{\theta 2} = 0$$

so

$$S_2 = 0$$

Accordingly

$$\bar{\bar{u}}_y^2 + \tilde{\bar{\bar{u}}}_\theta^2 = 1 \qquad \text{(A.2.2.13)}$$

A.2.2.2 The Case of Hyperbolic Acceleration Spectrum

Substitution of equations (2.15.a) and (2.15.b) into equation (A.2.2.4) yields

$$S_1 = \sum_{i=1}^{2} \left(\frac{\omega_i}{\omega_y}\right)^2 \alpha_{yi}^2 \left(\alpha_{yi}^2 + \tilde{\alpha}_{\theta i}^2\right)$$

$$= \sum_{i=1}^{2} \left(\frac{\omega_i}{\omega_y}\right)^2 \alpha_{yi}^2 \qquad \text{(A.2.2.14)}$$

From equation (2.2)

$$\left[1 - \left(\frac{\omega_i}{\omega_y}\right)^2\right]\alpha_{yi} - \frac{e}{r}\,\tilde{\alpha}_{\theta i} = 0 \qquad \text{(A.2.2.15)}$$

Substitution of equation (A.2.2.15) into equation (A.2.2.14) gives

$$S_1 = \sum_{i=1}^{2} \alpha_{yi}^2 - \frac{e}{r} \sum_{i=1}^{2} \alpha_{yi}\,\tilde{\alpha}_{\theta i} \qquad \text{(A.2.2.16)}$$

The orthogonality condition specifies that

$$\sum_{i=1}^{2} \alpha_{yi}^2 = 1 \qquad \text{and} \qquad \sum_{i=1}^{2} \alpha_{yi}\, \tilde{\alpha}_{\theta i} = 0 \tag{A.2.2.17}$$

hence

$$S_1 = 1$$

Substitution of equations (2.15.a) and (2.15.b) into equation (A.2.2.4) gives

$$S_2 = a_{12} \frac{\omega_1 \omega_2}{\omega_y^2}\, \alpha_{y1}\, \alpha_{y2}\, (\alpha_{y1}\, \alpha_{y2} + \tilde{\alpha}_{\theta 1}\, \tilde{\alpha}_{\theta 2}) \tag{A.2.2.18}$$

Since the orthogonality condition also holds here,

$$S_2 = 0$$

and hence the interaction equation still applies

$$\bar{\bar{u}}_y^2 + \bar{\bar{u}}_\theta^2 = 1 \tag{A.2.2.19}$$